Complex Formation of Protoporphyrinogen IX Oxidase and Ferrochelatase during the Tetrapyrrole Biosynthesis in *Thermosynechococcus elongatus*

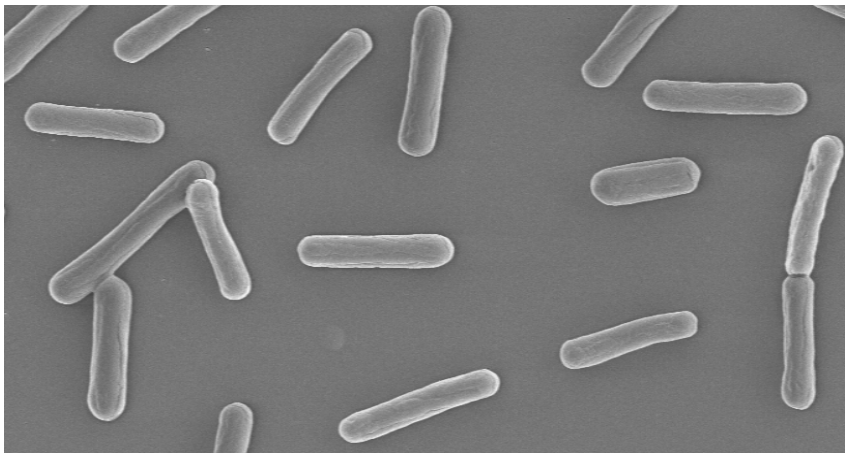

Von der Fakultät für Lebenswissenschaften

der Technischen Universität Carolo-Wilhelmina

zu Braunschweig

zur Erlangung des Grades einer

Doktorin der Naturwissenschaften

(Dr. rer. nat.)

genehmigte

D i s s e r t a t i o n

von Ava Masoumi
aus Khorram abad / Iran

1. Referent: Professor Dr. Dieter Jahn
2. Referent: Professor Dr. Ralf-Rainer Mendel
eingereicht am: 21.03.2007
mündliche Prüfung (Disputation) am: 19.07.2007

Druckjahr 2007

Vorveröffentlichungen der Dissertation

Teilergebnisse aus dieser Arbeit wurden mit Genehmigung der Fakultät für Lebenswissenschaften, vertreten durch den Mentor der Arbeit, in folgenden Beiträgen vorab veröffentlicht:

Publikationen

Layer, G., Grage, K., Teschner, T., Schunemann, V., Breckau, D., Masoumi, A., Jahn, M., Heathcote, P., Trautwein, AX., Jahn, D. Radical S-adenosylmethionine enzyme coproporphyrinogen III oxidase HemN: functional futures of the [4Fe-4S] cluster and the two bound S-adenosyl-L-methionines. *J Biol Chem*. 280(32): 29038-46 (2005)

Schulze, J.O.**,** Masoumi, A., Nickel, D., Jahn, M., Jahn, D., Schbert, W.D. & Heinz, D.W. Crystal structure of a non-discriminating glutamyl-tRNA synthetase. *J Mol Biol*. 361(5):888-97 (2006)

Heinemann, I.U., Diekmann, N., Masoumi, A., Koch, M., Messerschmidt, A., Jahn, M. & Jahn, D. Functional definition of the tobacco protoporphyrinogen IX oxidase substrate binding site. *Biochem J.* 402: 575-80 (2007)

Vorbereitete Publikationen

Masoumi, A., Heinemann, I., Rohde, M., Jahn, M. & Jahn, D. Metabolic channelling of photoreactive protoporphyrinogen IX in *Thermosynechococcus elongates* during the ultimate steps in porphyrin biosynthesis. Manuskript in preparation

Tagungsbeiträge

Masoumi, A., Heinemann, I., Rohde, M., Jahn, M. & Jahn, D. (2006). Protein complex of three enzymes involved in tetrapyrrole biosynthesis in *Thermosynechococcus elongates* VAAM-Jahrestagung, Jena, Germany, 19-22/03 (Poster).

Table of Contents

Abbreviations

α	anti
A	Ampere
ALA	5-Aminolevulinic Acid
amp	ampicillin
AP	Alkaline Phosphatase Buffer
APS	Ammonium Peroxodisulfate
ATP	Adenosine 5´-triphosphate
BCA	Bicinchoninic Acid
BCIP	5-Brom-4-Chloro-3-Indolyl Phosphate
bp	base pair
C	Celsius (° C)
Ci	Curie
cm	chloramphenicol
Copro	Coporporphyrin III
Coprogen	Coproporphyrinogen III
CPO	Coproporphyrinogen III oxidase
CV	Column Volume
Da	Dalton
DEAE	Diethylaminoethyl
D-GluRS	Discriminating Glutamyl tRNA Synthetase
DNA	Deoxyribonucleic Acid
(d)dNTP	(di)deoxyribonucleotide Triphosphate
DSMZ	Deutsche Sammlung von Mikroorganismen und Zellkulturen
DTT	1,4-dithio-D,L-threitol
EDTA	Ethylenediaminetetraacetic Acid
e.g.	*exempli gratia* (for instance)
et al.	*et alteri* (and others)
EtOH	Ethanol
FAD	Flavin-Adenine-Dinucleotide

g	*Centrifugation*: earth gravity
	Weight: gram
Gln	Glutamine
GlnRS	Glutaminyl tRNA Synthetase
Glu	Glutamate
GluRS	Glutamyl tRNA Synthetase
h	hour
H_2O_{deion}	deionised water
HemF	oxygen-dependent coproporphyrinogen III oxidase in prokaryotes
HemH	oxygen-dependent ferrochelatase in prokaryotes in prokaryotes
HemY	oxygen-dependent protoporphyrinogen IX oxidase in prokaryotes
HEPES	4-(2-hydroxyethyl)-piperazine-1-ethane sulfonic acid
i.e.	*id est* (that is to say)
IPTG	Isopropyl-1-Thio-ß-D-Galactopyranoside
k	kilo
kan	kanamycin
λ	wavelength
l	liter
LB	Luria Bertani
m	milli
µ	micro
M	Molar (mol/l)
mA	milli Ampere
MCS	Multiple Cloning Site
min	minute
m_r	relative moleculare mass
n	nano
NBT	Nitroblue-tetrazolium chloride
ND-GluRS	Non-Discriminating glutamyl tRNA Synthetase
Ni-NTA	Nickel-Nitrilotri- acetic acid
Ω	Ohm
OD_λ	Optical density at wavelength λ nm

Pa	Pascal
PBS	Phosphate Buffered Saline
PCR	Polymerase Chain Reaction
pH	negative decadic logarithm of the H^+ concentration of a solution
PPO	Protoporphyrinogen IX Oxidase
Proto	Protoporphyrin IX
Protogen	Protoporphyrinogen IX
PVDF	Polyvinylidenfluoride
RNase	Ribonuclease
rpm	rotations per minute
RT	Room Temperature
s	second
SDS-PAGE	Sodium Dodecyl Sulfate Polyacrylamide Gel Electrophoresis
TAE	Tris-Acetate/EDTA
Taq	*Thermus aquaticus*
TE	Tris-EDTA
TEMED	Tetramethylen diamine
tet	tetracycline
Tris	Tris-(hydroxymethyl)-aminomethane
Triton X-100	T-octylphenoxypolyethoxyethanol
tRNA	transfer Ribonucleic Acid
Tween	Polyoxyethylene sorbitol oleate
U	Unit
UV	Ultra Violet
UV-VIS	Ultra Violet and Visible Spectrum of light
V	Volt
v/v	volume per volume
W	Watt
w/v	weight per volume
Y	Cytosine or Guanine

I Introduction

I.1 Importance of Tetrapyrroles

Tetrapyrroles are molecules which contain four pyrrole rings. They include chlorophylls, hemes, chlorins, corrins and billins.

Tetrapyrroles participate in fundamental biological processes and are essential components of the metabolism of practically all organisms on earth. They play a central role in electron transfer-dependent energy generating processes such as photosynthesis and respiration. They also function as prosthetic groups for a variety of enzymes. Due to their typical colors, they have often been referred to as "pigments of life" (Sir Alan Battersby, 2000). The most commonly found tetrapyrrole in nature is chlorophyll. It is essential for light harvesting and energy transduction during photosynthesis. Magnesium-containing chlorophylls are responsible for the green colours in plants. Iron-chelating tetrapyrroles such as hemes represent the prosthetic group of haemoglobin (O'Brian *et al.*, 2002) responsible for the transport of oxygen. Hemes are responsible for the red color of blood. They also play an important role in membrane localized electron transfer reaction during respiratory energy generation.

I.2 Tetrapyrroles Structure and Functions

Four pyrrole rings of a tetrapyrrole molecule are mostly attached to each other in a cycle or linear form via methine bridges. The basic structure of a cyclic tetrapyrrole is the porphyrin macrocycle shown in figure 1.

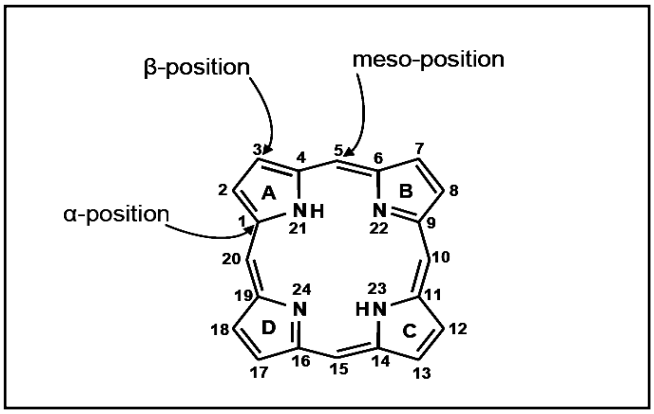

Figure 1: Basic structure of cyclic tetrapyroles, the porphyrin ring. The pyrrole rings are labled A – D, the carbon and nitrogen atoms are numbered 1 – 20 and 21 – 24, respectively. The α-carbon refer to carbon atoms adjacent to nitrogen atoms, the remaining pyrrole ring carbons are designated ß-carbons and the methine bridge carbons are in meso-position.

Eight different groups of tetrapyrroles are known. The functional properties of each group are mainly determined by the nature of the metal ion which is chelated by the nitrogen atoms in the center of the ring system, by the oxidation state of the macrocycle and by the nature of the substituents at the ß positions of the pyrrol rings. Structures of important representatives of different groups of of tetrapyrroles are shown in figure 2.

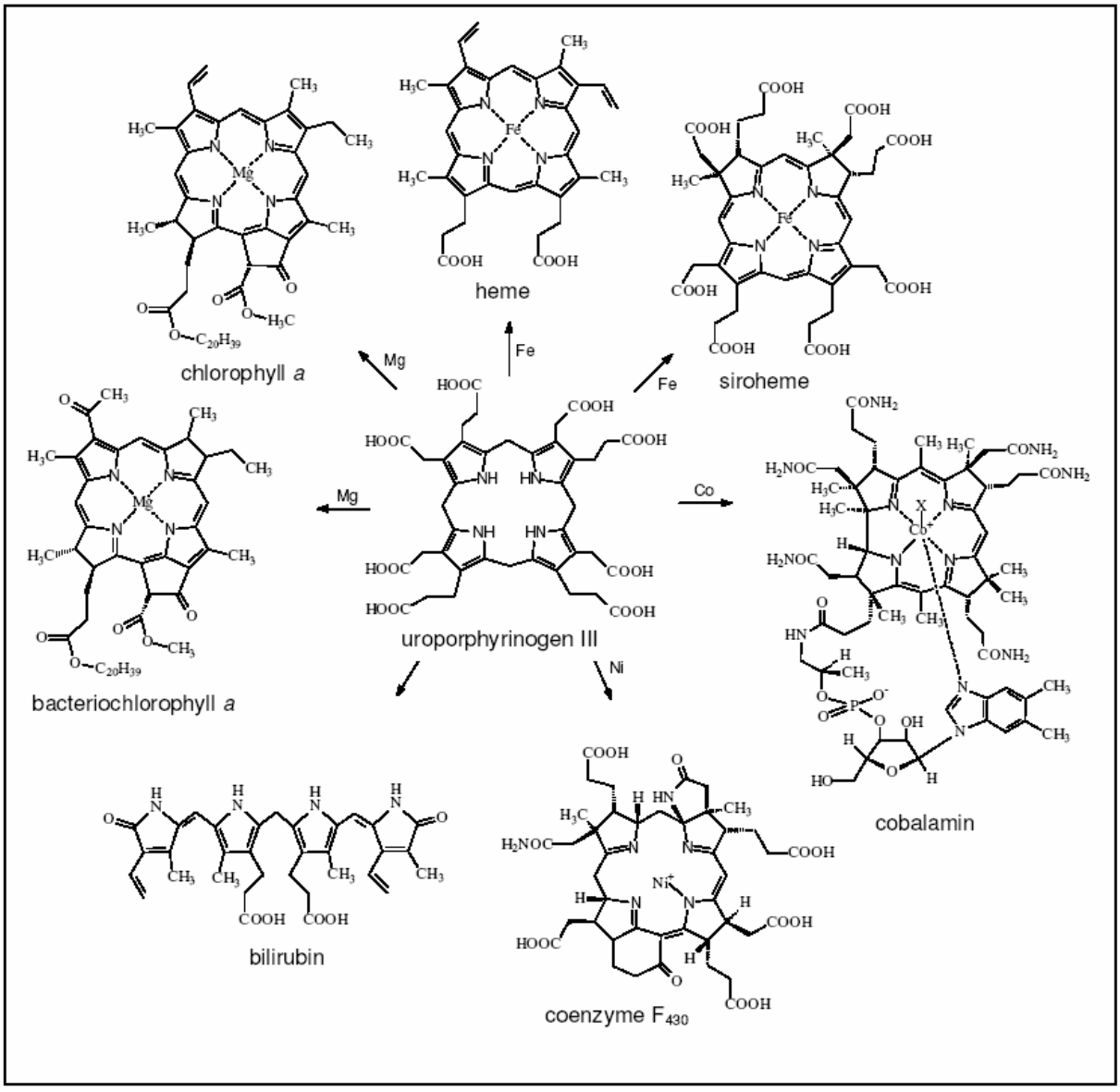

Figure 2: Important representatives of naturally occuring tetrapyrroles and their common precursor uroporphyrinogen III. The structure of the eighth representable heme d_1 is not shown.

Porphyrins represent molecules with multiple conjugated double bonds that cause a characteristic adsorption pattern in the visible spectrum of the light resulting in their color. Some intermediates

similarly have specific spectroscopic properties, which significantly help to the clear the biosynthetic pathways of tetrapyrroles (Battersby, 2000; Warren, 2005). Heme is a true porphyrin that acts as prosthetic group of hemoglobin, myoglobin, cytochromes, catalases and peroxidases. Heme proteins carry out electron transfer reaction with O_2 or alternatively nitrate, sulphate or other oxidants as electron acceptors. Exogenous heme serves as a nutritional iron source to some pathogenic bacteria. Finally, heme is a substrate for the synthesis of phytochrome and bilins, which serve as light-sensing and light-harvesting molecules in photosynthetic organisms.

Further examples for tetrapyrroles include more highly reduced cyclic tetrapyrroles such as chlorophylls (chlorins), bacteriochlorophylls (chlorins or bacteriochlorin), siroheme, coenzyme F_{430} and heme d_1. Magnesium containing chlorophylls and bacteriochlorophylls function as photoreceptors during photosynthesis (Beale and Weinstein, 1990, 1991). Siroheme and heme d_1 are the cofactors of assimilatory sulfite and nitrite reductase and of dissimilatory nitrite reductase, respectively (Chang, 1994; Warren *et al*., 1994). Both contain iron as central atom. Cofactor F_{430}, chelates nickel and serves as prosthetic group of methyl coenzyme M reductase, an enzyme involved in archaeal methanogenesis (Friedmann *et al*., 1991; Thauer and Bonacker, 1994). Finally, tetrapyrroles like coenzyme B_{12} belong to the class of corrinoids characterized by a missing methine bridge (C20) (Scott and Santander, 1991; Martens *et al*., 2002). Members of the cobalt-containing corrinoids are e.g cofactors in methyl transfer reactions. Linear tetrapyrroles are derived from cyclic tetrapyrroles by oxidative cleavage. The cleavage product of heme, biliverdin serves as a precursor for the biosynthesis of phycobilins (e.g chromophores of cyanobacterial phycobiliproteins) and phytochrome chromophores (Beale, 1993; Beale and Yeh, 1999; Frankenberg and Lagarias, 2003).

I.3 Biosynthesis of Tetrapyrroles

In accordance with their common structural core all currently known tetrapyrroles are derived from a single precursor molecule, 5-aminolevulinic acid (ALA). Consequently, the initial steps of the biosynthetic pathway from ALA are conserved throughout the different biosynthetic routes. Only after the formation of the first cyclic intermediate, uroporphyrinogen III, the pathways diverge. Representing a major branching point in tetrapyrrole biosynthesis, uroporphyrinogen III is converted either into protoporphyrin IX or into precorrin-2 (dehydrosirohydrochlorin).

Protoporphyrin IX is the precursor for the synthesis of hemes, chlorophylls and bacteriochlorophylls, while precorrin-2 is used to synthesize the remaining classes of cyclic

tetrapyrroles, including siroheme, heme d_1, corrinoids and coenzyme F_{430}. An overview of the divergent biosynthetic pathways is provided in figure 3.

Only prokaryotes are capable of synthesizing all classes of tetrapyrroles. In eukaryotes tetrapyrrole biosynthesis is limited to the formation of hemes, chlorophylls and siroheme. Tetrapyrroles and their biosynthesis have been reviewed in numerous publications, some of which focus solely on heme biosynthesis (e.g. Lascelles, 1964; Dailey, 1990; Jordan, 1991; Jahn *et al.*, 1996; Shoolingin-Jordan and Cheung, 1999; O'Brian and Thöny-Meyer, 2002; Frankenberg *et al.*, 2003).

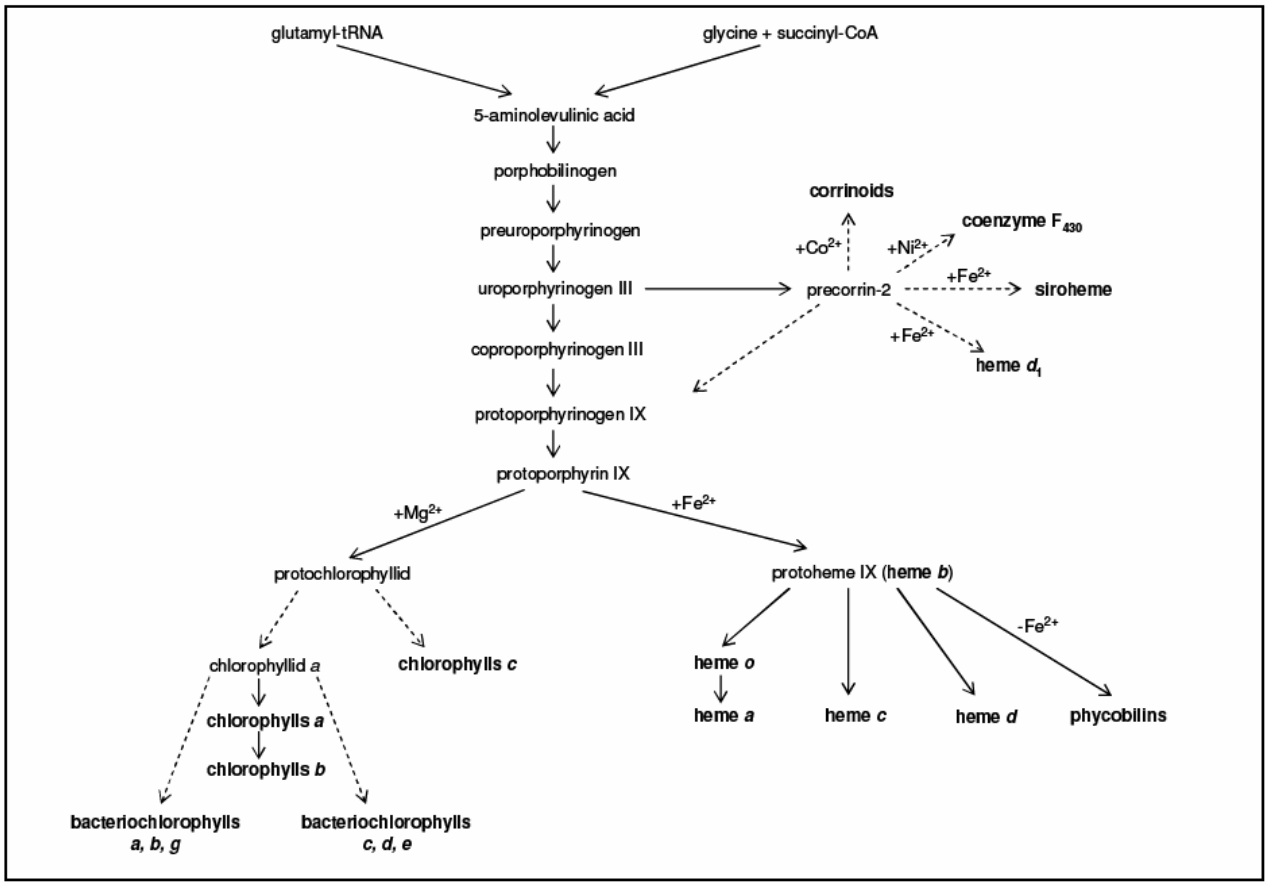

Figure 3: Overview of biosynthetic pathways of biologically relevant tetrapyrroles. Dotted arrows indicate pathways which are not shown completely or have not yet been entirely understood (modified from Jahn *et al.*, 1996).

I.4 Synthesis of Glutamyl-tRNA

The formation of 5-aminolevulinic acid can be achieved via two pathways (figure 3), one of which is the Shemin and the other is the C5 pathway (see I.5). The C5 pathway found in most

bacteria, archaea and plants (Beale and Castelfranco, 1973). This pathway uses an activated $tRNA^{Glu}$ as substrate (Figure 4). A Glutamyl-$tRNA^{Glu}$ serves as initial substrate and two enzymatic steps are required to form ALA (Jahn *et al*., 1992). The first enzyme of this pathway, glutamyl-tRNA reductase (**GluTR**), is NADPH-dependent and catalyzes the reduction of the glutamic acid residue of the glutamyl-tRNA to glutamate-1-semialdehyde (GSA) (Moser *et al*., 1999). In the following step glutamate-1-semialdehyde-2,1-aminomutase (**GSAM**) converts GSA to ALA in a pyridoxamine-5'-phosphate-dependent transamination reaction (Ilag and Jahn, 1992). Since GSA is a highly reactive aldehyde a coordinated action of the two enzymes is required. This led to the proposal of a GluTR/GSAM complex, based on the structural complementarity of the two enzymes (Moser *et al*., 2001). This complex was confirmed to exist *in vitro* (Lüer *et al*., 2005).

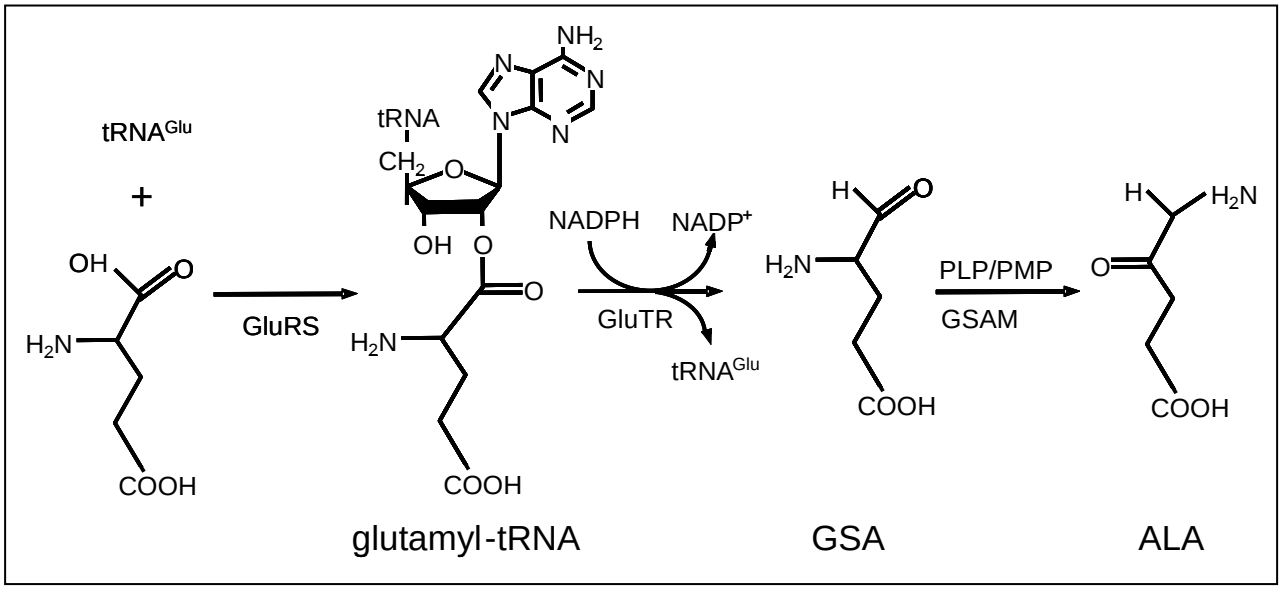

Figure 4: C5 pathway including the aminoacylation of $tRNA^{Glu}$ with glutamate by GluRS.

Glutamyl-tRNA is one of at least twenty tRNA molecules which upon aminoacylation through its corresponding cognate aminoacyl-tRNA synthetase enters the ribosomes for protein biosynthesis. It is the identical glutamyl-tRNA which is employed in tetrapyrrole biosynthesis. However, serving as a substrate for the C5 pathway in heme biosynthesis, glutamyl-tRNA has been of special interest in this work.

I.4.1 Aminoacyl-tRNA Synthetase Mechanism

Aminoacyl-tRNA synthetases catalyze a two-step reaction. In the first step they activate their substrate amino acid by forming an aminoacyl-adenylate, in which the carboxyl of the amino acid is linked to the alpha-phosphate of ATP, displacing pyrophosphate. When the correct tRNA is bound, the aminoacyl group of the aminoacyl-adenylate is transferred to the 2' or 3' terminal OH of the tRNA. In the cases of GluRS, GlnRS and ArgRS, the first step occurs only in the presence of the tRNA (Sekine *et al*., 2003).

I.4.2 Number of Aminoacyl-tRNA Synthetases

Most cells produce at least twenty different aminoacyl-tRNA synthetases, one for each type of amino acid. The corresponding twenty enzymes are widely different, each optimized for function with its own particular amino acid and the set of tRNA molecules appropriate for that amino acid. Recent analyses of entire genomes revealed that some archaea and bacteria do not possess genes for all twenty aminoacyl-tRNA synthetases. They do, however, use all twenty amino acids to construct their proteins. Glutaminyl- and Asparaginyl-tRNA synthetases (GlnRS and AsnRS) are among those that are frequently missing (*Campylobacter jejuni, Chlamydia trachomatis, Helicobacter pylori, Mycobacterium tuberculosis* and *Rickettsia prowazekii*) (Raczniak *et al., 2001)*. In *Methanococcus janaschii* (Bult *et al*., 1996) and *Methanobacterium thermoautotrophicum* (Smith *et al*., 1997) there are only 16 of 20 aminoacyl-tRNA synthetases present. This gave rise to the question how the accuracy of translation ensuring the genetic code is guaranteed.

I.4.3 Natural tRNA Mischarging

To explain the absence of an aminoacyl-tRNA synthetase, the existence of an alternative pathway was suggested (Wilcox *et al*., 1968). This pathway involves mischarging of a tRNA with a noncognate amino acid. For example, $tRNA^{Gln}$ and $tRNA^{Asn}$ are aminoacylated with glutamate (Glu) and aspartate (Asp) by GluRS and AspRS, respectively. Then they are subsequently converted to the glutaminylated and aspartylated tRNAs by the action of tRNA-specific amidotransferases (Ibba and Söll 2000). The amide donors of these enzymes are glutamine (Gln) and asparagine (Asn), respectively.

I.4.4 Discriminating and Nondiscriminating GluRS

In many organisms two types of glutamyl-tRNA synthetase exist; the discriminating enzyme (D-GluRS) forms solely Glu-tRNA^{Glu}, while the non-discriminating one (ND-GluRS) also synthesizes Glu-tRNA^{Gln} besides Glu-tRNA^{Glu}.

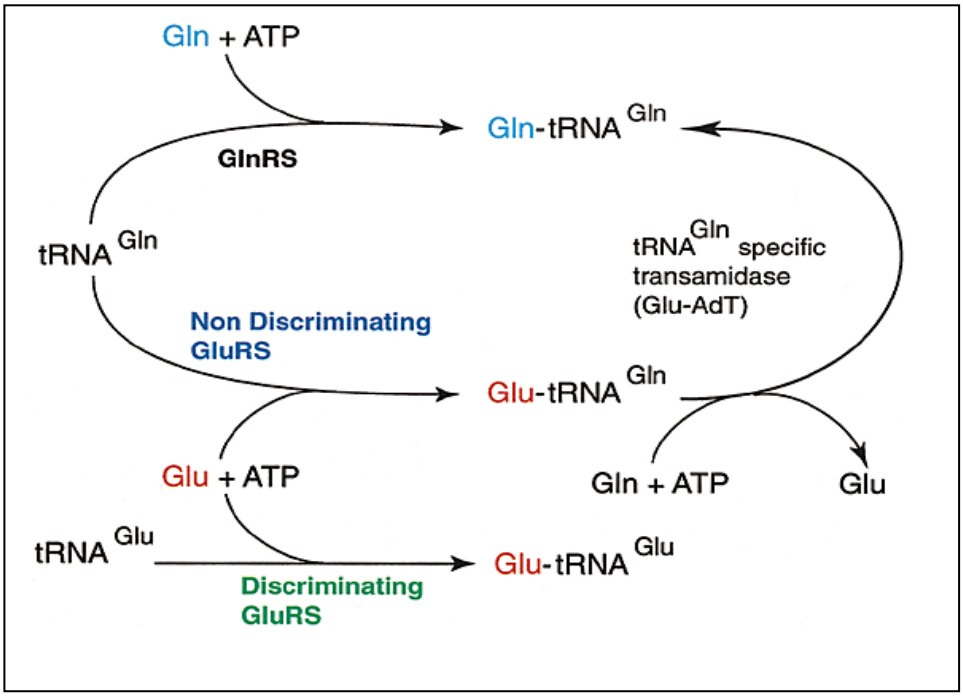

Figure 5: Formation of Glu-tRNA^{Glu} and Gln-tRNA^{Gln} by discriminating and nondiscriminating GluRS. The tRNA synthetases responsible for catalyzing the respective aminoacylation reactions are indicated, as well as the tRNA^{Gln} specific amidotransferase responsible for transferring a terminal amino group to the glutamylated-tRNA^{Gln} (Francklyn, 2001).

ND-GluRS must accept both tRNA^{Gln} (anticodon 5´-YUG-3`) as well as tRNA$^{Glu}$ (anticodon 5´-YUC-3`) as substrates. These reactions contradict a key assumption originally made for protein biosynthesis namely that each enzyme is restricted to the set of tRNAs specific for the amino acid cognate for that tRNA synthetase. The co-crystal structure of a discriminating GluRS and its cognate tRNA was described. Structural details of the recognition of the tRNA^{Glu} anticodon by GluRS were provided (Sekine *et al*., 2001). The authors showed how the mutation of a single arginine in the GluRS anticodon binding domain abolishes discrimination between the anticodons for tRNA^{Glu} and tRNA^{Gln}. While not being a fully 'nondiscriminating' version of GluRS, this mutant enzyme nonetheless serves as a model for how evolution of tRNA specificity might have proceeded.

Genetic studies revealed that *Thermosynechococcus elongatus* does not posses a gene for GlnRS (Nakamura *et al*., 2002). Instead, the genes *gatC*, *gatA* and *gatB* for the heterotrimeric amidotransferase Glu-AdT (or GatCAB) are present (Curnow *et al*., 1997). Most likely, GluRS of *T. elongatus* ($GluRS_{Tel}$) is a non-discriminating enzyme, acylating both $tRNA^{Glu}$ and $tRNA^{Gln}$ followed by the conversion of misacylated Glu-$tRNA^{Gln}$ into Gln-$tRNA^{Gln}$ by GatCAB.

The recently solved crystal structure revealed that the ND-$GluRS_{Tel}$ consists of five domains (Schulze et al., 2006, figure 6). The catalytic domain has a dinucleotide binding or Rossmann fold (Rao and Rossmann, 1973). A deep pocket accommodates the active site, including binding sites for glutamate and the acceptor end of tRNA. The conserved ATP-binding motifs form part of the active site pocket. The acceptor binding-site or connective polypeptide (CP) causes the helical tRNA acceptor end to change its conformation during binding to allow the 3′ end to fit into the active site. The other domains are one stem contact (SC) domain (four α-helices) and two anticodon-binding domains.

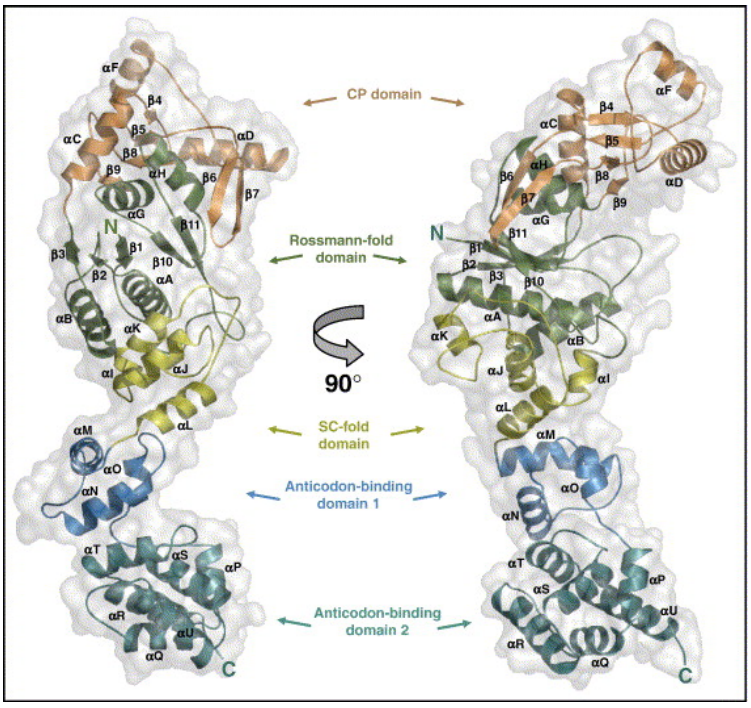

Figure 6: Representation of non-discriminating GluRS from *T. elongatus* (ND-$GluRS_{Tel}$) with transparent surface. The right view is rotated by 90° relative to the left view. The catalytic domain is shown in green, the connective peptide (CP) domain in orange, the stem contact (SC)-fold domain in yellow, and anticodon-binding domains 1 and 2 in light blue and cyan, respectively (Schulze *et al*., 2006).

I.5 Heme Biosynthesis

I.5.1 Glutamyl-tRNA Dependent and Independent 5-Aminolevulinic Acid Formation

The shared structural core of tetrapyrroles implies a highly conserved biosynthetic pathway. All tetrapyrroles derive from a common precursor 5-aminolevulinic acid (ALA). There are, however, two alternate routes leading to ALA formation. The pathway discovered first is termed 'Shemin pathway' (Shemin *et al*., 1953; Neuberger *et al*., 1953) and occurs in animals, fungi and the α-group of p*roteobacteria*. Here the pyridoxal-5'-phosphate dependent enzyme ALA synthase (**ALAS**) synthesises ALA in a single step through condensation of glycine and succinyl-CoA (Kikuchi *et al*., 1958).

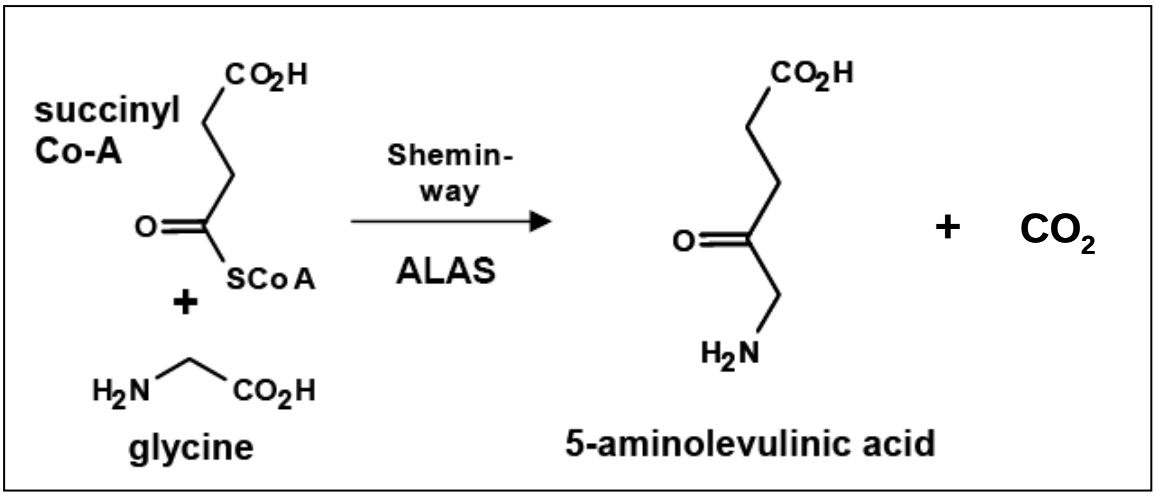

Figure 7: The Shemin pathway for aminolevulinic acid formation.

I.5.2 Formation of Porphobilinogen

In the next step of heme biosynthesis, two molecules of 5-aminolevulinic acid are condensed asymmetrically to yield the pyrrole derivative porphobilinogen (PBG). This reaction is catalyzed by porphobilinogen synthase (**PBGS**) (Frankenberg *et al*., 1999). **PBGS** enzymes from different organisms are all metal-ion dependent, some enzymes require Zn^{2+} for catalysis and others Mg^{2+} and/or K^{+} (Shoolingin-Jordan, 2002).

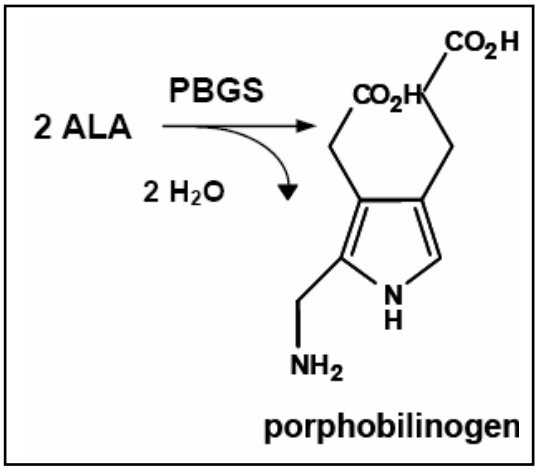

Figure 8: Porphobilinogen-formation by porphobilinogen synthase (PBGS).

Four molecules of PBG are linked consecutively by porphobilinogen deaminase (**PBGD**) to produce the linear tetrapyrrole pre-uroporphyrinogen (Warren *et al*., 1987). this is converted into the first cyclic intermediate of the pathway, uroporphyrinogen III, by the uroporphyrinogen III synthase (**UROS**). The uroporphyrinogen III synthase catalyzes the inversion of ring D creating the asymmetric tetrapyrrole uroporphyrinogen III (Chadwick and Ackrill, 1994). Uroporphyrinogen III, the first cyclic intermediate, is the common precursor for two distinct groups of tetrapyrroles the porphinoids (siroheme, heme d_1, coenzyme F430 and vitamin B12) and the porphyrins (hemes and chlorophylls) (fig. 9).

The intermediates in the biosynthesis of chlorophylls and hemes are synthesized by the successive decarboxylation of the four acetate side chains of uroporphyrinogen III to produce coproporphyrinogen III. Uroporphyrinogen III decarboxylase (**UROD**) catalyses this decarboxylation in clockwise direction beginning with the acetate side chain of ring D (Luo *et al*., 1993).

In the next step two different coproporphyrinogen III oxidases (**CPO**) catalyzes the conversion of coproporphyrinogen III to protoporphyrinogen IX (Layer *et al*., 2002; Breckau *et al*., 2003). Protoporphyrinogen IX oxidase (**PPO**) converts protoporphyrinogen IX into the aromatic and colored protoporphyrin IX as further described in section I.5.4. The last step of heme biosynthesis is the insertion of iron into protoporphyrin IX catalyzed by ferrochelatase (**FC)** (Dailey, 2002).

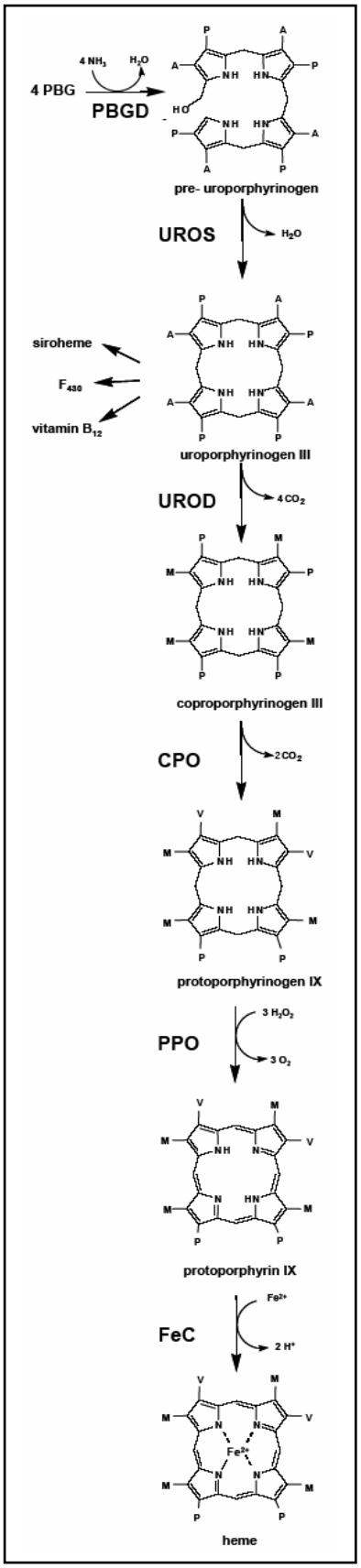

Figure 9: Biosynthesis of heme. The abbreviation for the involved enzymes and their catalyzed reactions are explained in the text. A: acetate side chain; M: Methylgroup; P: propionate side chain; V: vinyl group.

I.5.3 Formation of Protoporphyrinogen IX by Coproporphyrinogen III Oxidase

In the antepenultimate step of heme synthesis, which is illustrated in figure 10, the propionate side chains of rings A and B of coproporphyrinogen III (coprogen) (positions C3 and C8; compare figure 1) are consecutively converted into the corresponding vinyl groups of the product protoporphyrinogen IX (protogen) (Sano and Granick, 1961; Akhtar, 1991). During this oxidative decarboxylation reaction two molecules of CO_2 are released and a terminal electron acceptor is required. Two types of enzymes catalyzing the reaction are found in nature.

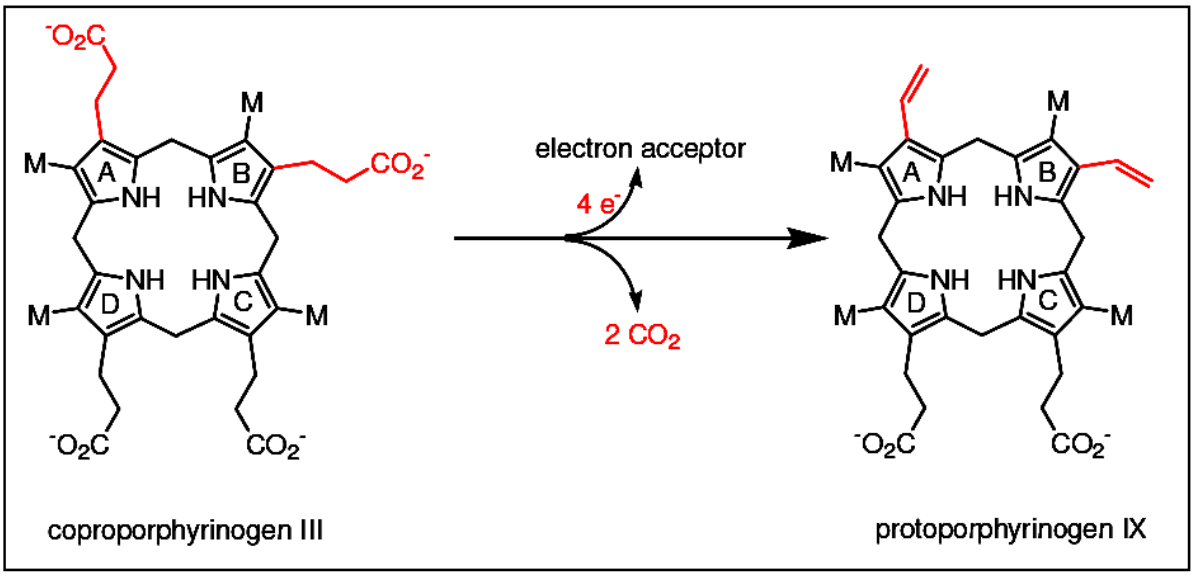

Figure 10: The oxidative decarboxylation of coproporphyrinogen III to protoporphyrinogen IX catalyzed by the enzyme coproporphyrinogen III oxidase. The two propionate side chains to be decarboxylated and the resulting vinyl groups are shown in red. M, methyl group.

One is the oxygen-dependent coproporphyrinogen III oxidase, which catalyzes the reaction under aerobic conditions using molecular oxygen as electron acceptor (Breckau *et al.*, 2003). The other is the oxygen-independent coproporphyrinogen III oxidase, which functions independent of oxygen utilizing an alternative electron acceptor. For the aerobic reaction the isolation of harderoporphyrinogen (C3: vinyl group, C8: propionate group) as an intermediate has provided evidence that the propionate side chain of ring A is decarboxylated prior to that of ring B (Kennedy *et al.*, 1970; Jackson *et al.*, 1980). Oxygen-dependent CPO is mainly a eukaryotic enzyme although it has been found in a few bacteria, where it is termed HemF. In prokaryotes, however, the O_2-independent radical SAM enzyme HemN is prevalent (Panek and O'Brian, 2002; Layer *et al.*, 2003). Oxygen-dependent CPO proteins from several - mostly eukaryotic - organisms have been investigated and quite different results have been obtained e.g. with regard

to their metal content (Dailey, 2002). Human oxygen-dependent CPO does not contain any detectable cofactors or metals (Medlock and Dailey, 1996) while the mouse enzyme was reported to contain copper (Kohno *et al.*, 1996). The recently purified and characterized *E. coli* enzyme was shown to be manganese-dependent (Breckau *et al.*, 2003). The first crystal structure of an O_2-dependent CPO - the yeast enzyme - has been solved, revealing the absence of any bound metal ion (Phillips *et al.*, 2004). Recently the crystal structure of the human CPO was reported (Lee *et al.*, 2005).

I.5.4 Formation of Protoporphyrin IX by Protoporphyrinogen IX Oxidase

The penultimate step of heme biosynthesis – the conversion of protoporphyrinogen IX (protogen) into protoporphyrin IX (proto) – is catalyzed by protoporphyrinogen IX oxidases (PPO). During this reaction two of the four imino groups of the pyrrole and the four bridging carbons (C5, C10, C15 and C20) are oxidized (Dailey, 2002). This six electron oxidation gives rise to a completely conjugated, planar and colored macrocycle.

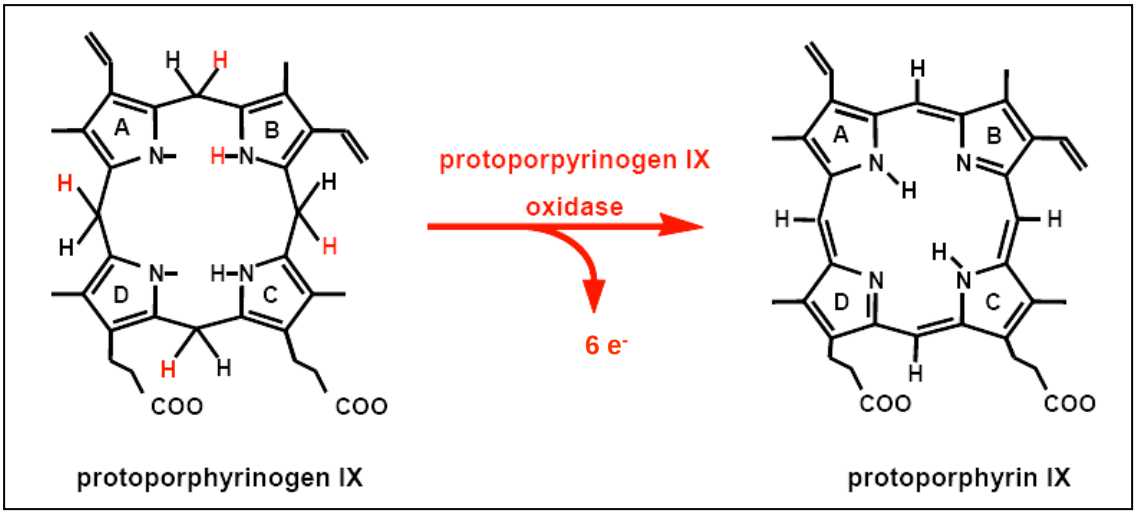

Figure 11: Conversion of protoporphyrinogen IX into protoporphyrin IX.

The oxygen-dependent PPO (HemY in prokaryotes) is encoded by the *hemY* gene and produced in eukaryotes as well as in *Myxobacteria* and Gram positive bacteria. Oxygen-dependent PPO is also found in bacteria such as *Bacillus subtilis* (Hansson and Hederstedt, 1992, 1994; Daily *et al.*, 1994, Corrigall *et al.*, 1998), *Myxococcus xanthus* (Dailey *et al.*, 1996) or *Aquifex aeolicus* (Wang *et al.*, 2001).

Under aerobic conditions, molecular oxygen serves as the terminal electron acceptor during the formation of protoporphyrin IX. Three moles of O_2 are consumed per mole of substrate yielding three moles of H_2O_2.

PPOs are generally dimeric enzymes. Only the enzyme of *Bacillus subtilis* has been described to exist as monomer (Dailey *et al*., 1994). The relative molecular masses of PPO monomers range from M_r = 36.000 (barley) to M_r = 65.000 (cattle). They are located in the inner mitochondrial membrane while their active sites facing the perimitochondrial space.

Two isoforms have been found in plants, plastidal PPO I and mitochondrial PPO II (Jacobs *et al*., 1984, 1987). PPO I and II from *Nicotiana tabacum* share a sequence identity of only 27% (Lermontova *et al*., 1997).

Oxygen-dependent PPO belongs to the superfamily of flavin-containing oxidases (Dailey *et al.*, 1998) and mostly bind FAD (Siepker *et al*., 1987; Camadro *et al.*, 1994; Koch *et al.*, 2004). The mitochondrial PPO of *N. tabacum* was the first PPO to be crystallized followed by the structure resolution (Koch *et al*., 2004). As expected, the structure revealed a homodimer in which each monomer consists of a FAD, substrate and membrane binding domain (Koch *et al.*, 2004). Recently, a second 3-D structure was solved for the *Myxococcus xanthus* PPO (Corradi *et al*., 2006).

Similar to CPOs there exists an O_2-independent form of PPO. This obviously bacteria-specific enzyme channels the six abstracted electron-transport chains of respiration (Jacobs and Jacobs, 1987).

I.5.5 Formation of Protoheme

The last step in heme biosynthesis the insertion of a ferrous ion into protoporphyrin IX to form protoheme is catalyzed by ferrochelatase (Labbe - Bios, 1990; Brenner *et al.*, 1991) .

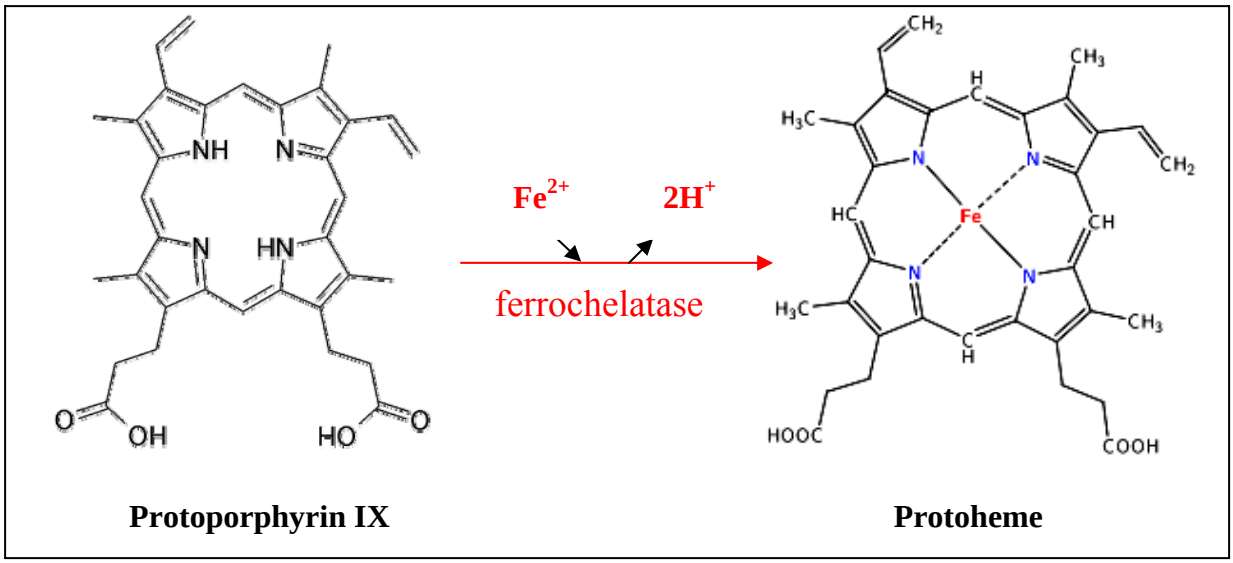

Figure 12: Chelation of ferrous ion into protoporphyrin IX via ferrochelatase to form protoheme.

In prokaryotes FC (HemH) is encoded by the *hemH* gene. Environmental iron is primarily in the ferric form, and thus it must be reduced prior to chelation. Other divalent ions such as Co^{2+} and Zn^{2+} can also serve as metal substrates *in vitro*, whereas others such as Mn^{2+}, Cd^{2+} and Pb^{2+} are competitive inhibitors (Dailey, 1987). The crystal structures of *B. subtilis* and human ferrochelatase have been solved (Al-Karadaghi *et al.*, 1997; Wu *et al.*, 2001). The human enzyme exists as a homodimer. Each subunit contains one [2Fe-2S] cluster. The monomer is folded into two similar domains, each with a four-stranded parallel beta-sheet flanked by an alpha-helix in a beta-alpha-beta motif that is reminiscent of the fold found in the periplasmic binding proteins. The topological similarity between the domains suggests that they have arisen from a gene duplication event. However, significant differences exist between the two domains, including an N-terminal section (residues 80-130) that forms part of the active site pocket, and a C-terminal extension (residues 390-423) that is involved in coordination of the [2Fe-2S] cluster and in stabilization of the homodimer. The [2Fe-2S] cluster ligands are Cys196, Cys403, Cys406 and Cys411. The experiments with Co(II) binding show that His230 and Asp383 are part of the enzyme active site (Wu *et al.*, 2001).

FC seems to have a structurally conserved core region that is common to the enzyme from bacteria, plants and mammals. Porphyrin binds in the identified cleft. This cleft also includes the metal-binding site of the enzyme. It is likely that the structure of the cleft region will have

different conformations upon substrate binding and release (Al-Karadaghi *et al.*, 1997; Medlock *et al*., 2007).

I.5.6 Probability of the Existance of a Complex between Protoporphyrinogen IX Oxidase and Ferrochelatase

Mutations in the different human heme biosynthetic genes cause inherited disorders commonly named porphyrias (Sarkani, 1999). Patients suffering from these genetic inherited diseases accumulate highly toxic intermediates which induce cellular damage via peroxidation of membrane lipids and ultimative cell death. They suffer from cutaneous photosensitivity and develop acute neurovisceral crises (Meissner *et al*., 1996). The disorder connected to the PPO and FC genes are known as variegate porphyria (VP) (Murphy *et al.*, 1986) and erythropoietic porphyria (EP) (Brenner *et al.*, 1992), respectively. The skin is one of the major organs involved in most of these diseases. In EP, porphyrin accumulation causes photosensitivity of the patient. When excited by light, porphyrins generate reactive oxygen species, which cause skin lesions. VP manifests itself with skin lesions and acute neurologic attacks.

In eukaryotic cells PPO binds to the outer surface of the inner mitochondrial membrane while FC is associated with the matrix side. Deduced from the solved PPO- and FC-structures a complex between these two enzymes was proposed to protect the highly toxic intermediate protoporphyrin IX (Koch *et al.,* 2004). It was suggested that possibly CPO, the enzyme catalyzing the previous reaction, is also part of this protein complex. CPO is present in the intermembrane space of mitochondria and is loosly associated with the outside of the inner mitochondrial membrane.

In figure 13, the dashed lines symbolize the channel within the PPO and FC molecules where the substrates are channelled, processed and transported from PPO to ferrochelatase. From left to right, the reaction sequence is shown starting with protoporphyrinogen IX uptake by PPO from CPO (1), reaction to protoporphyrin IX in PPO and channelling to the active site of FC (2), insertion of the iron into protoporphyrin IX resulting in protoheme or heme b (3) and its release into the membrane (4). The channel from PPO to FC is opened towards the membrane at the PPO side of the PPO–FC complex. Here it is possible for molecules to enter or leave the complex. One possibility for the release of heme is that heme leaves through the channel opening of the assembled complex as shown here. Alternatively, the complex that has been described as not very stable by Ferreira and coworkers (1988) and could therefore disassemble after step 2.

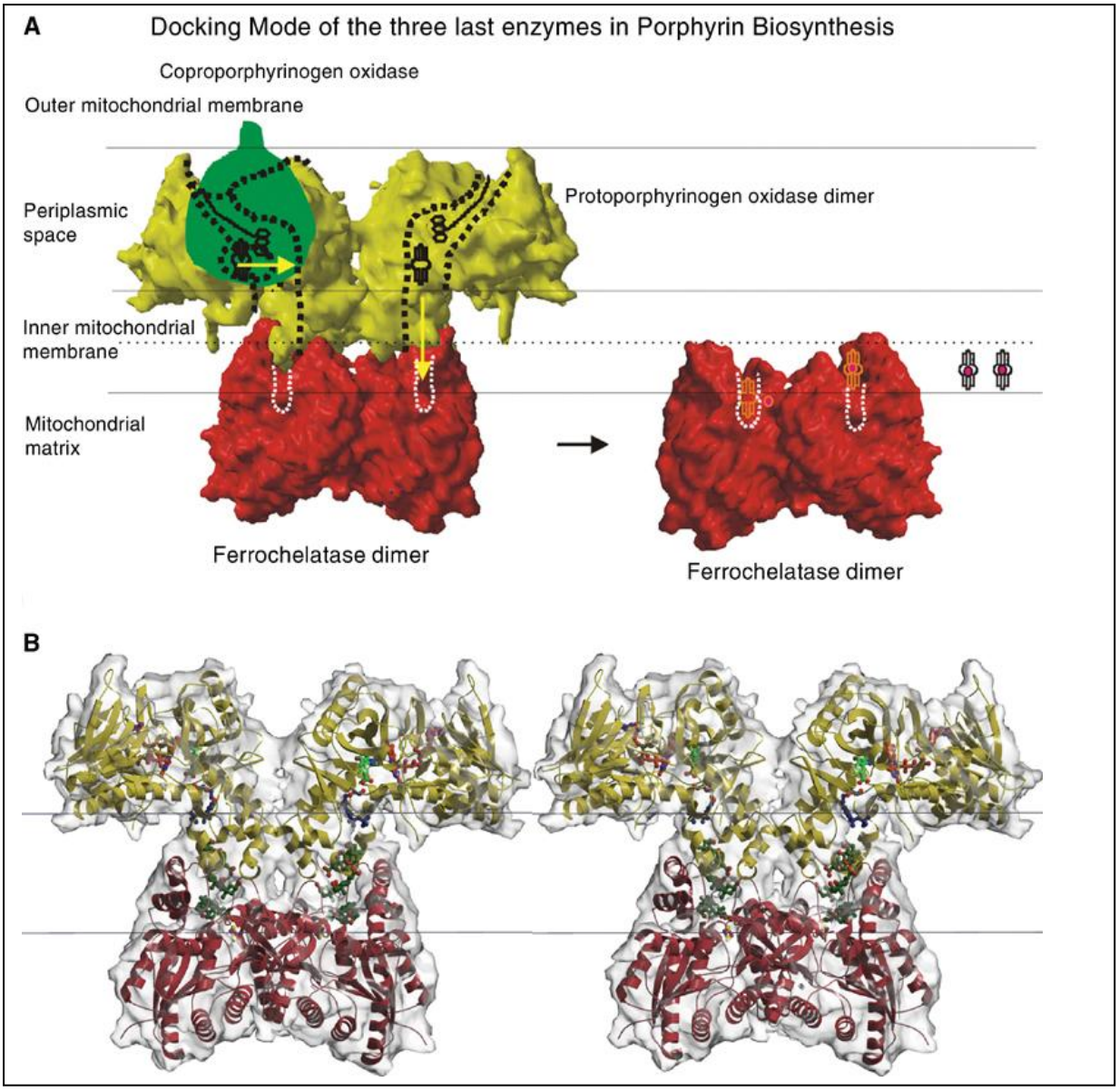

Figure 13: Supposed interaction mode of the last three enzymes in the human mitochondrial heme biosynthesis. (**A**) Localization of coproporphyrinogen III oxidase (Santana *et al*, 2002) (CPO, EC green), PPO (surface of the tobacco structure in yellow) and human ferrochelatase (Wu *et al*, 2001) (FC, red) in the mitochondrial periplasm. (**B**) Stereo-view of the putative PPO–FC complex, the PPO is shown in yellow, FC in red. The channel in the complex is filled with the PPO inhibitor (INH, green) below the cofactor FAD (PPO, red–orange), the detergent molecules Triton X-100 (PPO-part of the channel, blue) and three cholate molecules (FC, olive-green). The inner mitochondrial membrane is symbolized by black lines. (Koch *et al.*, 2004)

I.6 Objectives of the Work

T. elongatus genome does not posses a gene coding for GlnRS. So the first objective of this thesis was to unambiguously identify *T. elongatus* GluRS as a non-discriminating enzyme by biochemical means. For this purpose $tRNA^{Glu}$ and $tRNA^{Gln}$ of *T. elongatus* had to be isolated. Aminoacylation experiments with L-[^{14}C]Glu by purified recombinant *T. elongatus* GluRS i*n vitro* should allow the determination of kinetic parameters characteristic of a non-discriminating GluRS.

The second objective of this work was to proof the existence of the postulated protein complex of the three terminal enzymes in tetrapyrrole biosynthesis consisting of CPO, PPO and FC, respectively. For this purpose these three *T. elongatus* enzymes should be produced recombinantly. Subsequently, antibodies had to be generated against the three purified recombinant proteins. Finally, these antibodies should provide the basis for co-immunoprecipitation and electron microscopic experiments in order to prove the existence of such a complex *in vitro* as well as *in vivo.*

II Materials and Methods

II.1 Instruments and Chemicals

II.1.1 Instruments

Agarose Gel Electrophoresis	Agagel	Biometra
Agarose Gel Documentation	GelDoc	Bio-Rad
Autoclav	LVSY 50/70	Zirbus
Bioreactor	Biostat B2	B. Braun
Blotting	Trans Blot apparatus (semi dry transfer cell)	Bio-Rad
CD Spectropolarimeter	Jasco J810	Jasco
Centrifuges	Centrifuge 5403	Eppendorf
	Centrifuge 5415 C	Eppendorf
	miniSpin	Eppendorf
	L7-65 Ultracentrifuge	Beckmann
	RC 5B Plus	Sorvall
	SpeedVac SPD 110B with Refrigerated Vapor Trap RVT400	Savant
Digital Camera	Camedia C5050	Olympus
DNA Sequencing	ABI PRISM™ 310 Genetic Analyzer	Applied Biosystems
Electroporation	Gene Pulser® II with Pulse Controller Plus	Bio-Rad
Fluorescence Spectrometer	PE LS50B	PerkinElmer
FPLC	Äkta prime™	GE Healthcare
Luminescence Spectrometer	LS50B	PerkinElmer
Mikro- Dismembrator		Braun Biotech
pH Determination	pH-Meter C 6840 B	Schott
Pipettes	LABMATE	Abimed HTL
Protein concentrating Device	Stirred ultrafiltration Cell	Millipore
Scales	BL 1500	Sartorius

	BP 61S	Sartorius
	SBA 52	Scaltec
Scintillation Analyzer	Tri-Carb 2900 TR	PerkinElmer
SDS-PAGE	Mini Protean II	Bio-Rad
Sonication	SONOPLUS	Bandelin electronics
Spectrophotometer	Ultrospec 2000	GE Healthcare
Thermocycler	Tpersonal	Biometra
Thermomixer	Thermomixer compact	Eppendorf
UV-Crosslinker	UV Stratalinker 2400	Stratagene, La Jolla, USA
Water Purification	Synthesis A10	Millipore

II.1.2 Chemicals and Kits

Benzonase	Merck
Bio-Rad Protein Assay	Bio-Rad
Blocking Reagent	Roche
5'-biotinylated, gel-purified DNA oligonucleotides	Biomers.net
Chelating Sepharose™ Fast Flow	GE Healthcare
Crystal Screen™ Crystallization Kit	Hampton Research
Crystal Screen II™ Crystallization Kit	Hampton Research
PEG/ION Screen™ Crystallization Kit	Hampton Research
Crystal Screen Cryo™ Crystallization Kit	Hampton Research
Enzymes for Molecular Biological Applications	GE Healthcare
	Genecraft
	MBI-Fermentas
	NewEngland
	Biolabs, Promega
Glycogen	Invitrogen
L-[^{14}C]Gln	Hartmann Analytic
L-[^{14}C]Glu	Hartmann Analytic
MagneHis™ Ni-Particles	Promega

Mini Dialysis Units (Slide-A-Lyzer)	Pierce
Oligonucleotides	Biomers.net
OptiPhase HiSafe 2 (scintillation cocktail)	PerkinElmer
Polyclonal rabbit α-HemF antibodies	Eurogentec
Polyclonal rabbit α-HemH antibodies	Eurogentec
Polyclonal rabbit α-HemY antibodies	Eurogentec
Protease Inhibitor (Complete, Mini, EDTA-free)	Roche
Protein A Sepharose™ CL-4B	GE Healthcare
Q500 Maxi Kit	Qiagen
QIAquick Gel Extraction Kit	Qiagen
QIAquick nucleotide removal kit	Qiagen
QIAquick PCR Purification Kit	Qiagen
RNaseOut™ Ribonuclease Inhibitor	Invitrogen
Seize® X Protein A Immunoprecipitation Kit	Pierce
Size Standards for Agarose Gels:	
GeneRuler™ DNA Ladder Mix	MBI Fermentas
MassRuler™ DNA Ladder Mix	MBI Fermentas
Size Standards for SDS-PAGE:	
PageRuler Prestained Protein Ladder	MBI Fermentas
Protein Molecular Weight Marker	MBI Fermentas
Dalton Mark VII-L	Sigma
Size Standards for Polyacrylamide / Urea Gels:	
O'GeneRuler™ DNA Ladder Ultra Low Range	MBI Fermentas
GeneRuler™ 50 bp DNA Ladder	MBI Fermentas
Sterile filter	Millipore
Streptavidin-AP-conjugate	IBA BioTAGnology
UltraLink Immobilized Streptavidin	Pierce

Chemicals and reagents not specifically listed here were purchased from the following manufacturers: GE Healthcare, Difco, Fluka, Gerbu, Merck, Pierce, Roth and Sigma.

II.2 Bacterial Strains and Plasmids

All bacterial strains and plasmids used for this study are listed in tables 1 and 2.

Table 1: Strains Used in This Study

Name	Description	Reference or source
Escherichia coli strains		
BL21CodonPlus(DE3)-RIL	F$^-$ *omp*T *hsd*S(r_B- m_B-) *dcm*+ Tet^r *gal* λ(DE3) *end*AHte[*arg*U *ile*Y *leu*W Cam^r]	Novagen
BL21(λDE3)pLysS	F$^-$*ompT hsdS*$_B$($r_B^-m_B$) *gal dcm* λ(DE3) pLysS (Cam^R)	Stratagene
DH10B	F- *mcrA* Δ(mrr-*hsd*RMS-*mcr*BC) Φ80*lac*ZΔM15 Δ*lac*X74 *deo*R *rec*A1 *end*A1 *ara*D139 Δ(*ara*, *leu*)7697 *gal*U *gal*K λ- *rps*L (StrR) *nup*G	Gibco Life Technologies
Thermosynechococcus elongatus strain		
BP-1	Wild type	Berlin university Dr. Athina Zouni

Table 2: Plasmids Used in This Study

Plasmid designation	Description	Reference or source
pET-22b*hemF*TE	pET-22b(+), codes for a C-terminal fusion of His_6-tag with HemF from *T. elongatus*	Dr. Daniela Breckau Ph.D thesis
pET-32a(+)	Expression vector, T7 promoter, *Amp^r*	Novagen
pET-32a*hemH*TE	pET-32a(+), codes for a N- and C-terminal fusion of His_6-tag with HemH from *T. elongatus*	This work
pET-32a*hemY*TE	pET-32a(+), codes for a N- and C-terminal fusion of His_6-tag with HemY from *T. elongatus*	This work

pACYCDuet-1*hemH* TE	pACYCDuet-1, codes for a N-terminal fusion of His_6-tag with HemH from *T. elongatus*	This work
pTe*RS*	pET-29-Derivative, codes for a C-terminal fusion of His_6-tag with GluRS from *T. elongatus*	Dr. Jörg O. Schulze PhD thesis

II.3 Growth Media and Media Additives

II.3.1 Media for *Escherichia coli* and *Thermosynechococcus elongatus* Growth

As a standard medium for growth of all bacterial strains, Luria Bertani (LB) medium (Sambrook *et al.*, 1989) was used unless indicated otherwise. For solid media 1.5 % (w/v) agar-agar was added prior to sterilisation.

LB medium	Tryptone	10.0	g
	Yeast extract	5.0	g
	NaCl	5.0	g
	H_2O_{deion}	ad 1.0	l

For *T. elongatus* cultivation D-Medium supplemented with micronutrients was used.

D medium	Titriplex III	0.19	g
	$MgSO_4$ x 7 H_2O	0.10	g
	KNO_3	0.10	g
	$NaNO_3$	0.69	g
	Na_2HPO_4 x 2 H_2O	0.14	g
	$CaCl_2$ x 6 H_2O	0.08	g
	NaCl	0.008	g
	H_2O_{deion}	ad 1.0	l
after filtration, addition of:	$NaHCO_3$	5.0	g
	$FeCl_3$ x 6 H_2O	0.001	g
	Micronutrients stock solution (2000x)	0.5	ml

titrated with NaOH to pH 7.5-7.8

Micronutrients stock solution (2000x)	H_2SO_4 concentrated	0.5	ml
	$MnSO_4$ x 1 H_2O	2.28	g
	$ZnSO_4$ x 7 H_2O	0.5	g
	H_3BO_3	0.5	g
	$CuSO_4$ x 5 H_2O	0.025	g
	Na_2MoO_4 x 2 H_20	0.025	g
	$CoCl_2$ x 6 H_20	0.045	g
	H_2O_{deion}	ad 1.0	l

II.3.2 Additives

Antibiotics and other additives were prepared as concentrated stock solutions, sterilized by filtration and added after autoclaving to the chilled medium. For light sensitive additives such as tetracycline, incubation occurred in the dark. Solutes and concentrations are summarized in the next table.

Substances	Solute	Concentration of stock solution		Final concentration in growth medium	
Ampicillin	H_2O_{deion}	100.0	mg/ml	100.0	µg/ml
Chloramphenicol	Ethanol 70 % (v/v)	34.0	mg/ml	34.0	µg/ml
IPTG	H_2O_{deion}	1.0	M	0.5	mM
Kanamycin	H_2O_{deion}	10.0	mg/ml	30.0	µg/ml
Riboflavin	H_2O_{deion}	0.5	mg/ml	5.0	µg/l
Tetracycline	Ethanol 70 % (v/v)	5.0	mg/ml	10.0	µg/ml

II.4 Microbiological Techniques

II.4.1 Sterilisation

Unless otherwise noted, all media were vapour sterilized at 121 °C and 1 bar positive pressure for

20 min. Other substances and solutions were either vapour sterilized or, if temperature sensitive, sterilized by filtration (pore width of the filter was 0.2 µm). Work surfaces were desinfected using 70 % (v/v) ethanol.

II.4.2 Growth of Bacteria

II.4.2.1 *Escherichia coli* Cultivation

II.4.2.1.1 Liquid Cultures

Aerobic liquid pre-cultures (volume 3 - 5 ml) were inoculated using a single colony from a LB agar plate. The medium was supplemented with the appropriate antibiotics where required. Pre-cultures were shaken at 180 - 200 rpm in test tubes over night at 37 °C. Cultures of 300 - 500 ml were inoculated with 1% (v/v) of the precultures. The incubation times varied according to the desired optical densities. For protein production, after induction of gene expression cultures were incubated at 25 °C or 37 °C for indicated intervalls.

II.4.2.1.2 Plate Cultures

Agar plates were utilized for plating 50 - 100 µl of a bacterial cell suspension with a Drygalski spatula, for streaking cells from another plate with an inoculating loop or a single colony from another plate with a sterile toothpick or pipette tip. They were incubated overnight at 37 °C.

II.4.2.2 Large - Scale Cultivation of *T. elongatus* in a 5 l - Bioreactor

T. elongatus BP1 cells were cultivated in a 5 – liter bioreactor (Braun Biotech; Melsungen; Germany) at 55 °C with continuous illumination using fluorescent white lamps (~80 µmol of photons $m^{-2}s^{-1}$). The cells were grown in D-Medium supplemented with micronutrients at pH 7.5-7.8 in an CO_2-enriched atmosphere of 10 % for circa 4 days to an OD_{700} of 2.0.

II.4.3 Determination of Cell Density

The cell densities of *E. coli* liquid cultures were determined by measuring the optical density at a wavelength of 595 nm (OD_{595nm}). For cell densities with an $OD_{595nm} \geq 0.6$, dilutions of the cell

culture broth were prepared before measurement. An OD_{595nm} of 1 corresponded to approximately 1 x 10^9 cells ml^{-1}.

In batch cultivations of *T. elongatus*, the cell density of the culture was determined by measuring the optical density at a wavelength of 700 nm (OD_{700nm}). For cell densities with an $OD_{700nm} > 0.6$, dilutions of the cell culture broth were prepared before the measurement. A correlation between OD_{700nm} and cell dry weight (CDW) was determined: $OD_{700} = 2.0$ equals 1.4 g cells l^{-1}.

II.4.4 Storage of Bacteria

E. coli strains were kept on agar plates at 4 °C for up to four weeks. For long-term storage glycerol stocks were prepared. This was done by growing a culture for 6 to 8 h, cooling it on ice for 30 min and mixing of the culture with sterile glycerol (80% (v/v) (final concentration of 30% glycerol). Stocks were immediately frozen and kept at -80 °C.

T. elongatus cells were harvested by centrifugation (5000 x g, for 20 min) and frozen at -80 °C.

II.5 Molecular Biology Techniques

Protocols employed in this study are generally based on the methods described by Sambrook *et al.* (2001). Modifications of these denoted methods will be described below.

II.5.1 Preparation of Plasmid DNA from *Escherichia coli*

2 ml of an overnight culture were harvested by centrifugation (3 min, 14000 x g) and the cell pellet resuspended in 300 µl of buffer P1. Approximatly 300 µl of buffer P2 were added, the sample carefully mixed by inverting the tube and incubated at room temperature for 5 min. Then 300 µl of buffer P3 were added, the sample again carefully inverted and incubated on ice for another 5 min. After centrifugation (15 min at 15000 g and 4 °C) 800 µl of the supernatant were added to 560 µl isopropanol in a fresh tube. Precipitation of plasmid DNA was allowed to proceed during a 10 min incubation step at 4 °C, followed by a 30 min centrifugation step also at 4 °C (15000 x g). The DNA pellet was washed once with 70% (v/v) ethanol. Finally, the DNA precipitate was dried and dissolved in 50 - 100 µl H_2O_{deion} or TE buffer.

Buffer P1	Tris-HCl (pH 8.0)	50.0	mM
	EDTA	10.0	mM
	RNase A	100.0	mg/l

Buffer P2	NaOH	200.0	mM
	SDS	1.0%	(w/v)
Buffer P3 (pH 5.5)	KOAc	3.0	M
Buffer TE	Tris-HCl (pH 8.0)	50.0	mM
	EDTA	10.0	mM
	dissolved in H_2O_{deion}		

II.5.2 Determination of DNA Concentration

The concentration and purity of a DNA solution was determined by measuring the absorbance at 260 nm and additionally at 280 nm to account for protein impurities by an Ultrospec 2000-Photometer. For a pure DNA solution an A_{260} of 1 corresponds to a dsDNA concentration of 50 µg/ml. The puritiy of DNA solution can be deduced from the ratio of A_{260} to A_{280}. With A_{260}/A_{280} = 1.8 - 2.0 the DNA can be considered as pure.

For determination of the prepared plasmid DNA concentration and purity, the plasmid was linearized enzymatically and visualized by agarose gel electrophoresis (see II.5.4).

II.5.3 Agarose Gel Electrophoresis

For analytical separation of DNA fragments, agarose gels consisting of 0.7 to 1 % (w/v) agarose in TAE buffer were prepared. The DNA samples were mixed with 6 x loading dye to facilitate loading and to indicate the progress of the samples in the gel. GeneRuler™ DNA Ladder Mix or MassRuler™ DNA Ladder Mix (MBI Fermentas; St. Leon-Rot; Germany) were used as size standards according to the manufacturer's instructions. Depending on the size of the gel, a voltage of 80-100 V was applied. The DNA fragments migrate towards the positive anode with a velocity that is proportional to the negative logarithm of their length. After electrophoresis, gels were incubated in an 0.1% ethidium bromide solution for 10 min and briefly rinsed with H_2O. The DNA was detected via its fluorescence under UV light (λ = 312 nm).

TAE buffer	Tris-acetate (pH 8.0)	40.0	mM
	EDTA	1.0	mM
6 x DNA loading dye	Bromophenol blue	350.0	µM
	Xylene cyanol FF	450.0	µM
	Glycerol	50.0%	(w/v)

	dissolved in H_2O_{deion}		
Ethidium bromide solution	Ethidium bromide dissolved in H_2O_{deion}	0.1%	(w/v)

II.5.4 Amplification of DNA by Polymerase Chain Reaction (PCR)

Oligonucleotide primers for the PCR based amplification of the *hemY* and *hemH* genes from *T. elongatus* for the subsequent cloning into expression vector pET-32a(+) were designed. Recognition sequences for restriction endonucleases were inserted via these primers at both ends of the generates PCR fragments. All oligonucleotide primers are listed below. Recognition sequences of restriction endonucleases are underlined. Primers were purchased from MWG Biotech AG (Ebersberg; Germany) or biomers.net GmbH (Ulm; Germany).

Primer designation	Primer sequence (5' – 3')
T.elon.hemYEcoRI	CCGGAATTCCGGGTGATTGAGGTAGATGTTGC
T.elonhemYXhoIrev	CCGCTCGAGCGGCTAGGACTGGCCTCCTGCAAG
hemH T.e.EcoRI	CCGGAATTCCGGGTGATTTTGGGAATGGCGAGCC
hemH T.e.rev XhoI	CCGCTCGAGCGGACTGATGAGTTCAATCATCAAC

T. elongatus *hemY* (1404 bp) was amplified using primers T.elon.hemYEcoRI and T.elonhemYXhoIrev. T.elongatus *hemH* (1179 bp) was amplified using primers hemH T.e.EcoRI and hemH T.e.rev XhoI. Both were cloned after restriction digest in the appropreately cut pET-32a.

II.5.4.2 PCR Reaction Conditions

Taq DNA polymerase (GE Healthcare) was used for all reactions. A standard reaction was composed as listed below.

Standard PCR composition

Template DNA	200 ng
Forward primer	50 pmol
Reverse primer	50 pmol

10 x reaction buffer	5 µl
dNTPs (2 mM)	5 µl
Taq polymerase	2.5 U
H_2O_{deion}	ad 50 µl

After an initial DNA denaturation step, 30 cycles consisting of denaturation, primer annealing and primer elongation step were performed and the reaction terminated by a final elongation step. The denaturation temperature of 95 °C and the elongation temperature of 72 °C remained unchanged. The annealing temperature depended on oligonucleotide length and G+C content and was furthermore influenced by the insertion of mismatches. The annealing temprature was calculated as follows:

$$Tm\ [°C] = 69.3 + 0.41\ (\%\ G+C) - 650/n$$

%G+C represents the G+C content of the primer in % and *n* represents the number of nucleotides. The 10 x reaction buffer was supplied by taq polymerase manufacturer (GE Healthcare).

The duration of the elongation step is chosen according to the length of the DNA fragment to be amplified. To search for the perfect annealing temperature the PCR reaction was done in a gradient cycler. The enzyme Taq polymerase inserts approximately 1000 nucleotides per minute.

Standard Thermocycle program:

Denaturation	95°C	5 min	
Denaturation	95°C	60 s	30x
Annealing	T_m [°C]	60 s	
Elongation	72°C	60 s	
Elongation	72°C	10 min	

After the PCR reaction, an aliquot of the reaction mixture was analyzed by agarose gel electrophoresis. If only one PCR product was detected in the gel, the entire sample was subjected to purification with the QIAquick PCR Purification Kit (Qiagen; Hilden; Germany). If more than one PCR product was visible in the gel, the entire reaction mixture was separated electrophoretically. The DNA fragment of interest was then excised from the gel and purified using the QIAquick Gel Extraction Kit (Qiagen; Hilden; Germany). All kits were used according to the manufacturer's instructions.

II.5.5 Enzymatic Modification of DNA

II.5.5.1 Cutting DNA with Restriction Endonucleases

Restriction of DNA (vectors and PCR products) was carried out using restriction endonucleases purchased from New England BioLabs (NEB; Ipswich; USA) or MBI Fermentas (MBI Fermentas; St. Leon-Rot; Germany). Reaction buffers, concentrations of enzymes and DNA as well as incubation temperatures were chosen according to the manufacturer's instructions. The digestion was allowed to proceed for up to 16 h and was followed by heat inactivation of the restriction endonucleases (20 min at 65 °C or 80 °C, depending on the enzyme).

II.5.5.2 Ligation of DNA

In order to avoid re-circularization of digested vector DNA, the 5'-phosphate groups of linearized vectors were removed prior to the ligation reaction. The dephosphorylation was achieved by adding 1 U /µg DNA shrimp alkaline phosphatase (Promega; Mannheim; Germany) to the sample immediately after endonuclease based restriction and incubation at 37 °C for 15 - 30 min, followed by heat inactivation for 15 min at 65 °C. The DNA was purified using the gel extraction purification kit (QIAgen; Hilden; Germany) following the manufacturer's instruction.
Ligation of DNA was carried out using the Takara Kit (Takara Bio; Japan) or T4 DNA ligase (MBI Fermentas) in a reaction buffer supplied by the manufacturer. Approximately 30 - 60 ng of vector DNA were used and insert DNA was added in excess. Insert to vector ratio with regard to molar concentrations were 1 : 1 to 10 : 1. Usually, 200 U of T4 DNA ligase were added and the reaction incubated overnight at 4 °C.

II.5.6 DNA-Sequencing

Cloning experiments were confirmed by sequence determination of the respective created DNA construct after transformation of competent *E. coli* cells and plasmid preparation. The correct sequences of *T. elongatus hemY* and *T. elongatus hemH* and their correct insertions into the vector pET-32a(+) were conducted on an ABI PRISM 310 Genetic Analyzer (Applied Biosystems; PerkinElmer; Rodgau - Jügesheim; Germany) after the instructions of the manufacturer. The analysis of all sequencing results was done using the software Lasergene 6 (GATC Biotech; Konstanz; Germany).

II.5.7 Transformation of Bacteria

II.5.7.1 Transformation of *Escherichia coli* by Electroporation

Starting out from an individual *E. coli* colony a 5 ml overnight culture was inoculated. This culture was used to inoculate 500 ml of LB medium. The bacteria were incubated at 37°C and 200 rpm in baffled flasks until the culture reached an OD_{595nm} of 0.6. After cooling the cultures in ice water for 15 min, the cells were harvested by centrifugation (4500 x g; 15 min; 4°C). Then, the cell pellet was washed twice with 20 ml of ice-cold water (4500 x g; 8 min; 4°C) and resuspended in 20 ml of 10 % (v/v) glycerol. With a further centrifugation step (4500 x g; 8 min; 4°C), the obtained cell pellet was redissolved in 500 - 1000 µl of 10 % (w/v) glycerol. Competent cells were either used directly for transformation experiments or frozen at -80°C.

Competent *E. coli* cells were transformed with dialyzed ligation reactions by electroporation with a Gene Pulser™ apparatus (Bio-Rad; Munich; Germany). For this purpose, plasmid DNA was mixed with 50 µl of competent *E. coli* cells in a 2 mm electroporation cuvette. The electroporation was carried out in the Gene Pulser™ at settings of 2.5 kV at 25 µF and 200 Ω. The transformed cells were regenerated by incubation in 1 ml of LB medium at 37°C and soft shaking for 1 h. Depending on the expected colony density, different volumes were then applied on LB agar plates containing the appropriate antibiotics and plates incubated overnight at 37 °C.

II.5.7.2 Transformation of *Escherichia coli* Cells by the $CaCl_2$ Method

From an individual colony of *E. coli*, a 5 ml overnight culture was inoculated. This culture was used to inoculate 100 ml of LB medium in a ratio of 1 : 100. The bacteria were incubated at 37°C and 200 rpm in baffled flasks until the culture reached an OD_{595nm} of 0.8. After cooling the cultures in ice water for 10 min, the cells were harvested by centrifugation (4500 x g; 15 min; 4°C). After resuspension of the cells in 10 ml of ice-cold 100 mM $CaCl_2$/10% (w/v) glycerol the cell solution was again cooled for 15 min in ice water. After centrifugation (4500 x g; 10 min; 4°C), the cells were resuspended in 1 ml of ice-cold 100 mM $CaCl_2$/10 % (w/v) glycerol. The competent cells were either used directly for transformation or frozen at -80°C.

An aliquot of plasmid DNA was mixed with 50 µl of competent *E. coli* cells in a sterile reaction tube and was placed on ice for 20 min. After heating the cells for 45 s at 42°C, the cells were cooled down on ice for 2 min. To regenerate the transformed cells, they were further incubated in 250 µl of LB medium at 37°C and soft shaking for 1 h. The transformation reaction was streaked

out on a LB agar plate including the corresponded antibiotics. The plate was incubated overnight at 37°C.

II.5.7.3 Transformation of *Escherichia coli* Cells by Rubidium Chloride

From an individual colony of *E. coli* a 5 ml overnight culture was inoculated. Subsequently 2.5 ml culture was used to inoculate 250 ml of LB medium containing 20 mM $MgSO_4$ in a ratio of 1 : 100. The bacteria were incubated at 37°C and 200 rpm in baffled flasks until the culture reached an OD_{595nm} of 0.6. The cells were harvested by centrifugation (4500 x g; 10 min; 4 °C). The cells were resuspended in 100 ml of ice-cold TFB1 and then the cell solution was cooled for 5 min in ice water. After centrifugation (4500 x g, 5 min, 4 °C), the cells were resuspended in 10 ml of the original culture volume of ice-cold TFB2. The competent cells were incubated on ice for 15 - 60 min and then either used directly for transformation or frozen at -80°C. For transformation an aliquote of plasmid DNA was mixed with 50 µl of competent *E. coli* cells in a sterile reaction tube and was placed on ice for 20 min. After heating the cells for 45 s at 42 °C, the cells were cooled down on ice for 2 min. To regenerate the transformed cells, they were incubated in 250 µl of LB medium at 37 °C and gentle shaking for 1 h. The transformation volume was streaked out on a LB agar plate including the corresponded antibiotics. The plate was incubated overnight at 37 °C.

TFB1	CH_3COOK	30.0	mM
	$CaCl_2$	10.0	mM
	$MnCl_2$	50.0	mM
	RbCl	100.0	mM
	Glycerol	15.0%	(w/v)
	dissolved in H_2O_{deion}		

titrated with acetic acid to pH 5.8 and filter sterilized

TFB2	MOPS	10.0	mM
	$CaCl_2$	10.0	mM
	RbCl	10.0	mM
	Glycerol	15.0%	(w/v)
	dissolved in H_2O_{deion}		

titrated with KOH to pH 6.5 and filter sterilized.

II.6 Biochemical Methods

II.6.1 Recombinant Production and Purification of *Thermosynechococcus elongatus* GluRS

II.6.1.1 Cell Growth for Protein Production

Recombinant *T. elongatus* GluRS was produced as a His-tag fusion protein in *E. coli* BL21 Codon-Plus(DE3)-RIL cells carrying vector pTe*RS*. Protein production was induced at A_{595} of 0.6 with the addition of 200 µM isopropyl-1-thio-ß-D-galactopyranoside (IPTG) to the LB medium including 30 µg/ml kanamycin (kan) and 34 µg/ml chloramphenicol (cm). After induction of gene expression, cells were grown overnight at 20 °C. The cells were subsequently harvested by centrifugation (15 min, at 4500 x g and 4 ^{o}C).

II.6.1.2 Cell Disruption

The cell sediment obtained by centrifugation of 1 liter culture was resuspended in 15 ml lysis buffer (see II.6.2.3.1). Cells were disrupted by sonication (SONOPLUS; Bandelin electronics; Berlin; Germany) 5 times for 3 min with 50% cycle and 70% power with breaks of 5 min by MS 73 tip, and the insoluble protein fraction was removed by ultracentrifugation at 50000 rpm (Beckman Ultrazentrifuge, Rotor: Ti 70.1) for 45 min at 4. The obtained clear cell-free extract was separated from the pelleted cell debris and further filterated through a 0.2 µM sterile filter. The extract was then either detectly used for further experiments or stored at -20 ^{o}C.

II.6.1.3 Purification of *Thermosynechococcus elongatus* GluRS Using Affinity Chromatography on Ni-Nta-Sepharose

A 5 ml Ni-Nta-Sepharose column (GE Healthcare) was equilibrated with 30 ml of lysis buffer. After loading 15 ml *E. coli* cell-free extract containing the overproduced GluRS (flow rate 0.5 ml/min), the column was washed with 40 ml wash buffer to remove unbound proteins (flow rate 1 ml/min). Bound proteins were eluted using 20 ml wash buffers containing 100, 125, 200, 300 and 1000 mM imidazole. The eluate was collected in 5 ml fractions. Fractions containing GluRS were identified by SDS-PAGE and then GluRS solution was dialyzed against dialysis buffer.

Lysis Buffer	HEPES pH 8.0	20.0	mM
	NaCl	300.0	mM

	Imidazole	10.0	mM
	ß-Mercaptoethanol	10.0	mM
	Complete Protease Inhibitor	1.0	tablet
Wash buffer	HEPES pH 8.0	20.0	mM
	NaCl	300.0	mM
	ß-Mercaptoethanol	10.0	mM
	Complete Protease Inhibitor	1.0	tablet
Dialysis buffer	HEPES pH 7.5	50.0	mM
	KCl	25.0	mM
	$MgCl_2$	15.0	mM
	DTT	5.0	mM

II.6.2 Recombinant Production and Purification of *Thermosynechococcus elongatus* HemF

II.6.2.1 *Escherichia coli* Cell Growth for Protein Production

Recombinant *T. elongatus* HemF was produced as a His-tag fusion protein in *E. coli* BL21(λDE3)-pLysS cells carrying vector pET-22b*hemF*TE. Protein production was induced at A_{595} of 0.6 with 500 µM IPTG to LB medium including 100 µg/ml ampicillin (amp) and 34 µg/ml chloramphenocol (cm). After induction, cells were grown 4 hours at 37 °C. The cells were subsequently harvested by centrifugation (15 min, at 4500 x g and 4 ^{o}C).

II.6.2.2 Cell Disruption

The cell sediment of a 2 liter culture was resuspended in 10 ml Buffer A (II.6.2.3.1). Cells were disrupted by sonication (SONOPLUS; Bandelin electronics; Berlin; Germany) 3 times for 5 min with 50% cycle and 70% power with breaks of 5 min by MS 73 tip, and the insoluble protein fraction and cell debris were removed by ultracentrifugation at 50000 rpm (Beckman Ultrazentrifuge, Rotor: Ti 70.1) for 45 min at 4 ^{o}C. The obtained clear cell-free extract was separated from the pelleted cell debris and further filtrated through a 0.2 µM sterile filter. The extract was then used for further experiments.

II.6.2.3 Affinity Chromatography Using Ni-Nta-Sepharose

A 5 ml Ni-Nta-Sepharose column (GE Healthcare; Freiburg; Germany) was washed with 25 ml of H_2O_{deion} and then was equilibrated with 25-30 ml of buffer A. After loading the column with cell free extract containing the desired HemF protein. (flow rate 0.5 ml/min), the column was washed with 30 ml of buffer A to remove unbound proteins (flow rate 1 ml/min). Bound proteins were eluted using a 50 ml linear gradient of 10 - 500 mM imidazole in buffer A (i.e. 0 - 50% buffer B) at a flow rate of 1 ml/min. The eluate was collected in 1 ml fractions. Fractions containing HemF were identified by SDS-PAGE and determination of activity.

Buffer A	Tris pH 8.0	20.0	mM
	NaCl	350.0	mM
	Imidazole	10.0	mM
	Triton ®X-100	0.2%	(w/v)
Buffer B	Tris pH 8.0	20.0	mM
	NaCl	500.0	mM
	Imidazole	1.0	M
	Triton ®X-100	0.2%	(w/v)

II.6.3 Recombinant Production and Purification of *Thermosynechococcus elongatus* HemY

II.6.3.1 Cell Growth for Protein Production

Recombinant *T. elongatus* HemY was produced as a His-tag fusion protein in *E. coli* BL21-Codon-Plus(DE3)-RIL cells carrying vector pET32-a*hemY*TE. Protein production was induced at A_{595} of 0.6 – 0.8 with 500 µM IPTG, riboflavin 5 µg/l and additional ampicillin to 100 µg/ml and 34 µg/ml chloramphenicol. After induction of gene expression, cells were grown overnight at 25 °C. The cells were subsequently harvested by centrifugation (15 min, at 4500 x g and 4 °C).

II.6.3.2 *Escherichia coli* Cell Disruption and Recombinant HemY Purification

The cells from 500 ml culture were disrupted by incubation in 50 ml lysis buffer and soft shaking for 30 min and then by sonication (SONOPLUS; Bandelin electronics; Berlin; Germany) 1 - 2 times for 5 min with 50% cycle and 70% power with breaks of 5 min by MS 73 tip. Purification was performed using the Magne His™ Ni-Particles (Promega; Mannheim; Germany) with the wash buffer and elution buffer according to the manufacturer's instructions.

Lysis buffer	Tris pH 8.0	50.0	mM
	$MgCl_2$	10.0	mM
	NaCl	350.0	mM
	Triton ®X-100	0.5%	(w/v)
	NP-40	0.5%	(w/v)
	Benzonase (10,000 u/ml)	0.1%	(v/v)
	RNaseA (10 mg/ml)	0.1%	(v/v)
	Tween 80	0.05%	(w/v)
	Lyzosyme from hen egg white	8.0	mg/ml
Wash buffer	HEPES buffer pH 7.5	100.0	mM
	NaCl	500.0	mM
	Imidazole	10.0	mM
	Triton ®X-100	0.2 %	(w/v)
Elution buffer	Tris pH 8.0	20.0	mM
	NaCl	500.0	mM
	Triton ®X-100	0.2 %	(w/v)
	Imidazole	1.0	M

II.6.3.3 Dialysis for Buffer Exchange

Buffer exchange was achieved at 4 °C using dialysis membranes with a molecular cut off of 14000 kDa. Approximately 5-10 ml of protein solutions were dialyzed overnight (approx. 14 h) against 1 liter of dialysis buffer. The resulting pellet, containing denatured proteins, was removed by centrifugation (15 min, at 10000 x g and 4 ^{o}C).

Dialysis buffer	Tris pH 8.0	20.0	mM
	NaCl	50.0	mM
	Triton ®X-100	0.1 %	(w/v)

II.6.4 Recombinant Production and Purification of *Thermosynechococcus elongatus* HemH

II.6.4.1 Cell Growth for Protein Production

Recombinant *T. elongatus* HemH was produced as a His-tag fusion protein in *E. coli* BL21-Codon-Plus(DE3)-RIL cells carrying vector pET-32a*hemH*TE. Protein production was induced at A_{595} of 0.6 with IPTG (final concentration 500 µM) including 100 µg/ml ampicillin, 34 µg/ml chloramphenicol. After induction of gene expression, cells were grown at 37 °C for 2.5 hours. Medium was exchanged by centrifugation at 4500 x g for 15 min to remove IPTG. The cells were washed by LB again a second time. After centrifugation at 4500 x g for 15 min, LB medium including 100 µg/ml ampicillin, 34 µg/ml chloramphenicol and 10 µg/ml tetracycline was added to cells, and cells were incubated further overnight at 25 ^{o}C in order to allow proper protein refolding when protein synthesis is arrested (Carrio and Villaverde, 2001).

II.6.4.2 Cell Disruption and Purification

The cell sediment obtained by centrifugation of 1 liter culture was resuspended in 5 - 8 ml binding buffer. To avoid protein degradation by intracellular host proteases, protease inhibitor (Complete Mini EDTA-free; Roche; Mannheim; Germany) was used as described in the manufacturer's manual. The cells were disrupted by sonication (SONOPLUS; Bandelin electronics; Berlin; Germany) 3 times for 5 min with 50% cycle and 70% power with breaks of 5 min using MS 73 tip. The insoluble protein fraction was removed by ultracentrifugation at 50000 rpm (Beckman Ultrazentrifuge, Rotor: Ti 70.1) for 30 min at 4 ^{o}C. The pellet was resuspended in binding buffer and sonicated for three times. The supernatants were collected and purified by cobalt sepharose chromatography manually. Also 1 ml of 6 M urea buffer was added to the insoluble fraction in order to completely unfold HemH from inclusion bodies. This denatured HemH preparation was used for α-HemH antibody production in rabbit.

II.6.4.3 HemH Purification Using Affinity Chromatography on Cobalt Sepharose

A 10 ml Poly-Prep chromatography column (Bio-Rad; Munich; Germany) was packed with 3 ml of Chelating Sepharose^{TM} Fast Flow (GE Healthcare; Freiburg; Germany). The material was first loaded with two column volumes (CV) of 100 mM of Co_2SO_4 and subsequently equilibrated with 5 CV of H_2O_{deion} followed by 5 CV of binding buffer. The supernatants containing the soluble proteins were loaded onto the prepared affinity column. Alternatively, the prior prepared column material was incubated with the protein solution in a batch process with soft shaking for 1 h at

4°C. Then column material was washed with 3 CV of binding buffer. Proteins were step-eluted at different imidazole concentrations of 50, 150, 250, and 500 mM in washing buffer. An aliquot of 500 µl of each fraction was collected. Fractions containing HemH were identified by SDS-PAGE.

Binding buffer	Tris pH 8.0	50.0	mM
	KCl	150.0	mM
	Triton ®X-100	0.2 %	(w/v)
Elution buffer	Tris pH 8.0	50.0	mM
	KCl	150.0	mM
	Triton ®X-100	0.2 %	(w/v)
	Imidazole	50.0 – 500.0	mM

II.6.5 Concentration of HemY by Ultrafiltration

Several trials to concentrate *T. elongatus* HemY by stirred ultrafiltration cells with a YM30 membrane (Millipore; USA) at 3 x 10^5 Pa or vivaspin concentrator (Vivascience; Germany) failed. Therefore, a classical concentration via DEAE sepharose column was performed.

II.6.5.1 Concentration of HemY by DEAE Sepharose Chromatography

A Poly-Prep chromatography column (Bio-Rad; Munich; Germany) was packed with 1 ml of DEAE Sepharose™ Fast Flow (GE Healthcare; Freiburg; Germany). The material was first equilibrated with 5 CV of H_2O_{deion} followed by 5 CV of equilibration buffer. The supernatant containing soluble HemY after dialysis and centrifugation was loaded onto the prepared chromatography column. The column material was washed with 5 CV of equilibration buffer. Proteins were eluted with 3 - 5 ml elution buffer. An aliquot of 500 µl of each fraction was collected. Fractions containing concentrated HemY were identified by SDS-PAGE.

Equilibrating buffer	Tris pH 8.0	20.0	mM
	NaCl	50.0	mM
	Triton ®X-100	0.2 %	(w/v)
	$MgCl_2$	5.0	mM
Elution buffer	Tris pH 8.0	20.0	mM
	NaCl	1.0	M

Triton ®X-100	0.2 %	(w/v)
$MgCl_2$	5.0	mM

II.6.6 Determination of Protein Concentration

II.6.6.1 Bicinchoninic Acid Protein Assay

An alkaline solution containing Cu^{2+} and bicinchoninic acid (BCA) was used in this assay. In an alkaline solution proteins act on copper ion. The formation of a Cu^{2+}-protein complex under alkaline conditions, followed by reduction of the Cu^{2+} to Cu^{+} is observed. The degree of Cu^{2+} reduction is proportional to the amount protein present. The reduction of alkaline Cu^{2+} by proteins at absorbance maximum 562 nm. A series of BSA dilution, each containing a known amount of protein, as standard was made. The outlined assay with these standard solutions and the unknown protein sample was performed and their absorbances measured. After creating the standard curve, the amount of protein in the standard with the amount of protein in the sample was calculated.

II.6.6.2 Photometric Determination of Protein Concentration

Extinction coefficient of a protein at 280 nm can determined from the protein sequence by the method of Gill and van Hippel :

$\varepsilon_{280} = (nTrp \cdot 5'690 + nTyr \cdot 1'280 + nCys \cdot 120) \cdot M^{-1}cm^{-1}$

n_x = Number of partial amino acids in protein

ε_{280} = Molar extinction coefficient in 280 nm

After measuring OD_{280} by Ultrospec 2000-Photometer, protein concentration (c) was calculated based on this equation :

$c\ [mg/ml] = M_r \cdot A_{280}/\varepsilon_{280} \cdot d$

d = Diameter of cuvette [cm]

II.6.7 Determination of HemY Activity

In HemY activity assay first coproporphyrinogen (corprogen) III was converted into protoporphyrinogen (protogen) IX by the HemF activity. Protogen IX was subsequently oxidized to protoporphyrin (proto) IX by the addition of HemY. Excitation of the product proto IX at a wavelength of 409 nm resulted in an emission at 633 nm which was detected fluorimetrically and

was clearly distinguishable from protogen as this substance reveals no fluorimetric properties. The substrate protogen was obtained through the reduction of proto according to a modified instruction of Sano and Granick (1961). Approximately, 0.85 mg (500 µM) proto were dissolved in 3 ml 10 mM KOH, 20% ethanol in a stream of N_2 and reduced with freshly prepared 6 g of 3% Na-amalgam. When the solution had lost its color after incubation for no longer than 2 min at 80 °C, it was filtered through glass wool. DTT (50.0 mM) was added and the pH was adjusted to 7-8 with 20% (v/v) phosphoric acid. The protogen IX solutions were aliquoted anaerobically and stored in the dark at -20 °C to avoid autooxydation of the substrate by oxygen as well as of light.
The standard assay mixture contained 334 nM recombinant purified *T. elongatus* HemF and 20 µM coprogen in kinetic buffer in a total volume of 300 µl. The mixture was incubated at 37 °C for 30 min under rigorous shaking at 1000 rpm in the dark. Reactions were continued by the addition of 0.5 µM (final concentration) *T. elongatus* HemY or H_2O_2 (as control reaction) to oxidize generated protogen. After 10 min of oxidation, the amount of enzymatically formed proto IX was determined by fluorescence spectrometry (PerkinElmer; Rodgau - Jügesheim; Germany) with an excitation wavelength of 409 nm, an emission scan range of 570-680 nm, a scan speed of 200 nm/min and a slit width of 5 nm for excitation and emission.

Kinetic buffer	MES/HCl, pH 6.0	50.0	mM
	Triton ®X-100	0.1 %	(w/v)

II.6.8 Determination of HemH Activity

In the HemH activity assay ferrous ion is inserted into the porphyrin macrocycle to form protoheme IX. HemH activity is monitored fluorimetrically at 633 nm by recording the decrease of proto concentration. For this perpose 36 µl Proto solution (100 µM in water containing 15 mg/ml Tween 80) was added to 600µl of the standard assay mixture. The reaction was started by the addition of 0.1 µM HemH in water containing 15 mg/ml Tween 80. HemH catalysis was determined by the decrease of fluorescence at 633 nm after 5 min of incubation using a fluorescence spectrometer (PerkinElmer; Rodgau - Jügesheim; Germany). The excitation wavelength was 409 nm. An emission scan range of 570 - 680 nm, at a scan speed of 200 nm/min and a slit width of 5 nm for excitation and emission was used.

Standard buffer	Tris pH 7.2	100.0	mM

Tween 80	0.3%	(w/v)
$ZnCl_2$	100.0	µM

II.6.9 Determination of Kinetic Parameters of *T. elongatus* HemY by Fluorescence Stopped Flow Spectrometery

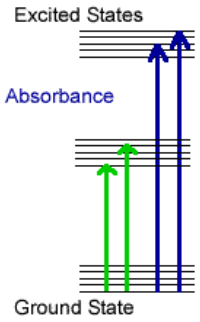

A molecule absorbs light once it accomodates the additional energy of the light by promoting electrons to higher energy levels. However the energy of the absorbed light must match the energy required to excite the electron. The absorption of light of a specific wavelength by a fluorescent molecule leads exactly to the transfer of electrons to a defined excited state. Relaxation to the ground state occurs upon losing energy either non-radiatively or by emission of light of longer wavelengths. Consequently, fluorescence is the light emitted by excited molecules in order to relax back to their ground state energy level. In order to measure these fluorescence reactions we employed a Jasco 810 stopped-flow spectrometer. Since the initial phase of velocity of enzyme reaction is characteristic for the investigated reactions we employed stopped flow analysis. A simplified schematic of the basic components of a stopped flow fluorescence instrument is shown below:

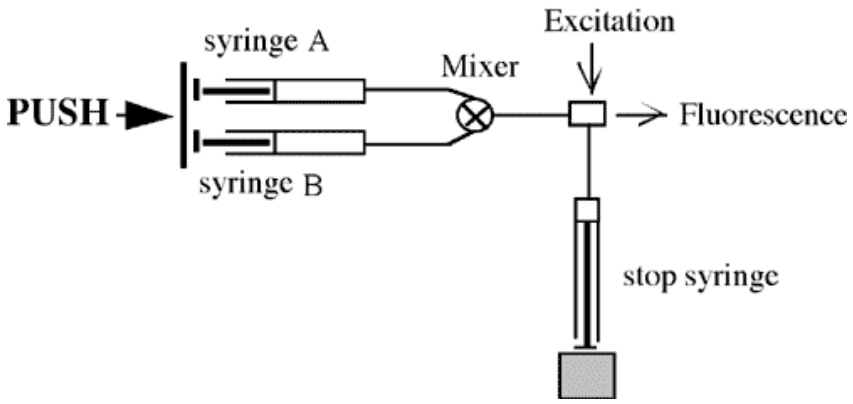

Figure 15: A schema of a stopped flow fluorescence instrument

After filling the drive syringes with solutions A (enzyme) and B (substrate), the syringes were pushed within milliseconds. Solution A was rapidly mixed with solution B and entered the

spectrophotometer cell. Subsequently the flow was stopped and the change in fluorescence was monitored.

In order to determine the kinetic parameters of *T. elongatus* HemY, the change in fluorescence during proto production from protogen was measured by a Jasco 810 stopped-flow spectrometer. A 10 ml syringe was filled with a soluton containing 5 ml kinetic buffer and 60 µl protogen solutions (460, 230, 115, 57.5 and 28.75 µM). A one ml syringe was filled with purified recombinant *T. elongatus* HemY (0.1 mg/ml). The substrate and protein were mixed of a ratio 1 : 5 (Enzyme : Protogen) in total volume 304 µl in a cuvette. A solution of enzyme without protogen and a solution of protogen without enzyme were used as negative controls.

Kinetic buffer	MES pH 6.0	50.0	mM
	Triton ®X-100	1.0%	(w/v)
	EDTA	20.0	mM
Protoporphyrinogen solution	Protoporphyrinogen	Various	
	Ethanol	20.0%	(v/v)
	KOH	10.0	mM

The excitation wavelength was 409 nm. The fluorescence of proto at 633 nm was measured.

Table 3: Parameters of the fluorometric HemY test.

Excitation wavelength	409.0	nm
Total measure time	35.0	s
Time base	0.005	s
Band width	8.0	nm
High voltage	variable between 880 - 940	V
Flow	2.0	ml/s
Acquisition start	10.0	ms before stop
Total volume	304.0	µl

Fluorescence from Proto production was measured by the photometer in relative voltage intensity. In order to quantify produced proto a calibration curve with different concentrations of protoporphyrin was prepared. The corresponding calibration curve is shown in Figure 16. In

accordance to the calibration curve 1 µM protoporphyrin is equal 2.4998 voltage. The setting was: High voltage 930 V, Measure time 4 s and time base 1ms.

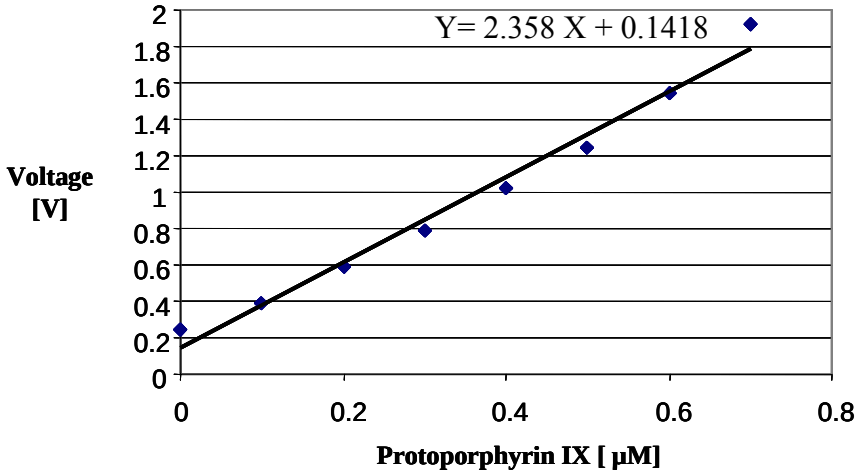

Figure 16: Calibration curve for determination of protoporphyrin concentrations in relation to voltage intensity from fluorescence stopped flow measurement.

Enzyme activity measurement with different concentration of substrate were performed. All assays were performed in triplicate. The initial velocity of the reactions was deduced from the linear regressions of saturation curves. The velocity of the enzyme reaction was plotted against respective substrate concentration in a Michaelis-Menten graph. The K_m and v_{max} values were determined by the computerized Michaelis-Menten curve fitting using SigmaPlot 8.0 Enzyme Kinetics v1.1. The k_{cat} value was calculated according to Voet und Voet, 1995 :

$$k_{cat} = v_{max} / [E]$$

k_{cat}: catalytic constant
v_{max}: maximal velocity
[E]: Enzyme concentration

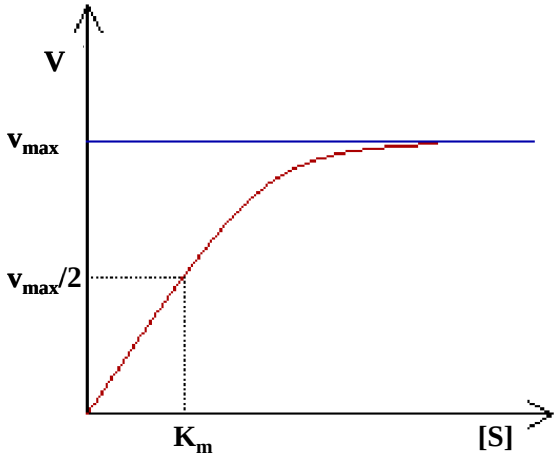

Figure 17: Schema of Michaelis – Menten Diagram

Plotting the reciprocals of the Michaelis-Menten representation yields a "double-reciprocal" or Lineweaver-Burk plot. This provides a more precise way to determine v_{max} and K_m. The v_{max} value can be deduced from the point where the line crosses the $1/V_i = 0$ axis. Note that the magnitude represented by the data points in this plot decrease from lower left to upper right. The K_m value equals v_{max} times the slope of line. This is easily determined from the intercept of the X axis.

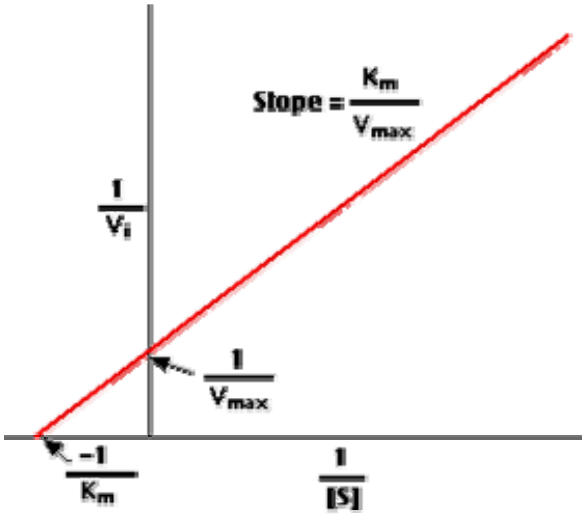

Figure 18: Schema of Lineweaver-Burk Diagram

II.6.10 Discontinuous SDS Polyacrylamide Gel Electrophoresis (SDS-PAGE)

Proteins were analyzed by SDS-PAGE (sodium dodecyl sulfate-polyacrylamide gel electrophoresis) as described by Laemmli (1970) with modifications by Righetti *et al.* (1990) for discontinuous SDS-PAGE. Protein samples were prepared by heating to 95 °C for 5 min in SDS loading dye. Samples were loaded onto 12% polyacrylamide gel (7 cm x 10 cm x 0.75 mm) which was run at 45 mA. During electrophoresis, proteins were first focused in the stacking gel and subsequently separated according to their relative molecular masses in the running gel. The size standards employed were Dalton Mark VII-L (Sigma) and Protein Molecular Weight Marker (MBI Fermentas). Gels were stained with Coomassie Brilliant Blue G-250 and destained until stained proteins were clearly visible.

Acrylamide stock solution	Acrylamide	30.0 %	(w/v)
	Bisacrylamide	0.8 %	(w/v)
Running gel buffer	Tris pH 6.8	500.0	mM

	SDS	0.4 %	(w/v)
Stacking gel buffer	Tris pH 8.8	1.5	M
	SDS	0.4 %	(w/v)
Running gel (12 % (v/v))	Acrylamide stock solution	2.0	ml
	Running buffer	1.25	ml
	H_2O_{deion}	1.75	ml
	APS solution	5.0	µl
	TEMED 1.0 % (w/v)	50.0	µl
Stacking gel (6 % (v/v))	Acrylamide stock solution	500.0	µl
	Stacking gel buffer	625.0	µl
	H_2O_{deion}	1.375	ml
	APS solution	3.0	µl
	TEMED 1.0 % (w/v)	30.0	µl
Electrophoresis buffer	Tris pH 8.4	50.0	mM
	Glycin	380.0	mM
	SDS	0.1 %	(w/v)
SDS loading dye	Tris pH 6.8	100.0	mM
	Glycerol	40.0 %	(v/v)
	ß-mercaptoethanol	10.0 %	(v/v)
	SDS	3.2 %	(w/v)
	Bromophenol blue	0.2 %	(v/v)
Staining solution	Acetic acid	10.0 %	(v/v)
	Ethanol	25.0 %	(v/v)
	Coomassie Brilliant Blue G-250	0.25%	(v/v)
Destaining solution	Acetic acid	10.0 %	(v/v)
	Ethanol	30.0 %	(v/v)
Fixation solution	Acetic acid	10.0 %	(v/v)

II.6.11 Preparation of *T. elongatus* Cell-Free Extract Containing the Membrane Proteins

Bacterial cell pellet of 5.5 g *T. elongatus* was resuspended in 6 ml of HEPES or Tris buffer, pH 8.0, containing 5 mM $MgCl_2$ and 300 mM NaCl, 1% n-Dodecyl-ß,D-maltoside (Gerbu; Gaiberg;

Germany) and 0.5% Triton X-100. Cells were disrupted by sonication using a sonotrode (SONOPLUS; Bandelin electronics; Berlin; Germany) 5 times for 3 min with 50% cycle and 70% power with breaks of 5 min by MS 73 tip. The disrupted cells were treated in a Mikro-Dismembrator (Braun Biotech; Melsungen; Germany) for 30 min. Cell debris were removed by centrifugation at 4000 x g for 15 min. The supernatant was subjected to the dismembrator for 40 min again. After incubation at 4 ^{o}C for 60 min, cell debris was removed again by centrifugation at 4 °C and 50000 rpm (Beckman Ultrazentrifuge, Rotor: Ti 70.1) for 45 min.

II.6.12 Co-Immunoprecipitation Experiments Using Cell-Free *T. elongatus* Extracts

In immunoprecipitation assay an antibody against a specific target antigen forms an immune complex with its target in cell free extract. The immune complex is then bound to Protein A-coupled sepharose which subsequently separated from the residual extract protein by centrifugation. The process of capturing this complex from the solution is referred to as precipitation. Any proteins not "precipitated" by the immobilized Protein A are washed away. Finally both antigen and antibody are eluted from the sepharose matrix and analyzed by SDS-PAGE. Western blot analysis is performed to verify the identity of the antigen and potential proteins bound to the antigen which were recovered by the employed antibody. This co-immunoprecipitation is most commonly technique used to identify interactions between two proteins which are associated *in vitro* (figure 19).

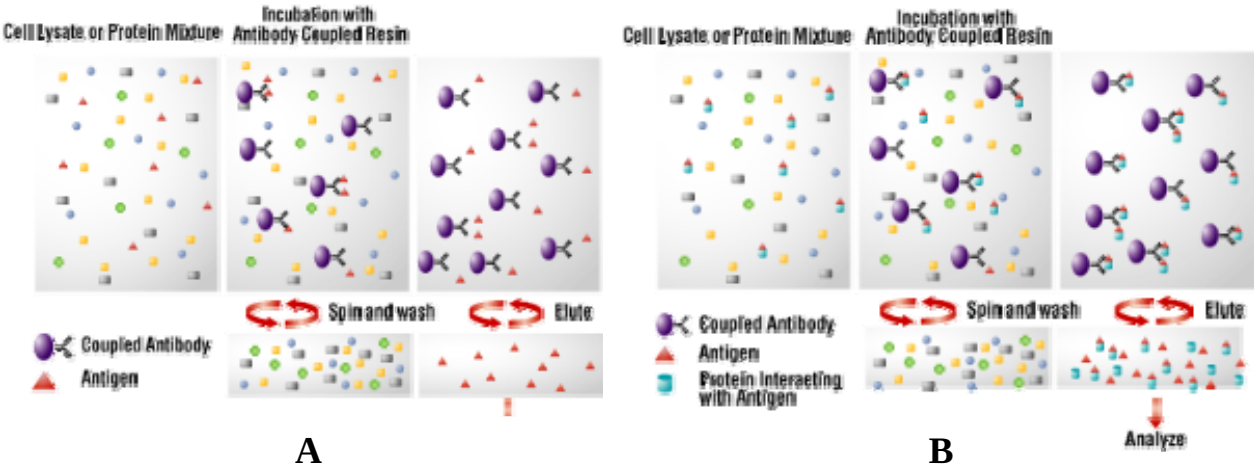

Figure 19: Schemata of immunoprecipitation (A) and co-immunoprecipitation (B) assays.

So, 350 µl of the *T. elongatus* cell extracts were mixed with 2.5 µl of antibody solution (α-HemF,

α-HemY and α-HemH antibodies) and incubated at 1400 rpm and 4 °C. After 1-2 h, 5 mg protein A sepharose™ CL-4B (GE Healthcare; Germany) was added to the cell extract-antibody mixture. The mixture was incubated at 1400 rpm and 4 °C for 1 h. The immobilized antigen-antibody was recovered by centrifugation at 10000 x g for 1 min and washed 3 times by resuspension in wash buffer. The proteins were eluted and dissociated from the beads by addition of 20 µl of SDS loading dye and boiling for 5 min at 95 °C prior to being separated on a 8% or 12% SDS-PAGE and transferred to a nitrocellulose membrane (Millipore; Eschborn; Germany).
In order to remove heavy and light chains bands in western blots (II.6.13), the Seize™ X Protein A Immunoprecipitation Kit (Pierce; USA) was used according to the manufacturer's instructions.

Wash buffer	Tris pH 8.0	20.0	mM
	$MgCl_2$	5.0	mM
	NaCl	300.0	mM
	Triton ®X-100	0.5 %	(w/v)

II.6.13 Western Blotting

For further analysis, proteins separated during SDS-PAGE were transferred in a semi-dry process onto a Polyvinylidenfluoride (PVDF) membrane, which binds the proteins by polar interactions (Western-Blot). Therefore, PVDF-membranes were incubated in methanol for 15 min and afterwards, parallel to the SDS-gel and blotting papers, incubated in transfer-buffer and assembled in the following order on the blotting apparatus: Cathode, blotting paper, PVDF-membrane, SDS-gel, blotting paper, and anode. A current of 0.8 mA/cm^2 was applied for 30 min at 10 V.

10 x Transfer buffer	Tris pH 8.0	250.0	mM
	Glycin	1.92	M
Methanol	Methanol	20.0%	(v/v)

Proteins immobilized on a PVDF-membrane can be detected by antibodies. The primary antibody is directed against an epitope of the protein of interest and the secondary antibody directed against the primary antibody is coupled to an enzyme which catalyses a detectable color developing reaction. For immunodetection of proteins, after blotting onto a PVDF-membrane non-specific binding sites of the membrane were saturated overnight in blocking-solution at RT and slight shaking. Incubation with the primary antibody was carried out in incubating-solution

for 1.5 h (RT) and slight shaking (rabbit α-HemF or α-HemY or α-HemH antibodies diluted 1:5,000 in incubating-solution separatly). The membranes were washed three times for 5 min each step with washing-buffer (1 x PBS) and incubated for 90 min with the secondary antibody (anti-rabbit diluted 1:20,000 in incubating-buffer), which is coupled to an alkaline phosphatase. After three further washing steps with washing buffer for 5 min, membranes were incubated for 5 min in alkaline phosphatase-buffer (APB) and exposed to staining-solution until detected proteins became visible. During exposure alkaline phosphatase, the enzyme bound to the antibody, catalyzes the reaction of 5-brom-4-chloro-3-indolylphosphate (BCIP) with nitroblue-tetrazolium (NBT). The resulting insoluble dye precipitates immediately on the membrane. Color development was stopped by the addition of water and the membranes were air dried in the dark.

10 x Phosphate Buffered Saline (PBS) pH 7.4	NaCl	1.37	M
	KCl	22.0	mM
	Na_2HPO_4	100.0	mM
	KH_2PO_4	17.0	mM
	dissolved in H_2O_{deion}		
Blocking solution	Skim milk powder	5.0 %	(w/v)
	Triton ®X-100	0.1 %	(w/v)
	dissolved in 1 x PBS		
Incubating solution	Skim milk powder	3.0 %	(w/v)
	dissolved in 1 x PBS		
APB solution	Tris pH 9.5	100.0	mM
	$MgCl_2$	5.0	mM
	NaCl	100.0	mM
Staining solution	NBT solution (100 mg/ml in 70% DMF)	132.0	µl
	BCIP solution (50 mg/ml in DMF)	60.0	µl
	APB solution	20.0	ml

II.6.14 Double-Immunogold Labelling

T. elongatus cells were fixed in a fixation solution of 0.5% formaldehyde and 0.2% glutaraldehyde in cacodylate buffer (0.1 M cacodylate, 0.09 M sucrose, 10 mM $MgCl_2$. 10 mM

$CaCl_2$, pH 6.9) for 1 h on ice, washed with cacodylate buffer containing 10 mM glycine and embedded into 1.75% aqueous agar and after solidification cut into small cubes. Samples were then dehydrated with ethanol following the progressive lowering of temperature method (PLT) applying a graded series of ethanol. The 10% and 30% ethanol steps were carried out on ice for 15 min, followed by the 50% step at –20°C for 30 min. The subsequent ethanol steps (70, 90, 100%) were carried out at –35 °C, each step for 30 min and the 100% step was repeated twice. The Lowicryl resin K4M was infiltrated in several steps, first 1 part K4M/ 1 part 100% ethanol for overnight, 2 parts K4M/ 1 part ethanol for 24 h and pure resin for 36 h with several changes. The resin was polymerized at –35 °C with UV-light (366 nm) for 1 day and further polymerized at room temperature for another 2 days. Ultrathin sections were cut with a diamond knife and collected onto formvar-coated 300 mesh nickel grids. Sections were incubated in a 1:25 dilution of protein A-sepharose purified anti-the first protein of interest (stock solution 1.9 mg/ml IgG protein) at 4°C for overnight. Sections were then washed with PBS (II.6.13) and incubated on a 1:200 dilution of protein A/G gold (15 nm in diameter) for 30 min at room temperature. After washing with PBS containing 0.01% Tween 20 sections were incubated with 100 µg/ ml protein A for 15 min at room temperature and washed again with PBS. Sections were then incubated with a 1:25 dilution of purified anti-the second protein of interest (stock solution 1,9 mg/ml) and incubated for 3 h at room temperature. After washing with PBS sections were incubated with a 1:75 dilution of protein A/G gold (10 nm in diameter) for 30 min at room temperature. After washing with PBS containing 0.01% Tween 20 sections were washed with TE buffer (20 mM Tris, 2 mM EDTA, pH 7.0), distilled water and air-dried. Sections were counterstained with 4% aqueous uranyl acetate for 3 min and washed with water. After air-drying samples were examined in a Zeiss transmission electron microscope EM910 with an acceleration voltage of 80 kV. Images were recorded onto negative film (Kodak SO-163). Prints were generated on Ilford Multigrade paper and then scanned and processed using Adobe Photoshop 6.0.

These experiments were performed in the laboratory of Dr. Manfred Rohde (Helmholtz Centre for Infection Research, Braunschweig)

II.7 RNA Methods

II.7.1 Preparation of Cell Free Extracts for *T. elongatus* RNA Isolation

A total of 40 g of cells were dissolved in 160 ml dissolving buffer. The cell solution was divided into 5 parts and every part was disrupted by sonication (SONOPLUS; Bandelin electronics;

Berlin; Germany) 4 times for 5 min with 50% cycle and 70% power with breaks of 5 min by MS 72 tip.

Dissolving buffer	Tris pH 7.5	50.0	mM
	$MgOAc_2$	10.0	mM
	DTT	3.0	mM
	RNaseOut	1.5	mg/l

II.7.2 Total RNA Isolation

One volume of acidic phenol was added to the cell free extract, mixed and shaked vigorously for 30 min at RT. Then the sample was centrifuged for 30 min at 15000 x g and 4 ^{o}C and the aqueous phase was removed. One volume of dissolving buffer was added to the phenol phase and everything reextracted. The aqueous phase from the first extraction also was reextracted with 1 volume acidic phenol. After centrifugation of both reextractions for 30 min at 15000 x g and 4 ^{o}C, both aqueous phases were transfered to fresh tubes. In order to separate DNA from RNA, ice cold 20% isopropanol was added and mixed. After 10 min incubation at -20 ^{o}C, genomic DNA was harvested by centrifugation at 15000 x g and 4 ^{o}C for 20 min. Ice-cold isopropanol in a final concentration of 60%, 20 µl glycogen (stock solution 20 µg/µl) and 10 µl RNaseOUT (stock solution 40 u/µl) were added to the remaining supernatant. After 30 - 60 min incubation at -20 ^{o}C, total RNA was precipitated by centrifugation at 15000 x g and 4 ^{o}C for 45 min.

II.7.3 Total tRNA Isolation by Anion Exchange Chromatography

Two Qiagen-Q500 columns (Qiagen; USA) were equilibrated with 40 ml equilibration buffer. Total RNA pellet was dissolved in 40 ml loading buffer and loaded onto the columns. Every column was washed with 100 - 120 ml wash buffer and tRNA was eluted with 40 ml elution buffer. One volume 100% ice cold isopropanol, 10 µl glycogen (stock solution 20 µg/µl) and 10 µl RNaseOUT (stock solution 40 u/µl) were added and incubated at -20 ^{o}C overnight. The RNA was precipitated by centrifugation at 15000 x g and 4 ^{o}C for 40 min. The resulting pellet was washed with 10 ml 70% ice-cold ethanol containing 10 µl RNaseOUT and 20 µl glycogen and centrifuged at 15000 x g and 4 ^{o}C for 40 min. The pellet was dried by dry speed vaccum for 2 - 3 min.

Loading buffer	Mops pH 7.0	100.0	mM

	EDTA	1.0	mM
	ß-Mercaptoethanol	10.0	mM
Equilibration buffer	Mops pH 7.0	50.0	mM
	Isopropanol	15.0 %	(v/v)
	Triton ®X-100	1.0 %	(w/v)
	ß-Mercaptoethanol	5.0	mM
Wash buffer	Mops pH 7.0	50.0	mM
	NaCl	200.0	mM
	ß-Mercaptoethanol	5.0	mM
Elution buffer	Mops pH 7.0	50.0	mM
	NaCl	750.0	mM
	Ethanol	15.0 %	(v/v)
	ß-Mercaptoethanol	5.0	mM

II.7.4 tRNA Deacylation

30 mg unfractionated tRNA were deacylated by addition of 9 ml of 200 mM Tris acetate pH 9.0 and incubated at 37 ^{o}C for 1 h. Afterwards, 2.5 volumes of 300 mM sodium acetate pH 5.2 in ethanol, 5 µl RNaseOUT (stock solution 40 u/µl) and 10 µl glycogen (stock solution20 µg/µl) were added to the tRNA-fraction and incubated at -20 ^{o}C for 30 min. The tRNA-fraction was precipitated by centrifugation at 15000 x g and 4 ^{o}C for 30-40 min. The precipitate was dried by dry speed vaccum for 2-3 min. Purity of the tRNA was determined by denaturing 12% polyacrylamide / 8 M urea gel electrophoresis.

II.7.5 Gel Electrophoretical Method for the Analysis of Nucleic Acids

II.7.5.1 Denaturing Polyacrylamide Gel Electrophoresis

The denaturing polyacrylamide-gel electrophoresis was used to separate nucleic acids according to their molecular weight. The the addition of 8 M urea prevents the formation of secondary structures of RNAs or DNAs in the gels which could result in an alteration of their electrophoretic behavior. For detailed descripition and preparation of the gels see Sambrook *et al*., 1989. After gel setup, samples are loaded onto a urea-based denaturing gel (7 cm x 10 cm x 0.75 mm) which is run in 1 x TBE buffer at 90 mA and 300 V until the lower dye leaves the gel. The gel is stained for 5 minutes by staining solution and destained with water.

10 x TBE buffer	Tris base	108.0	g
	Boric acid	55.0	g
	EDTA	9.3	g
	dissolved in H_2O_{deion} (Total volume 1.0 liter)		
12% denaturing gel	Urea	2.4	g
	10 x TBE buffer	0.5	ml
	Acrylamide/Bisacrylamide 40% (19:1)	1.5	ml
	dissolved in H_2O_{deion} (Total volume 5.0 ml) by heating		
	10% APS	30.0	µl
	TEMED	5.0	µl
2 x tRNA Loading buffer	Urea	24.0	g
	Sucrose	10.0	g
	dissolved in H_2O_{deion} (Total volume 50.0 ml) by heating		
	Bromphenolblue	12.5	mg
	Xylene cyanol	12.5	mg
Staining solution	Methanol	200.0	ml
	Acetic acid	5.0	ml
	Toluidine blue	0.5	g
	dissolved in H_2O_{deion} (Total volume 500.0 ml)		

II.7.6 Individual tRNA Isolation with Chaplet Column Chromatography

Individual tRNAs were purified from total tRNA with 5´biotinylated DNA oligonucleotides, complementary to the target tRNA, immobilized on streptavidin sepharose. This improved solid-phase DNA probe method is named chaplet column chromatography (Kaneko *et al*., 2003).

II.7.6.1 5´-Biotinylated DNA Oligonucleotide Attachment to Streptavidin Sepharose

5´-biotinylated, gel purified DNA oligonuclotides, complementary to $tRNA^{Glu}$ and $tRNA^{Gln}$ of *T. elongatus* with the sequences 5′-biotin-GGAGGTGTCCTAGGCCACTAGACGATGGGGGC-3′ and 5′-biotin-CCCGCTGCCTTACCGCTTGGCGACACCCCA-3′, respectively, were synthesized (Biomers.net; Ulm; Germany).

In a reaction tube 300 µl UltraLink Immobilized Streptavidin (Pierce; USA) were washed twice with 1 ml of 10 mM Tris pH 7.5. Subsequently, 150 µg of each purified biotinylated DNA probe was mixed with Streptavidin sepharose in 500 µl of 10 mM Tris pH 7.5 and incubated at RT for 2 h under rotation. The Sepharose was centrifuged for 1 min at 10000 x g and washed four times with 10 mM Tris pH 7.5. Finally, the oligo-beads were equilibrated in 6 x NTE solution.

II.7.6.2 Individual tRNA Purification

An amount of 10 - 13 mg total *T. elongatus* tRNA was dissolved in 500 µl of 6 x NTE solution and then added to one of the oligo-beads. The mixture was incubated at 65 - 68 °C for 30 min under vigorous shaking at 1000 rpm and then allowed to cool to RT. Beads were washed three times in 500 µl of 3 × NTE, twice in 500 µl of 1 × NTE and once in 500 µl of 0.1 × NTE at RT until the absorbance at 260 nm was essentially not detectable anymore in the washing steps. Individual tRNAs were eluted three to four times with 400 µl of 0.1 × NTE at 65 – 68 °C and 1000 rpm for 5 min until the absorbance at 260 nm of the eluate was approximately zero. The eluates including RNaseOUT and glycogen were mixed with 2.5 volume ice cold 100% ethanol and after 10 min incubation at -20 °C, precipitated via centrifugation at 15000 x g and 4 ^{o}C for 30 - 40 min.

Further purification was achieved using the QIAquick Nucleotide Removal Kit (Qiagen; Hilden; Germany) and Dnase (Boehringer; Germany) according to the manufacturer's instructions. The purity of tRNAs were controlled by Northern dot-blot-analysis.

20 x NTE solution	Tris pH 7.5	100.0	mM
	NaCl	4.0	M
	EDTA	50.0	mM
	ß-Mercaptoethanol	5.0	mM

II.7.7 Northern dot-Blot

A total of 0.5 −1 µg tRNA was crosslinked onto a positively charged nylon membrane (Roche; Mannheim; Germany) by UV irradiation. The membrane was incubated with 20 ml hybridization solution at 68 °C for 1 h. Subsequently, 10 µg individual 5´-biotinylated DNA oligonuclotide with 20 ml hybridization solution were mixed and incubated at 68 °C for 10 min. The membrane was incubated in this mixture overnight and then washed four times with 50 ml wash buffer at 68 °C for 15 min, and three times with 20 ml PBS including 0.1% Tween 20 at RT for 5 min.

Attached biotinylated oligonucleotides were detected by incubation with detection buffer at RT for 90 min. The membrane was washed with PBS including 0.1% Tween 20 twice, and then with APB and exposed to staining-solution (II.6.14.1) until color became visible.

Maleic acid buffer	Maleic acid	100.0	mM
	NaCl	150.0	mM
	NaOH	175.0	mM
	dissolved in H_2O_{deion}		
titrated with NaOH to pH 7.5			
Prehybridization solution	Na_2HPO_4 x 7 H_2O	250.0	mM
	EDTA	1.0	mM
	dissolved in H_2O_{deion}		
titrated with phosphoric acid to pH 7.2 and autoclaved			
	SDS	20.0 %	(w/v)
10% Blocking buffer	Blocking Reagent	2.0	g
	Maleic acid buffer pH 7.5	20.0	ml
Hybridization solution	Prehybridization solution	38.0	ml
	10% Blocking buffer	2.0	ml
Wash buffer	Na_2HPO_4 x 7 H_2O	250.0	mM
	EDTA	1.0	mM
	dissolved in H_2O_{deion}		
titrated with phosphoric acid to pH 7.2 and autoclaved			
	SDS	1.0	% (w/v)
Detection buffer	PBS - 0.1% Tween 20	20.0	ml
	Streptavidin-AP-conjugate	5.0	µl

II.7.8 Determination of RNA Concentration

The concentration and purity of a RNA solution was determined by measuring the absorbance at 260 nm and additionally at 280 nm to account for protein impurities by Ultrospec 2000-Photometer. For a pure RNA solution an A_{260} of 1 corresponds to a RNA concentration of 40 µg/ml. The puritiy of DNA solution can be indicated from the ratio of A_{260} to A_{280}. With $A_{260}/A_{280} = 2.0$ the RNA is considered as pure.

Additionally, RNA purity can be determined by denaturing polyacrylamide gel electrophoresis.

II.7.9 Analysis of Protein : Nucleic Acid interactions

II.7.9.1 Aminoacylation of tRNAs by Aminoacyl-tRNA Synthetase

Aminoacylation assays were carried out by a modified method of Hoben and Söll, 1985. For qualitative assays, a series of dilutions of purified enzyme was made to establish the minimum of enzyme required for the acylation of 0.1 A_{260} units of tRNA. This quantity was then used in the assaying of a range of concentration of substrate samples. These concentrations were chosen to ensure complete acylation by the respective enzyme.

In vitro acylation experiments with *T. elongatus* GluRS were carried out at 37 °C and 600 rpm, in a 130 µl reaction mixture containing kinetic buffer, 5 mM ATP, 30 µM L-[^{14}C]Glu (237 mCi/ mmol) and 0.67 to 21.5 µg of the pure tRNA. The reactions were started by addition of 1.8 µM pure *T. elongatus* GluRS, which was dialyzed against kinetic buffer. Samples (15 µl) were taken at different time points (0, 10 s, 30 s, 60 s, 2 min, 5 min, 10 min and 30 min) spotted onto 3 MM Whatman filter paper discs and washed twice in 10%, once in 5% (w/v) trichloroacetic acid and finally in ethanol for 5 - 10 min. Filters were soaked in 4 ml scintillation liquid and radioactive amount was measured by liquid scintillation analyzer (Tri-Carb 2900 TR). Kinetic parameters were obtained by Michaelis-Menten plots.

Kinetic buffer	HEPES pH 7.5	50.0	mM
	KCl	25.0	mM
	$MgCl_2$	15.0	mM
	DTT	5.0	mM

II.8 Protein Crystallisation

II.8.1 HemY Crystallisation

After HemY concentration by DEAE Sepharose column chromatography, concentrated HemY was dialyzed against the buffers of a variety of buffered solutions overnight.

Buffer 1	Citric acid pH 3.0	20.0	mM

	NaCl	50.0	mM
	Triton ®X-100	0.1 %	(w/v)
Buffer 2	Citric acid pH 4.0	20.0	mM
	NaCl	50.0	mM
	Triton ®X-100	0.1 %	(w/v)
Buffer 3	Citric acid pH 6.0	20.0	mM
	NaCl	50.0	mM
	Triton ®X-100	0.1 %	(w/v)
Buffer 4	Tris pH 6.8	20.0	mM
	NaCl	50.0	mM
	Triton ®X-100	0.1 %	(w/v)
Buffer 5	Tris pH 8.0	20.0	mM
	NaCl	50.0	mM
	Triton ®X-100	0.1 %	(w/v)

In order to completely remove any solid particals which could initiate salt-precipitation during the crystallisation process, all buffered enzyme solutions were subjected to centrifugation (15 min, at 10000 x g and 4 ^{o}C. In this technique, 1.5 - 3 µl of HemY solutions with concentrations of 5.3 and 8 mg/ml mixed with 1.5 - 3 µl crystallization reagent of Crystal Screens I, II and Cryo and PEG/ION Screen crystallization kits (Hampton research; USA) in a well on a platform in vapor equilibration with the 100 µl reservoir. The plates were sealed with clear sealing tape and incubated at 17 ^{o}C.

II.8.2 HemY and HemF Co-Crystallisation

Co- crystallisation of HemF and HemY was performed like HemY crystallisation with Crystal Screens I and II.

III Results and Discussion

In the cyanobacterium *T. elongatus* heme is formed from glutamyl-tRNA (Glu-tRNA^{Glu}). Glutamyl-tRNA is synthesized by an ATP-dependent glutaminyl-tRNA synthetase (GluRS). In this thesis the non-discriminating nature of the enzyme was investigated. The kinetic behavior of purified tRNA^{Glu} and tRNA^{Gln} as substrates was determined. Obtained results were discussed in the light of the recently solved crystal structure of *T. elongatus* GluRS.

In a second part of this thesis the detailed characterization of the complex formation of the three heme-terminal enzymes CPO (HemF), PPO (HemY) and FC (HemH) from *T. elongatus* was investigated *in vitro* and *in vivo* (III.2).

III.1 Identification of *T. elongatus* Glutamyl-tRNA Synthetase as a Non-Discriminating Aminoacyl-tRNA synthetase

The genome sequence of *T. elongatus* revealed that the gene coding for glutaminyl-tRNA synthetase is not present. We proposed that the cyanobacterium synthesizes Glu-tRNA^{Glu} and Glu-tRNA^{Gln} via one single GluRS as determined for other bacteria. Glu-tRNA^{Gln} is formed via charging of tRNA^{Gln} with glutamate by this GluRS and the subsequent transamidation of mischarged Glu-tRNA^{Gln} by an amidotransferase.

The non-discriminating character (I.1.4.4) of GluRS was determined in aminoacylation assays using recombinantly purified enzyme, ^{14}C-labelled Glu, tRNA^{Glu} and tRNA^{Gln}. Kinetic parameters of glutamylation of both tRNA species were measured.

III.1.1 Isolation and Purification of *T. elongatus* tRNA^{Glu} and tRNA^{Gln}

Total RNA was isolated from 40 g of *T. elongatus* cells via acidic phenol extraction. Total tRNA was gained from total RNA via Qiagen-Q500 column chromatography. After tRNA deacylation, tRNA^{Glu} and tRNA^{Gln} were isolated by chaplet column chromatography. Further purification was achieved using the QIAquick Nucleotide Removal Kit. Degradation of the tRNAs was monitored by denaturing 12% polyacrylamide / 8 M urea gel electrophoresis (fig. 20) and purity of tRNAs was controlled via Northern dot-blot-analysis (fig. 21).

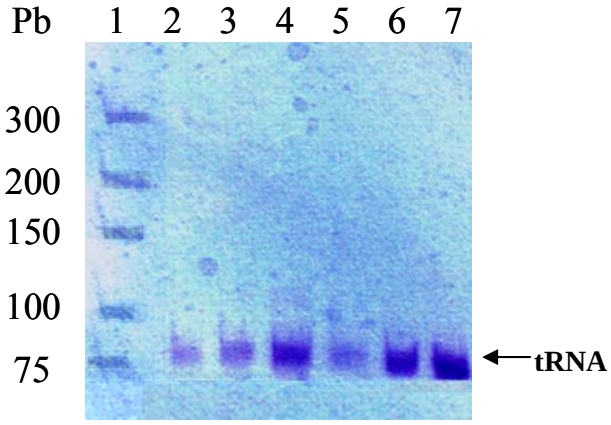

Figure 20: Analysis of purified *T. elongatus* $tRNA^{Glu}$ and $tRNA^{Gln}$ by denaturing polyacrylamid / 8 M urea gel electrophoresis. RNAs were separated by denaturing 12% polyacrylamide / 8 M urea gel electrophoresis as described in MATERIALS AND METHODS and visualized by staining with Toluidine blue. Lane 1 shows the DNA standards O'GeneRuler™ DNA Ladder Ultra Low Range. Sizes of significant marker bands are given. Lanes 2-4 show different amounts of the $tRNA^{Gln}$ and lanes 5-7 show different amounts of the $tRNA^{Glu}$.

Figure 20 shows the gel-electrophoretical separation of the purified tRNA-fractions. It presented that the purified $tRNA^{Glu}$ as well as $tRNA^{Gln}$ migrated in the denaturing polyacrylamide gel according to their expected nucleotide length. Moreover, no signs of degradation were detected.

In order to prove the complete separation of the individual tRNAs from one another to prevent cross-reactivity in the kinetic investigations, Northern dot-blot-analysis was performed. First, 1 µg of the tRNAs was crosslinked onto a positively charged nylon membrane. Then, the membrane was incubated with one of the individual 5´-biotinylated DNA oligonuclotides. The biotinylated oligonucleotide was then detected by incubation with a Streptavidin-AP-conjugate. Figure 21 demonstrates the purity and the successful separation of $tRNA^{Glu}$ and $tRNA^{Gln}$.

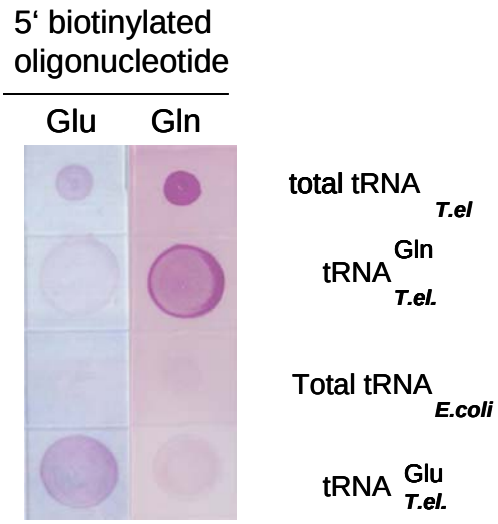

Figure 21: Demonstration of the purity of *T. elongatus* tRNA^{Glu} and tRNA^{Gln} via Norden dot blots analysis. To determine the degree of cross contamination of the tRNA^{Glu} preparation with tRNA^{Gln} and vice versa, purified tRNAs were analyzed for the presence of the corresponding counterpart. The left blot (Glu) was incubated with 5´-biotinylated DNA oligonuclotide complementary to tRNA^{Glu} and the right blot (Gln) was incubated with 5´-biotinylated DNA oligonuclotide complementary to tRNA^{Gln}. Color detection was achieved by a second incubation of the blot with streptavidin-AP-conjugated and succeeding BCIP and NBT detection.

The result of the Northern-dot blot analysis showed clearly that within the individual tRNA^{Glu} and tRNA^{Gln} preparation there was hardly any cross-contaminations between the two isolates. As a control total *E. coli* tRNA also was cross-linked onto the membrane and incubated with the respective biotinylated oligonucleotides directed against tRNA^{Glu} and tRNA^{Gln}. Again, no unspecific cross-reactivity was detected.

III.1.2 Purification *T. elongatus* GluRS

Recombinant *T. elongatus* GluRS was produced as a His-tag fusion protein in *E. coli* BL21 Codon-Plus(DE3)-RIL cells carrying vector pTe*RS* (Schulze *et al*., 2006*)*. Protein purification was performed via Ni^{2+} affinitiy chromatography. SDS-PAGE analysis of the purified protein (lane 3 in figure 22) revealed a band corresponding to a protein with a relative molecular mass of about 54.000, which was in good agreement with the calculated molecular mass of 54360.97 Da.

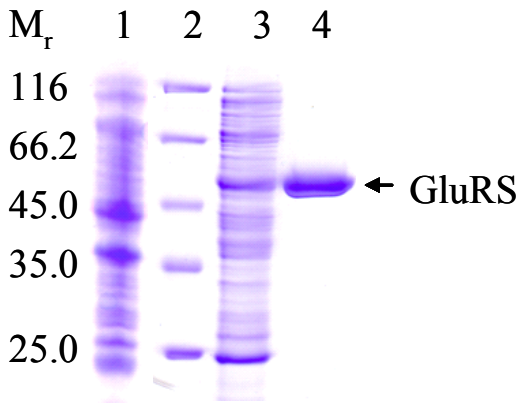

Figure 22: Production of recombinant *T. elongatus* GluRS. Proteins were separated by 12 % SDS-PAGE as described in MATERIALS AND METHODS and visualized by Coomassie Brilliant Blue staining. Lane 1 shows the crude extract of *E.coli* BL21-Codon-Plus(DE3)-RIL carrying pTe*RS* before induction. Lane 2 shows the proteins of the molecular weight marker, the respective relative molecular masses [x10^3] are indicated. Lane 3 shows the all free extract of *E. coli* BL21-Codon-Plus(DE3)-RIL carrying pTe*RS* after induction. Lane 4 shows the GluRS after purification via Ni^{2+} affinity chromatography.

III.1.3 Aminoacylation Assays

In order to prove whether *T. elongatus* GluRS is capable of glutamylation of both $tRNA^{Glu}$ as well as $tRNA^{Gln}$, aminoacylation assays were performed. Aminoacylation assays with *T. elongatus* GluRS carried out at 37 °C in a 130 µl reaction mixture containing kinetic buffer, L-[^{14}C]Glu and from 0.67 µg up to 21.5 µg of one of the purified tRNAs; for charging $tRNA^{Glu}$ and for mischarging $tRNA^{Gln}$. The reactions were started by addition of purified *T. elongatus* GluRS. Samples (15 µl) were sedimented at different time points onto filter paper discs by trichloroacetic acid treatment. This technique precipitates charged tRNAs bound to protein and leaves free amino acids in solution. Radioactivity on the filters, indicative of [^{14}C]Glu bound to tRNA was measured by liquid scintillation counting. Kinetic parameters were obtained by Michaelis-Menten plots (see fig. 23 and 24).

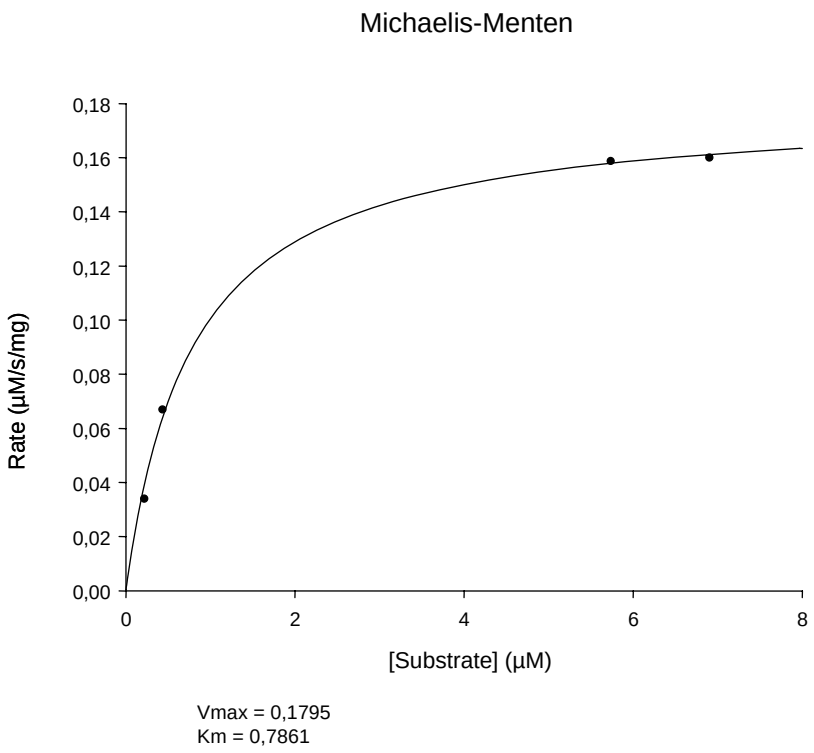

Figure 23: Michaelis Menten graph for tRNA^{Glu} glutamylation by *T. elongatus* GluRS (Charge)

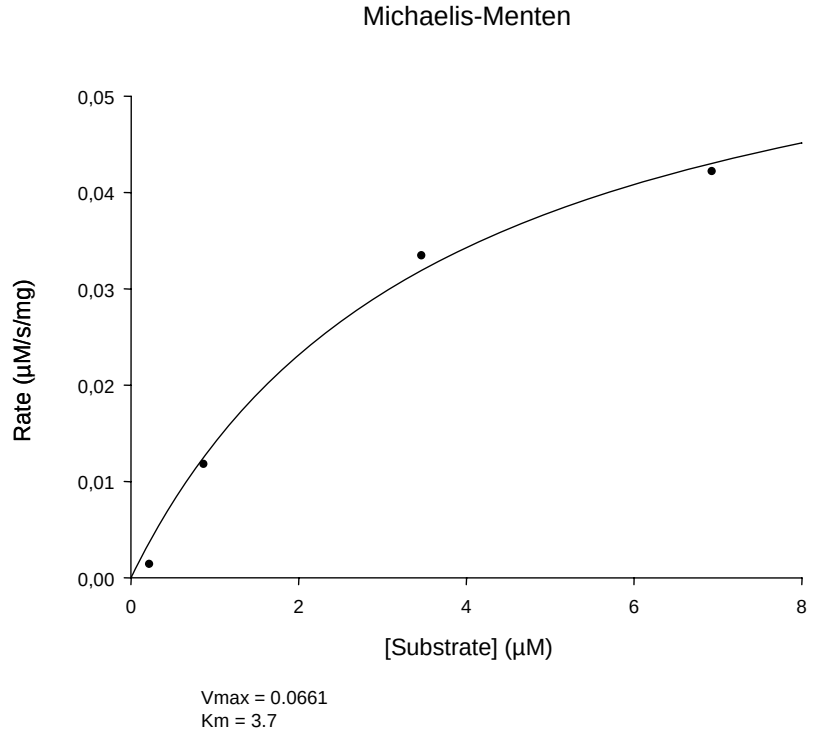

Figure 24: Michaelis Menten graph for tRNA^{Gln} glutamylation by *T. elongatus* GluRS (Mischarge)

K_m is defined as the substrate concentration at the half maximal velocity. The K_m-value of *T. elongatus* GluRS for $tRNA^{Glu}$ was lower compared to the one for $tRNA^{Gln}$. By comparing kinetic constants of *T. elongatus* GluRS for $tRNA^{Glu}$ and $tRNA^{Gln}$ (see table 4) we found that glutamylation of $tRNA^{Glu}$ is 13 fold more efficient than that of $tRNA^{Gln}$ by GluRS.

Table 4: Kinetic parameters for Glu-$tRNA^{Glu}$ and Glu-$tRNA^{Gln}$ formation by non-discriminating GluRS from *T. elongatus*.

tRNA	**K_m [µM]**	**kcat [s^{-1}]**	**kcat/K_m [s^{-1}mM]**
Glu-$tRNA^{Glu}$	0.79 ± 0.07	0.1 ± 0.03	126 ± 0.5
Glu-$tRNA^{Gln}$	3.7 ± 0.4	0.036 ± 0.003	9.7 ± 0.7

The kinetic data confirm the assumption that *T. elongatus* uses GluRS not only to charge its congate $tRNA^{Glu}$ but also misaminoacylates $tRNA^{Gln}$ due to the absence of a natural cognate glutaminyl-tRNA synthetase in *T. elongatus.* The misaminoacylated Gln- $tRNA^{Glu}$ gets corrected by an amidotransferase (Wilcox and Nirenberg., 1968; Curnow, 1997).

These results are in good agreement with the crystal-structure of *T. elongatus* GluRS recently solved by our co-operation partners in the laboratory of Prof. Dr. D. Heinz at the HZI, Braunschweig, Germany (Schulze *et al*., 2006). In order to be able to accommodate two different tRNA molecules for aminoacylation of either $tRNA^{Glu}$ and $tRNA^{Gln}$ with Glu, GluRS must possess a dual specificity for its two substrates.

The detailed molecular picture of GluRS-tRNA interaction was deduced from two GluRS crystal structures (see figure 25 A). The *T. elongatus* GluRS structure was solved without bound tRNA. Therefore, the crystallized GluRS-$tRNA^{Glu}$ complex from *Thermus thermophilus* was used to model the *T. elongatus* GluRS-$tRNA^{Glu}$ and GluRS-$tRNA^{Gln}$ complex.

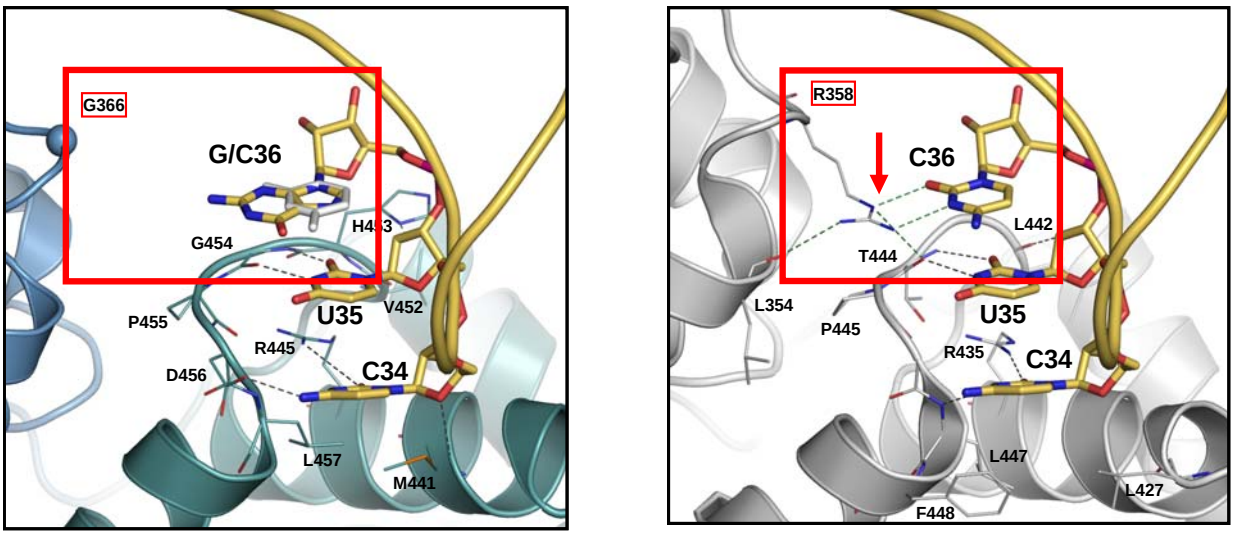

Figure 25: The structural basis of non-discrimination and discrimination for tRNA^{Glu} by *T. elongatus* and *T. thermophilus* GluRS. Structural comparison of the anticodon-binding domains of ND-GluRS from *T. elongatus* (A) and D-GluRS from *T. thermophilus* is shown (B). The importance of amino acid interaction with position 36 of tRNA^{Glu} and tRNA^{Gln} is emphasized.

To elucidate the molecular nature for the tRNA^{Glu} and tRNA^{Gln} binding, the non-discriminating *T. elongatus* GluRS was modeled in complexes with tRNA^{Glu} and tRNA^{Gln} and was compared with a discriminating enzyme in complex with tRNA^{Glu}.

T. thermophilus GluRS is a discriminating tRNA-synthetase, i. e. it glutamylates only its cognate tRNA^{Glu} to give rise to Glu-tRNA^{Glu}. The 3D-structure of the anticodon-binding site (figure 25, panel B) of *T. thermophilus* GluRS reveals a tight binding pocket where the cytidine36 of tRNA^{Glu} is coordinated by Arg358 (Nureki *et al.*, 1992). This picture diverges in the crystal structure of *T. elongatus* GluRS. Here, the coordinating amino acid residue Arg358 is missing. Instead, there is a Gly366 in the vicinity. However, no other amino acid seems to be involved in the coordination of the tRNA anticodon base 36. Thus, it seems possible for *T. elongatus* GluRS to accommodate both tRNA^{Glu} (^{34}CUC^{36}) as well as tRNA^{Gln} (^{34}CUG^{36}), since a large cavity in the anticodon binding pocket can bind to the larger pyrimidine.

The obtained experimental kinetic data prove the dual specificity of *T. elongatus* GluRS towards tRNA^{Gln} and this way explains the in nature occurring phenomenon.

III.2 Complex-Formation between the Terminal Enzymes in Tetrapyrrole Biosynthesis

Another important objective of this work was the investigation of the intraction between the terminal enzyme of tetrapyrrole biosynthesis CPO (HemF), PPO (HemY) and FC (HemH) of *T. elongatus*. These enzymes catalyze the interconvertion of coproporphyrinogen III onto protoheme. The structural model based on the crystal structure of tobacco PPO by Koch and coworkers suggested a complex between these three terminal enzymes in tetrapyrrole biosynthesis (Koch *et al*., 2004). According to this model the intermediate protoporphyrin IX is channelled from PPO directly to the FC. They suggested that coproporphyrinogen III oxidase is also part of this protein complex.

In order to prove the existance of such a protein complex, the three recombinant *T. elongatus* proteins HemF, HemY and HemH were produced and purified in order to obtain antibodies. Protein complex formation was studied using co-immunoprecipitation experiments. Furthermore, localization experiments were performed using double-immunogold labelled antibodies and electron microscopy.

III.2.1 Production and Purification of *T. elongatus* Recombinant Proteins

Vectors pET-22b*hemF*TE, pET32-a*hemY*TE and pET-32a*hemH*TE containing *T. elongatus hemF, hemY* and *hemH* genes were provided by Daniela Breckau (For HemF) and constructed in framework of this thesis (for HemY and HemH), respectively (II.2.2). These vectors were used to produce HemF, HemY and HemH proteins heterologously in *E. coli* cells.

III.2.1.1 Production and Purification of *T. elongatus* HemF

Production of recombinant HemF was carried out with the vector pET-22b*hemF*TE in the *E. coli* BL21(λDE3)-pLysS cells as a C-terminal His-tag fusion protein. Cultivation of this strain leads to an over-production of HemF. Cell-free extracts of this bacteria were used for purification of HemF via Ni^{2+} affinitiy chromatography. Fourty mg of HemF-containing cell-free extracts were loaded onto a 5 ml Ni-Nta-column, washed and bound proteins were eluted with 200 mM imidazole. Further purification was performed via 10 min heating of *T. elongatus* HemF containing fractions at 55 ^{o}C and subsequent collection of precipitated *E. coli* protein via

centrifugation (*T. elongatus* proteins optimal temperature is 55 °C). The solutions were identified by SDS-PAGE. The results are shown in figure 26.

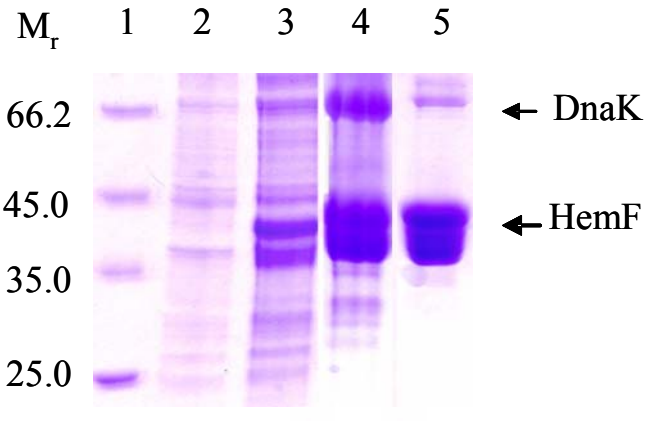

Figure 26: Production and purification of recombinant *T. elongatus* HemF. Proteins were separated by 12 % PAGE as described in MATERIALS AND METHODS and visualized by staining with Coomassie Brilliant Blue. Lane 1 shows the proteins of the molecular weight marker, the respective relative molecular masses [x10^3] are indicated. Lanes 2 and 3 show the crude cell free extract of *E.coli* BL21(λDE3)-pLysS carrying pET-22b*hemF*TE before (lane 2) and after (lane 3) induction with 500 µM IPTG. Lane 4 contains the semi-purified His-HemF fusion protein after the Ni^{2+}-affinity chromatography. Lane 5 contains purified His-HemF fusion protein that was purified via sedimentation of heat-labile proteins at 55 °C.

SDS-PAGE revealed a protein (lane 5, fig. 26) with a relative molecular mass of about 41.000 which corresponded to the calculated molecular mass of the expected His-tagged HemF. From 1 liter culture medium, HemF was purified in a volume of 4 ml with a protein concentration of 1.5 mg/ml. The additional protein(s) migrating below HemF in the gel most likely belong to degradation products of HemF. The other predominant protein of about 70 kDa in the gel was confirmed to be chaperon DnaK from *E. coli*. DnaK was identified by N-terminal sequencing of the protein (data not shown). The additional heating step of the HemF-fraction (as shown in lane 4) resulted in the partial sedimentation of the *E. coli* protein DnaK (lane 5), while HemF from *T. elongatus* remained the predominant protein of this fraction. The such purified HemF was then used for generating antibodies.

III.2.1.2 Production and Purification of *T. elongatus* HemY

Recombinant *T. elongatus* HemY was produced as a His-tag fusion protein in *E. coli* strain BL21-Codon-Plus(DE3)-RIL carrying vector pET32-a*hemY*TE. Cultivation of this strain led to an overproduction of HemY. Since, HemY is a membrane associated protein, the majority (≥ 90%) of the produced HemY was found in the insoluble membrane fractions. Attempts to solubilize

HemY out the membrane fractions by 8 M urea were only partly successful. Moreover, refolding of denatured HemY led to loss of enzyme activity (data not shown).

In an alternative approach to solubilize HemY 100, mg HemY containing *E. coli* host cells were disrupted by sonication and then the cell debris was resolved in isolation buffer (2 M urea, 20 mM Tris pH 7.2, 500 mM Nacl, 0.2% (w/v) Triton X-100) and further sonicated. After centrifugation, the pellet was resolved in 100 mM Tris pH 8.0 and sonicated again. The solubilized proteins were identified by SDS-PAGE. The results are shown in figure 27.

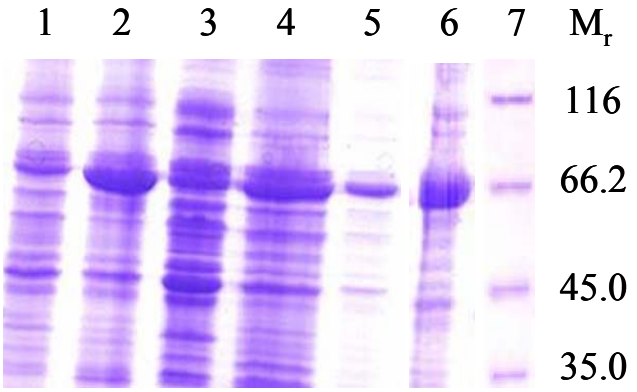

Figure 27: Production and solubilization of recombinant *T. elongatus* HemY. Proteins were separated by 12 % PAGE as described in MATERIALS AND METHODS and visualized by staining with Coomassie Brilliant Blue. Lanes 1 and 2 show the crude extract of *E.coli* BL21-Codon-Plus(DE3)-RIL carrying pET-32-a*hemY*TE before (lane 1) and after (lane 2) induction with 500 µM IPTG. Lanes 3, 4 and 5 contain the first, second and third soluble fractions (procedure, see text), respectively. Lane 6 contains the residual membrane fraction. Lane 7 shows the proteins of the molecular weight marker, the respective relative molecular masses [x10^3] are indicated.

Results showed that this method was successful to solubilize approximately 20% of produced HemY. Final purification of the collected soluble HemY was been performed via Ni^{2+}affinitiy chromatography.

For this purpose about 20 mg of HemY-containing soluble fractions were loaded onto a 5 ml Ni-Nta-column, washed and bound proteins were eluted with 150 mM imidazole. Eluates were collected and analyzed by SDS-PAGE analysis.

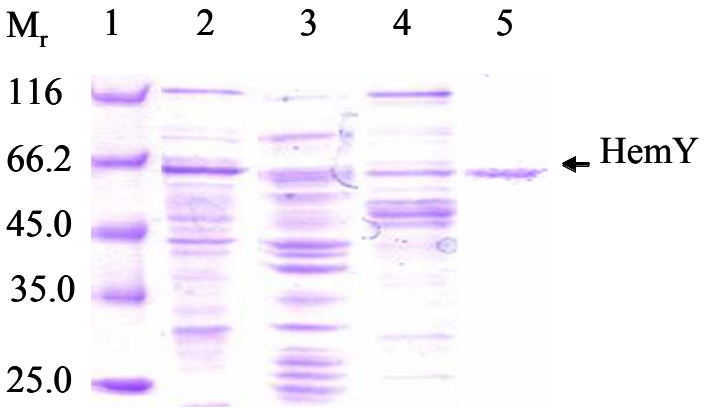

Figure 28: Purification of soluble recombinant *T. elongatus* HemY using Ni^{2+} affinity chromatography. Proteins were separated by 12 % PAGE as described in MATERIALS AND METHODS and visualized by staining with Coomassie Brilliant Blue. Lanes 1 shows the proteins of the molecular weight marker, the respective relative molecular masses [$x10^3$] are indicated. Lane 2 contains the collected soluble fractions (figure 27, lanes 3, 4 and 5) that were loaded onto the column. Lane 3 shows the flow through. Lane 4 shows the proteins belonging to the pre-elution step with 120 mM imidazole. Lane 5 shows the 150 mM imidazole eluate that contains the purified His-HemY fusion protein.

Figure 28 shows that soluble HemY was purified by Ni^{2+} affinity chromatography but its quantity and concentration was low (about 4 mg at a concentration of 0.3 mg/ml). HemY activity analysis showed that the collected soluble HemY was active (see figure 32). Several different attempts to further concentrate HemY-protein fractions were unsuccessful (data not shown).

The most effective enrichment of soluble and active HemY was achieved by using Magne His™ Ni-Particles (Promega). One hundred mg HemY containing cell-free extracts were subjected to Magne His™ Ni-Particles according to the manufacturer´s instructions and bound proteins were eluted with elution buffer containing 1 M imidazole. Eluates were analyzed by SDS-PAGE analysis and results are shown in figure 29.

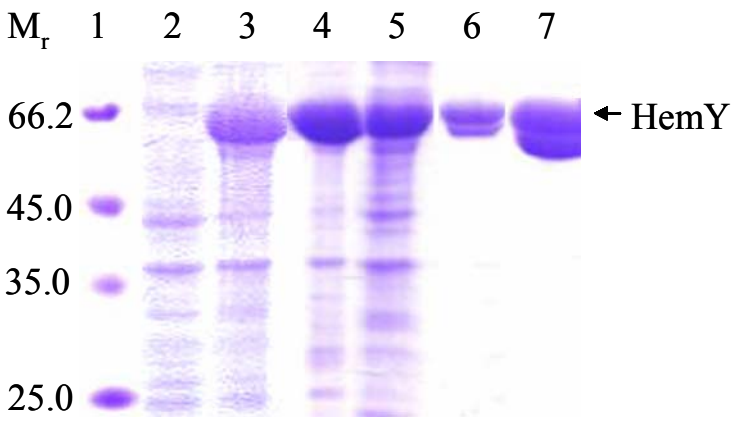

Figure 29: Purification and concentration of recombinant *T. elongatus* HemY by Magne His™ Ni-Particles and DEAE sepharose column chromatography, respectively. Proteins were separated by 12 % PAGE as described in MATERIALS AND METHODS and visualized by staining with Coomassie Brilliant Blue. Lane 1 shows the proteins of the molecular weight marker, the respective relative molecular masses [x10^3] are indicated. Lanes 2 and 3 show the crude extract of *E.coli* BL21-Codon-Plus(DE3)-RIL carrying pET-32-a*hemY*TE before and after induction of gene expression with IPTG. Lane 4 contains the collected proteins via magnet particles. Lane 5 consists of the supernatant of Magnet beads (lane 4). Lane 6 shows the eluted protein from magnet beads with 1 M imidazole contains elution buffer. Lane 7 shows the purified HemY (lane 6) that was concentrated by DEAE column chromatography.

Results of the purification of the Ni^{2+} affinity chromatography showed that 25 mg of active HemY were eluted (fig. 29, lane 6) at a concentration of 1.5 mg/ml. This protein fraction was further concentrated by a DEAE sepharose column chromatography. HemY was loaded at low salt conditions (50 mM NaCl) onto a 1 ml DEAE sepharose column and bound protein was eluted at 1 M NaCl. The eluted fraction was analyzed by SDS-PAGE (fig. 29, lane 7). A considerable concentration effect of 5-fold was achieved by using DEAE chromatography to yield 8 mg/ml of HemY. SDS PAGE analysis revealed a double band corresponding to a protein of the relative molecular mass of 65.000, which is in good agreement of the calculated molecular mass of the His-tagged HemY. N-terminal protein sequencing confirmed both proteins are *T. elongatus* HemY (data not shown). The purified HemY protein was then used for generating antibodies and analyzed in protein complex studies.

III.2.1.3 Production and Purification of *T. elongatus* HemH

Recombinant *T. elongatus* HemH was produced as a His-tag fusion protein in *E. coli* BL21-Codon-Plus(DE3)-RIL cells carrying vector pET-32a*hemH*TE. HemH, like HemY, is a membrane protein. To increase the percentage of soluble protein, after induction of gene expression with IPTG for 2.5 h at 37 °C, the cells were incubated overnight at 25 °C in LB medium including 100 µg/ml amp, 34 µg/ml cm and 10 µg/ml tet. Figure 30 provides

documentation of the HemH production. SDS-PAGE analysis of the protein fraction obtained after induction of gene expression revealed a single band corresponding to a protein with a relative molecular mass of about 60.000, which is in good agreement with the calculated molecular mass of the His-tagged HemH.

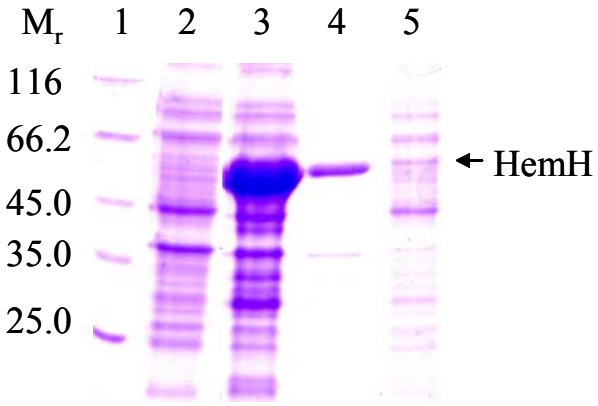

Figure 30: Production of recombinant *T. elongatus* HemH. Proteins were separated by 12 % PAGE as described in MATERIALS AND METHODS and visualized by staining with Coomassie Brilliant Blue. Lane 1 shows the proteins of the molecular weight marker, the respective relative molecular masses [x10^3] are indicated. Lanes 2 and 3 show the crude extract of *E.coli* BL21-Codon-Plus(DE3)-RIL carrying pET-32a*hemH*TE before and after induction of gene expression with 500 µM IPTG, respectively. Lanes 4 and 5 compare the insoluble fraction (lane 4) with the soluble fraction (lane 5).

Figure 30 shows about 95% of the produced HemH is found in the insoluble membrane fractions. In order to solubilize HemH, the insoluble protein fraction from *E. coli* grown in 1 liter culture medium was resuspended in fresh binding buffer containing 0.2% Triton ®X-100 (II.6.4.3**),** sonicated and centrifuged again. This step was repeated 3 times and the supernatants were collected (lanes 2-4, figure 31). Subsequently, the solubilized proteins containing HemH were loaded onto 2 ml cobalt-sepharose column and bound proteins were eluted with 140 mM imidazole. Figure 31 shows the solubilized and purified His-tag protein of HemH.

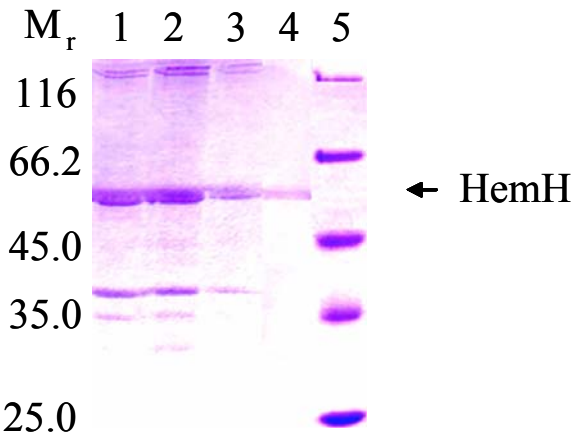

Figure 31: Solubilization and purification of recombinant *T. elongatus* HemH by cobalt-sepharose chromatography. Proteins were separated by 12 % PAGE as described in MATERIALS AND METHODS and visualized by staining with Coomassie Brilliant Blue. Lanes 1-3 show the soluble HemH after the in text outlined solubilization procedures. Lane 4 contains the purified soluble His-HemH after the the cobalt-affinity chromatography. Lane 5 shows the proteins of the molecular weight marker, the respective relative molecular masses [x10^3] are indicated.

According to this purification, it was possible to isolate approximately 0.5 mg of pure HemH protein out of 200 ml *E. coli* cell culture. The thus purified HemH protein was then used for HemH activity studies as well as for generating antibodies.

III.2.2 Determination of *T. elongatus* HemY and HemH Activity

The thermophilic cyanobacterium *T. elongatus* has an optimal growth-temprature of 55 - 60 ^{o}C (DSMZ, Braunschweig, Germany). Based on the information available for proteins from thermophilic bacteria about stability and enzymatic catalysis at high temperatures (Ladenstein and Antranikian, 1998), we decided to evaluate the enzyme activities of the recombinant *T. elongates* proteins HemY and HemH at 60 ^{o}C.

III.2.2.1 Determination of *T. elongatus* HemY Activity

The oxygen-dependent PPO assay was developed for mammalian cells by Brenner and Bloomer (1980). In this assay corprogen III is converted into protogen IX by the enzyme coprogen III oxidase (HemF). Then protogen IX is oxidized to proto IX by the addition of 0.5 µM protogen IX oxidase (HemY) or H_2O_2 as control reaction. Excitation of the product proto IX at a wavelength of 409 nm resulted in an emission at 633 nm which was detected fluorimetrically and was therefore clearly distinguishable from non fluorescent protogen. Formation of proto was

determined by the increase of the fluorescence intensity observed at 633 nm (see II.6.7.3 in materials and methods).

With regard to protein thermostability in thermophilic microorganisms (Kumar, S. and Nussinov, R., 2001), *T. elongatus* HemY activity testing was performed under two different conditions: once with recombinant *T. elongatus* HemY incubated at 60 °C for 10 min prior to the activity analysis. As a control, untreated HemY was used. In order to compare the measured activity parameters, the results are shown in figure 32.

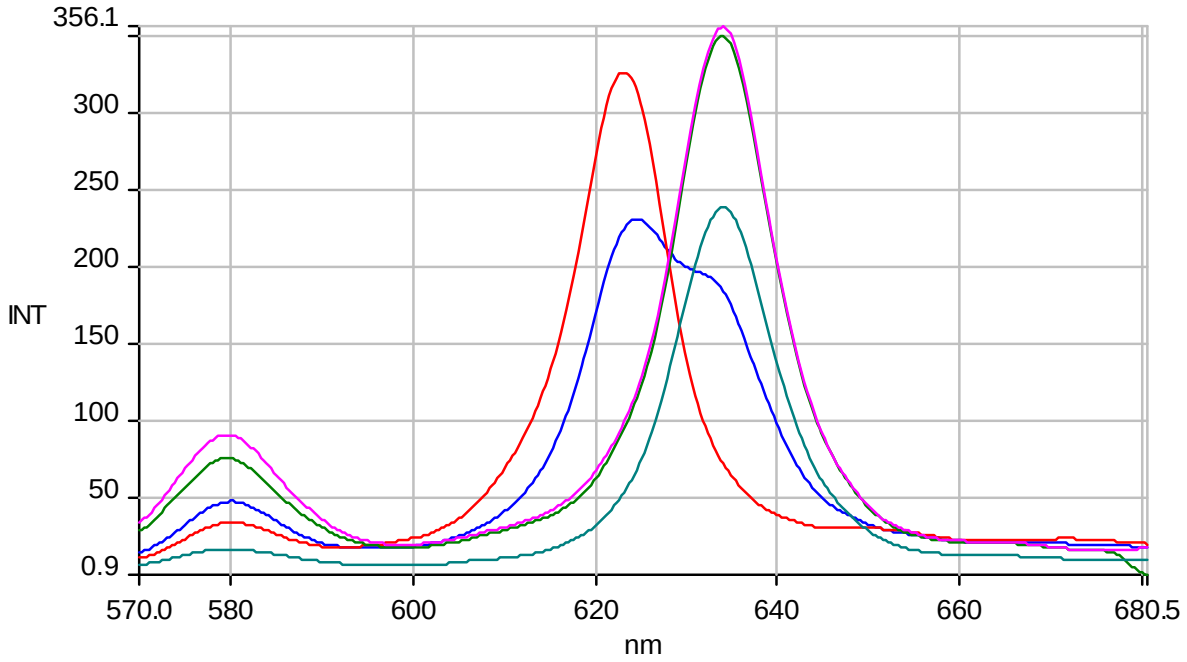

Figure 32: HemY activity test and comparison of the amounts of detected protoporphyrin IX after enzymatic oxidation of protoporphyrinogen by recombinant heated and non-heated *T. elongatus* HemY. A standard activity assay was carried out as outlined in MATERIALS AND METHODS, containing of 334 nM HemF and 20 µM coprogen in kinetic buffer. Solutions were incubated at 37 °C for 30 min under rigorous shaking at 1000 rpm in the dark. Reactions were continued by the addition of 0.5 µM protoporphyrinogen IX oxidase or H_2O_2 (as control reaction). After 10 min oxidation, the amounts of protoporphyrin IX formed during each treatment were determined by fluorimetric detection at the characteristic emission wavelength of 633 nm. _ Coproporphyrinogen, HemF and H_2O_2. _ Coproporphyrinogen and HemY. _ Coproporphyrinogen and HemF. _ Coproporphyrinogen, HemF and HemY. _ Coproporphyrinogen, HemF and heat-treated HemY.

The emission peak observed had a maximum at 633 nm which is characteristic for fluorescence properties of proto corresponding to data from Sano and Granick (1961).

Comparison of the emission peaks at 633 nm revealed that the induced heat-treatment of *T. elongatus* HemY did not alter enzyme activity. However, active *T. elongatus* HemY was purified.

III.2.2.2 Determination of *T. elongatus* HemH Activity

In order to determine ferrochelatase activity which catalyzes the insertion of ferrous ion into the porphyrin macrocycle to form protoheme IX, the *T. elongatus* HemH reaction was followed spectrometrically. After incubation of 100 µM proto with 100 nM HemH the specific activity was monitored by recording the disappearance of the protoporphyrin fluorescence at 633 nm (III.2.2.1). *T. elongatus* HemH activity assay was performed under two different temprature conditions: once HemH was incubated at 60 °C for 10 min prior to the activity analysis. As a control, HemH stored at RT was used. In order to compare measured the activity parameters, the results are shown in figure 33.

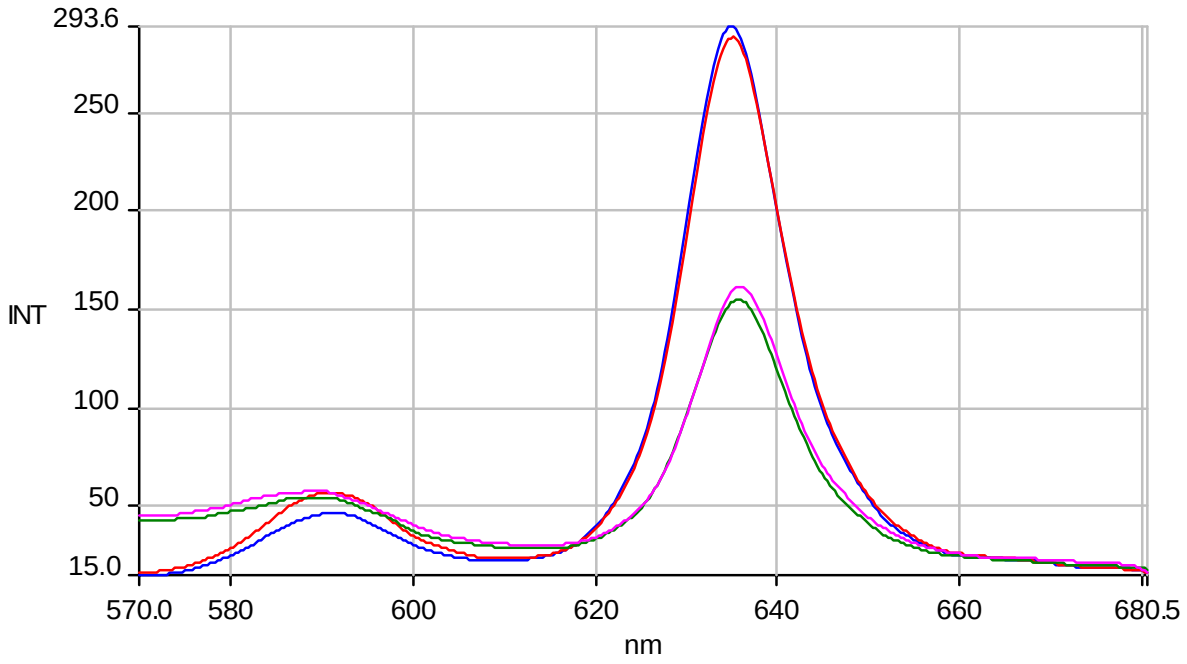

Figure 33: HemH activity test and comparison of the amounts of protoporphyrin IX decreasing after metal insertion into protoporphyrin by recombinant heated and non-heated *T. elongatus* HemH. A standard activity assay was carried out as outlined in MATERIALS AND METHODS. 36 µl Protoporphyrin solution was added to the 600 µl of standard buffer. The reaction was started by the addition of 100 nM HemH. The decrease of the fluorescence at 633 nm corresponding to the protoporphyrin substrate after HemH addition, determined the reaction velocity. _ Standard buffer and protoporphyrin. _ Standard buffer, protoporphyrin and heated HemH. _ Standard buffer, protoporphyrin and HemH. _ Standard buffer, protoporphyrin and additional standard buffer (negative control).

Figure 33 shows the results of the comparative activity analysis between heat-treated HemH and HemH tested at RT. Upon addition of HemH the emission peak at 633 nm of proto decreased.

The blue and red peaks show the emission peaks of proto prior to the activity assay, while the pink and green peaks correspond to the decreased emission when assayed with HemH at RT

(pink) and heat-treated HemH (green). As it was the case for HemY, heat-treatment of HemH did not alter enzyme activity, either.

III.2.3 Determination of Kinetic Parameters (K_m, v_{max}) of *T. elongatus* HemY by Fluorescence Stopped Flow Spectrometery

A continuous spectrofluorimetric PPO-activity assay was originally developed by Brenner and Bloomer (1980). Excitation of the product proto at a wavelength of 409 nm results in an emission at 633 nm which was detected fluorimetrically and was therfore clearly distinguishable from the substrate protogen as this revealed no spectroscopic properties.

In a Jasco 810 stopped-flow spectrometer a 10 ml syringe was filled with a solution containing 60 µl protoporphyrinogen solutions with concentration of 460, 230, 115, 57.5 and 28.75 µM and 5 ml kinetic buffer. The 1 ml syringe was filled with the purified *T. elongatus* protoporphyrinogen IX oxidase at a concentration of 0.1 mg/ml.

The solutions were mixed in 5 milliseconds with a mixing ratio of 1:5 (enzyme:protoporphyrinogen) in a total volume of 304 µl in a cuvette. The change in fluorescence at 633 nm during proto production from protogen was measured over time. As negative controls, a solution of enzyme without protogen and a solution of protogen without enzyme were used. For each sample the instrument showed proto production with a relative voltage intensity comparable to the curve shown in figure 34.

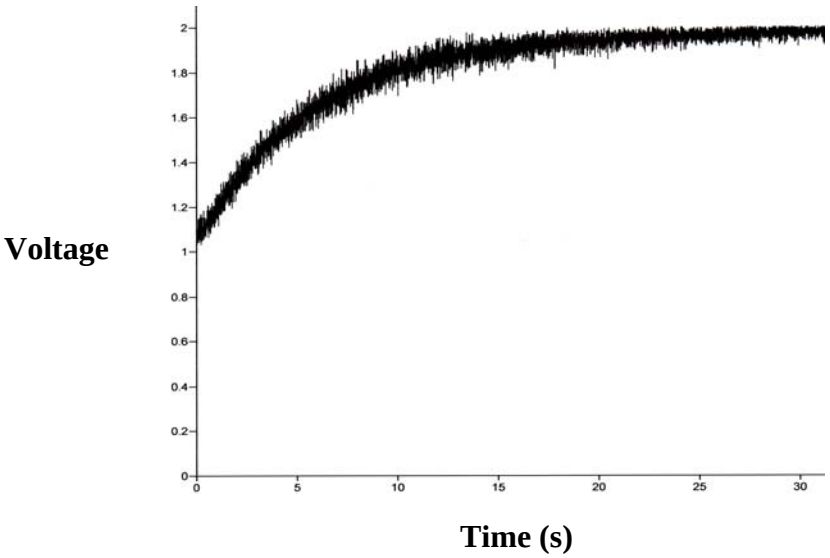

Figure 34: Fluorescence stopped flow analysis of protoporphyrin production given in relative voltage intensity at a substrate concentration of 2.72 µM using 0.242 µM purified HemY.

In order to quantify product formation a calibration curve with different concentrations of proto was prepared (II.6.9). In accordance to the calibration curve 1 µM of proto resulted in 2.5 fluorescence units (in Volt). Formation of proto was determined by the increase of the fluorescence intensity observed at 633 nm in the course of 35 s. Enzyme activity with 5 different substrate concentrations were measured. The velocity of the reaction was determined by linear regressions of saturation curves, and kinetic parameters of HemY were calculated.

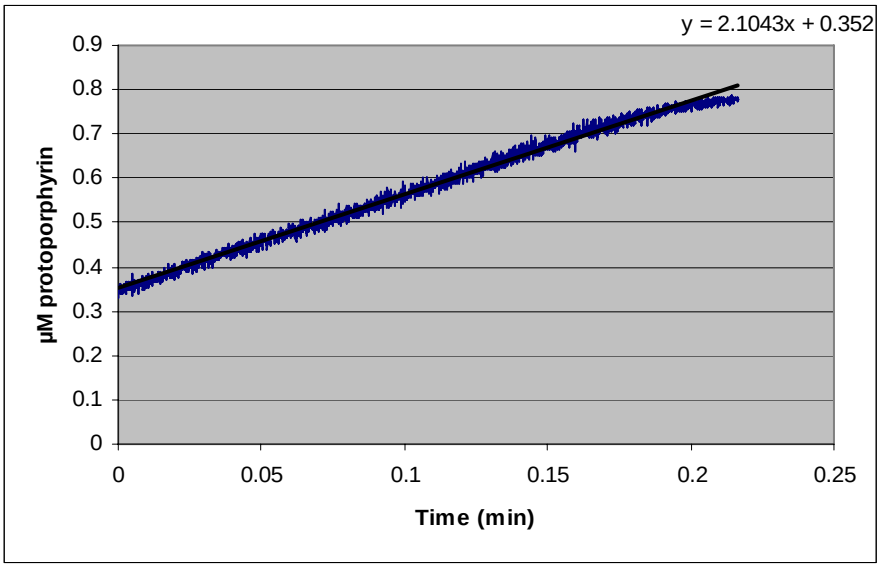

Figure 35: Linear regressions of the saturation curve for the experiment shown in Figure 34. µM protoporphyrin is plotted against reaction time.

The Michaelis Menten constant (K_m), the maximal velocity (v_{max}) and the catalytic constant (k_{cat}) were determined from substrate velocity plots by measuring the constant velocity formation of proto formation from protogen over a substrate range. Values were determined by the computerized Lineweaver-Burk interactive curve fitting using SigmaPlot 8.0 Enzyme Kinetics v1.1.

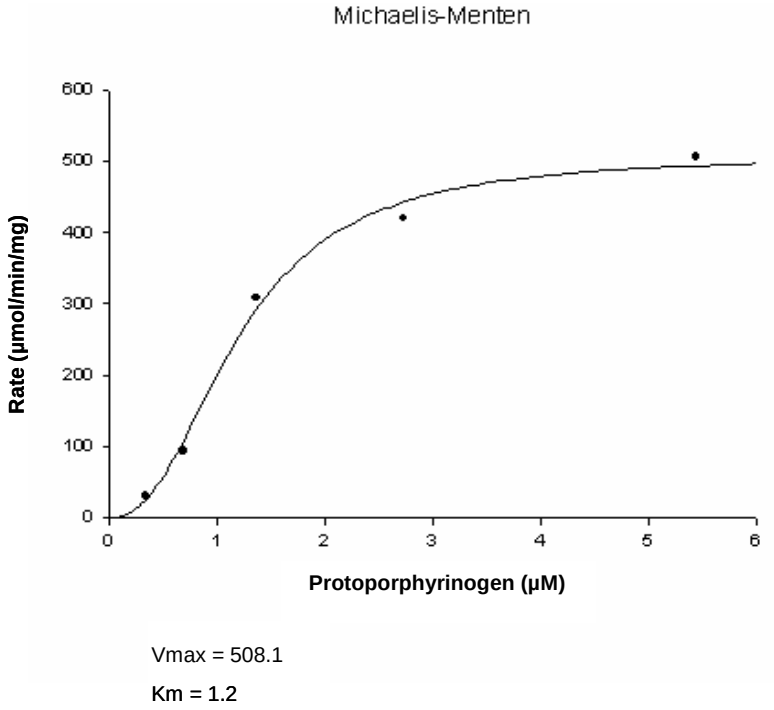

Figure 36: Michaelis Menten graph for protoporphyrinogen oxidation by *T. elongatus* HemY

The catalytic constant (k_{cat}) was calculated by dividing v_{max} by the enzyme concentration: $k_{cat} = \frac{v_{max}}{[E]}$.

Table 5: K_m, v_{max} und k_{cat} of *T. elongatus* HemY.

Protein	K_m [µM]	v_{max} [µmol min^{-1} mg^{-1}]	k_{cat} [s^{-1}]
T. elongatus HemY	1.2	508.1	1.67

The calculated K_m for *T. elongatus* was within the range of values reported for PPOs from other organisms. For example, the measured K_m for human PPO is 1.7 µM (Dailey *et al.*, 1996), for *Myxococcus xanthus* PPO 1.6 µM (Dailey *et al.*, 1996), for the extreme thermophilic bacterium *Aquifex aeolicus* PPO 2.8 µM (Wang *et al.*, 2001), for *Bacillus subtilis* 1.0 µM (Corrigall *et al.*, 1998) and for *Saccharomyces cerevisiae* PPO 0.1 µM (Camadro *et al.*, 1994).

The measured k_{cat} for human PPO is 0.175 s^{-1} (Dailey *et al.*, 1996) and for mitochondrial PPO from tobacco 6.0 s^{-1} (Heinemann *et al.*, 2007). The k_{cat} value of *T. elongatus* PPO showed an about 10 fold higher turnover compared to human PPO.

III.2.4 EPR Analysis of the HemY Cofactor FAD during Catalysis

The semiquinone forms of flavin and quinone co-factors are the main radical species known to occur in enzymatic catalysis. In order to discern whether FAD, the essential cofactor of HemY, transfers single electrons with intermediate formation of a FAD radical, EPR spectroscopy was performed in cooperation with Dr. Steve Rigby from Queen Mary´s College at the University of London. The basic physical concepts of the technique is analogous to those of NMR, but instead of the spins of the atom's nuclei, electron spins are excited. During an EPR experiment unpaired electrons are excited in a magnet field (for example by magnetic part of the radio wave). The excited electrons vibrate and are in resonance. These signals are detected by EPR spectroscopy.
T. elongatus HemY EPR spectroscopy showed less than 5% signals which does not proof of a radical mechanism (data not shown). So, occurrence of FAD electron transfer via free radical mechanisms could not be confirmed and probably electron transfer occurs via another mechanism.

III.2.5 Crystallization Attemps with the Purified *T. elongatus* enzymes

In order to study complex formation between the three terminal enzymes in tetrapyrrole biosynthesis, HemF, HemY and HemH crystallization experiments in various combinations were performed. The recombinant purified proteins were used for crystallization of the individual proteins alone or in combination with the expected complex partners, i.e, HemY/HemF, HemY/HemH and HemF/HemH, respectively.

III.2.5.1 *T. elongatus* HemY Crystallization Attemps

For HemY solutions with different pH (3.0, 4.0, 6.0, 6.8 and 8) and different protein concentrations (5 and 8 mg/ml), sitting drop crystallizations with Crystal Screens I, II and also Cryo and PEG/ION Screen crystallization kits (Hampton research) were performed. Unfortunately, after addition of the buffer solutions to the enzyme solution, HemY precipitated immediately. Only under a few conditions, crystals grew in a time period of 1 - 6 weeks at 17 ^{o}C:

Crystal Screen I: 9,15
Crystal Screen II: 2, 3, 4, 16, 17,30, 37
Crystal Screen PEG/ION: 45
Crystal Screen Cryo : -

The thus obtained crystals are shown in microscopic views in figure 37.

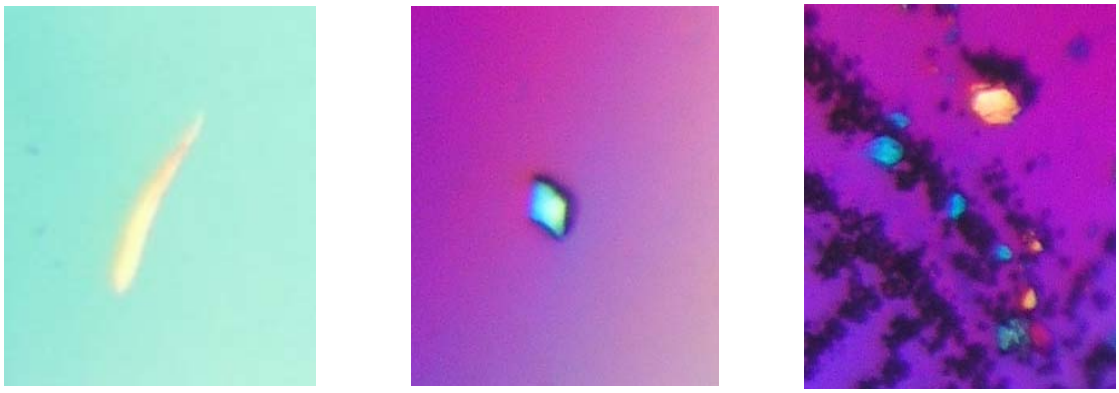

Figure 37: Three microscopic views of possible *T. elongatus* HemY crystals. In the right picture the black dots are protoporphyrin IX that was added to the protein sample to enzyme to co-crystallize the product of the enzyme reaction.

III.2.5.2 *T. elongatus* HemY and HemF Co-Crystallization

In order to solve problems like protein instablity and degradation, *T. elongatus* HemF and HemY were co-purifed and sitting drop crystallization with Crystal Screen I, II kits (Hampton research) were performed.

After incubation at 17 ^{o}C, microscopic views showed crystals under the following conditions:

Crystal Screen I: 9, 30, 43

Crystal Screen II: 1, 5, 14, 42

The obtained crystals are shown under microscopic views in fig. 38.

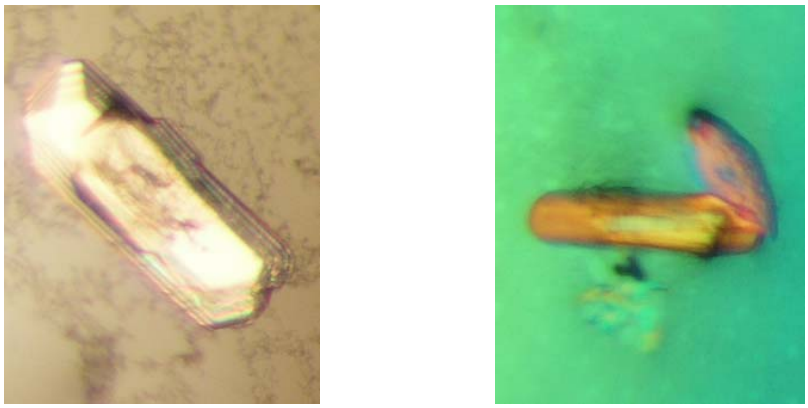

Figure 38: Two microscopic views of possible *T. elongatus* HemY and HemF crystals

Among the approximately obtained 30 crystals, which were repeatedly grown under the above mentioned conditions, the most prospective ones (~7) were harvested and subjected to x-ray analysis (HZI, Braunschweig, and Bessy, Berlin, Germany).
However, all the crystal analyzed in the x-ray beam did not result in a diffraction pattern. Thus, the obtained crystals were of poor quality and contained most likely precipitated salt crystals.

III.2.6 Co-immunoprecipitation experiments with *T. elongatus* HemF, HemY and HemH

An *in vitro* approach to study complex formation between the terminal enzymes of tetrapyrrole biosynthesis in *T. elongatus* was persued. Co-immunoprecipitation experiments with the investigated proteins with their respective antibodies were performed. Therefore, generation of polyclonal antibodies against HemF, HemY and HemH and the preparation of *T. elongatus* cell-free extracts became necessary.

III.2.6.1 Production of Antibodies against *T. elongatus* HemF, HemY and HemH

In order to perform co-immunoprecipitation analyses, purified recombinant *T. elongatus* HemF, HemY and HemH fractions were used to generate antibodies against each of the enzymes.
Therefore, solutions containing 1 mg HemF (lane 5 in figure 26), 1 mg HemY (lane 6 in figure 29) and 1 mg HemH (insoluble protein of lane 4 in figure 30 that was solubilized in 6 M urea) were sent to Eurogentec (Seraing, Belgium) for the generation of polyclonal rabbit antibodies against the recombinant *T. elongatus* proteins. The antibodies were analyzed by Western blot analysis and the specificity of antigen detection was evaluated. In figure 39 antigen recognition by these antibodies is documented.

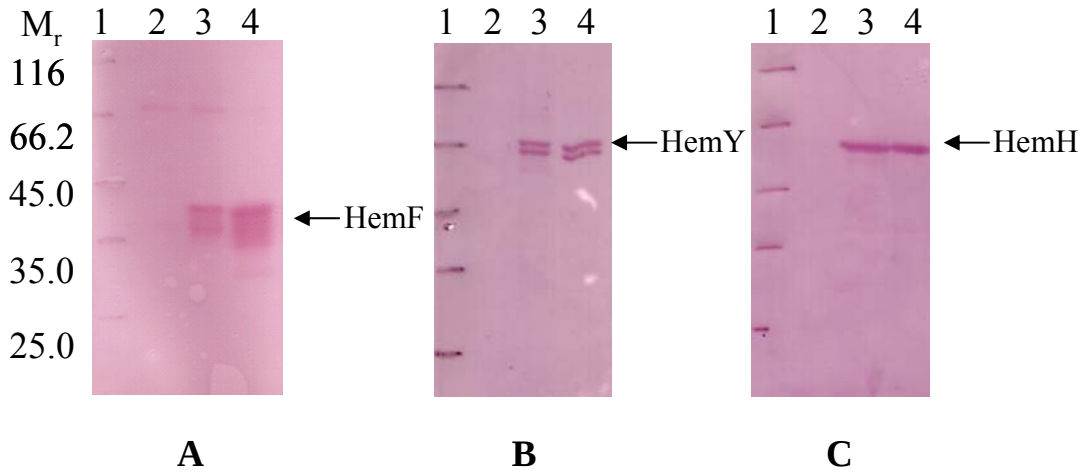

Figure 39: Detection of recombinant HemF, HemY and HemH by Western blots analysis with the corresponding polyclonal antibodies. Western-blots were performed after separation of 100 ng of each protein by SDS-PAGE at 45 mA. Proteins were detected primary with α-HemF antibody (A), α-HemY antibody (B) or α-HemH antibody (C) (1:100,000) and a secondry anti rabbit antibody (1:20,000) coupled to an alkaline phosphatase. Incubation with NBT and BCIP led to visualization of protein bands. Lanes 1 shows the proteins of the molecular weight marker, the respective relative molecular masses [$x10^3$] are indicated. Lanes 2 includes the extract of *E.coli* cells before induction of gene expression and lanes 3 and 4 contain 1 mg and 100 ng of purified recombinant HemF (A), HemY (B) and HemH (C), respectively.

The blots show that a dilution of 1/100000 of α-HemF, α-HemY and α-HemH antibodies can specifically detect 100 ng of purified recombinant HemF, HemY and HemH, respectively.

III.2.6.2 Preparation *of T. elongatus* Cell Free Extract

As described in MATERIALS AND METHODS, *T. elongatus* BP1 cells were cultivated in a 5 l fermenter at 55°C under continuous illumination from fluorescent white light in a CO_2-enriched atmosphere of 10 % for 4 days. About 5.5 g bacterial cell pellet was harvested by centrifugation. The resuspended bacterial cells were disrupted by sonication. In order to perform membrane protein solubilization, a process including the treatment of the cell free extract with a buffer containing 1% n-Dodecyl-ß,D-maltoside (Gerbu; Germany), 0.5 % Triton X-100 was performed. At last, cell debris was removed by ultracentrifugation.

III.2.6.3 Immunoprecipitation Experiments Using *T. elongatus* Cell Free Extracts

In an immunoprecipitation assay, an antibody against a specific antigen forms an immune complex with its antigen in a cell free extract.

In this work, 350 µl *T. elongatus* cell extract from 350 mg wet cells were mixed with 2.5 µl of α-HemF, α-HemY and α-HemH antibodies each. The mixtures were incubated at 4 ^oC under vigorous rotation. After 1 - 2 h, protein A sepharose^{TM} CL-4B (Amersham biosciences; Sweden)

was added to the mixtures. After 1 h incubation, the immobilized antigen-antibodies were recovered and proteins were eluted. Antibody heavy chains unfortunately result in a diffuse protein pattern at a relative molecular mass of 50.000 in SDS-PAGE and the succeeding Western blot analyses. Thus, they prevent the detection of signals for the expected immunoprecipitates of the formed HemY and α-HemY (data not shown). This problem was solved by using Seize™ X Protein A Immunoprecipitation Kit (Pierce), which successfully removed most of the antibodies heavy chains. In immunoprecipitation assays, after Western blot analysis, successful immunodetections of HemF, HemY and HemH were performed with antibodies raised against HemF, HemY and HemH, respectively (figure 40).

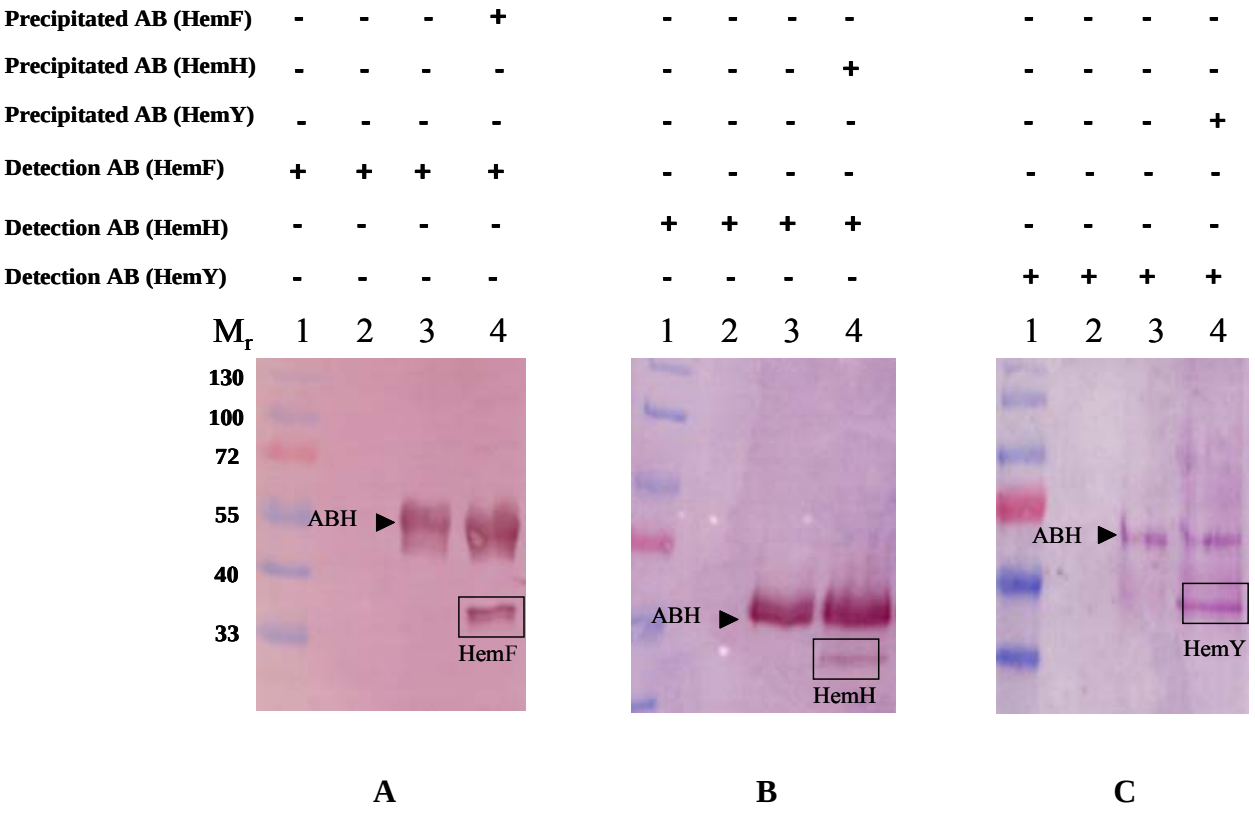

Figure 40: Detection of native HemF, HemH and HemY in *T. elongatus* cell free extract by immunoprecipitation. Western-blots were performed after separation of proteins by SDS-PAGE. Proteins were detected primary with α-HemF antibodies (A), α-HemH antibodies (B) and α-HemY antibodies (C) (1:5,000) and a secondary anti rabbit antibody (1:20,000) coupled to an alkaline phosphatase. Incubation with NBT and BCIP led to visualiation of the corresponding precipitated protein. Lane 1 shows the proteins of Page Ruler™Prestained Protein Ladder. The relative molecular masses (Mr x 10^3) of the marker proteins are given. Lane 2 consists of *T. elongatus* cell free extract and protein A sepharose. Lane 3 consists of *T. elongatus* cell free extract, pre-immune serum and protein A sepharose (negative control). Lane 4 contains *T. elongatus* cell extract, protein A sepharose and the antibodies against the protein (according to the given table, the protein presence was indicated by the + symbol).
ABH : Antibody Heavy chain.

The results of the immunoprecipitation experiment showed that the generated antibodies precipitated the respective proteins HemF, HemY and HemH from cell extract of *T. elongatus*. The control experiments with either pre-immune or protein A sepharose performed with cell free extracts showed no cross-reaction with HemF (fig. 40 A, lanes 2 and 3), HemY (fig. 40 C, lanes 2 and 3) and HemH (fig. 40 B, lanes 2 and 3), respectively.

The removal of the antibody-heavy chains was necessary in order to be able to detect the specific proteins of interest. Figure 40 lanes 4 in each panel show the results on the successful precipitation of HemF (panel A), HemY (panel C) and HemH (panel B).

III.2.7 Co-immunoprecipitation Experiments Using *T. elongatus* Cell Free Extract

In order to detect possible protein complex formation of HemF, HemY and HemH co-immunoprecipitation assays were performed. In a co-immunoprecipitation assay, the target antigen precipitated by the antibody "co-precipitates" a bound protein from the cell free extract. In this work, 350 µl *T. elongatus* cell extract from 350 mg wet cells were mixed with 2.5 µl of α-HemF, α-HemY and α-HemH antibody containing serum each. The mixtures were incubated at 4 ^{o}C under vigorous rotation. After 1 - 2 h, protein A sepharose^{TM} CL-4B (GE Healthcare; Uppsala; Sweden) was added to the mixtures. After 1 h incubation, the immobilized antigen-antibodies were recovered and proteins were eluted. Antibody heavy chains were removed by using Seize^{TM} X Protein A Immunoprecipitation Kit (Pierce). Finally immunodetection of each protein was performed by antibodies against the two other proteins (figure 41).

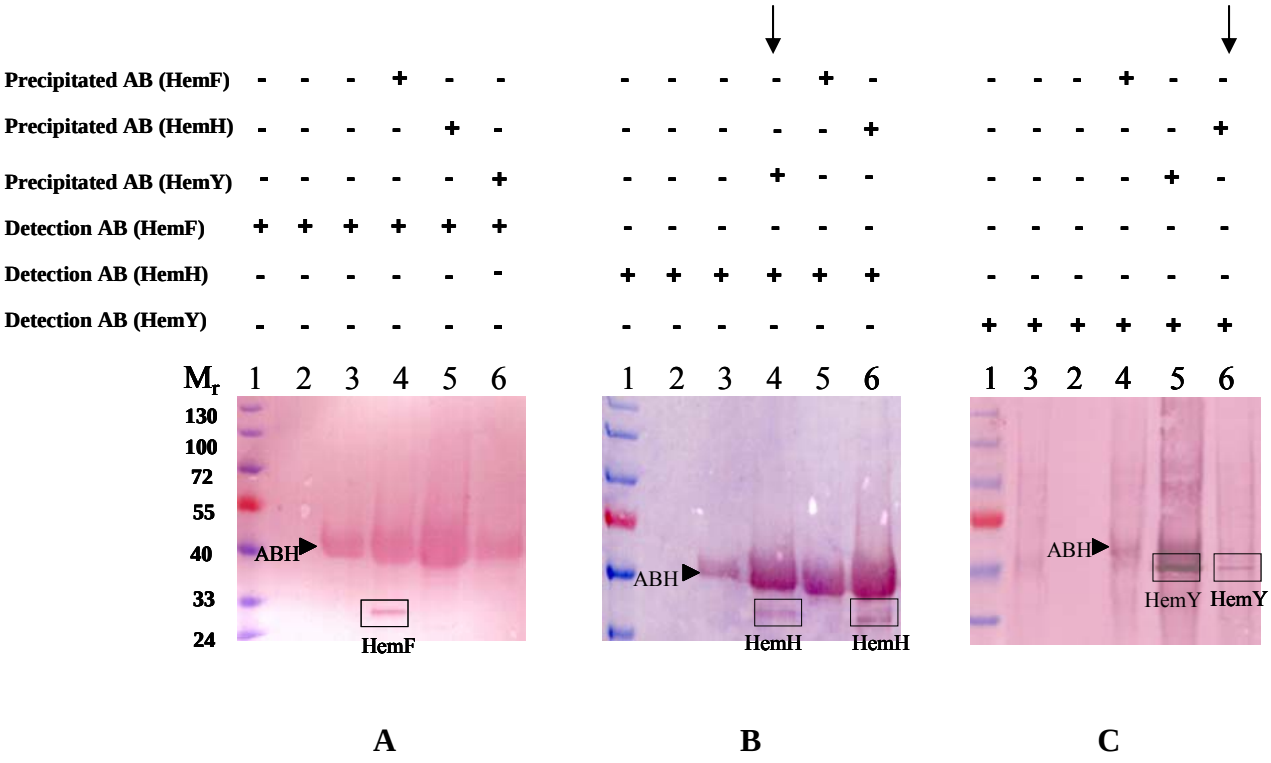

Figure 41: Detection of HemY-HemH complex in *T. elongatus* cell free extract by co-immunoprecipitation. Western-blots were performed after separation of proteins by SDS-PAGE. Proteins were detected primary with α-HemF antibody (A), α-HemH antibody (B) and α-HemY antibody (C) (1:5,000) respectively and a secondary α-rabbit antibody (1:20,000) coupled to an alkaline phosphatase. Incubation with NBT and BCIP led to exposure of protein bands. Lanes 1 shows the proteins of Page Ruler™Prestained Protein Ladder. The relative molecular masses (Mr x 10^3) of the marker proteins are given. Lanes 2 consists of *T. elongatus* cell extract and protein A sepharose. Lane 3 consists of *T. elongatus* cell extract, pre-immune serum and protein A sepharose (negative control). Lanes 4, 5 and 6 contain *T. elongatus* cell extract, protein A sepharose and antibodies against the proteins (according to the given table, presence of the protein was shown by the + symbol). Arrows indicated experiments demonstrating the HemY-HemH complex.
ABH : Antibody Heavy chain.

Blot B lane 4 in figure 41 shows HemH was detected after addition of α-HemY antibody to the cell free extract. In Blot C lane 6, HemY was detected after addition of α-HemH antibody to the cell free extract. Thus, HemY and HemH were bound to each other and were detected via the antibody against the other protein. These results confirm the existance of a complex of HemY with HemH in *T. elongatus* cells. However the existance of a complex between HemY and HemF (fig. 41, panel A, lane 6) or HemH and HemF (fig. 41, panel A, lane 5) was not detected.

III.2.8 Localization of HemF, HemY and HemH in *T. elongates* Cells with Immunogold Labelling and Electron Microscopy

In order to localize the proteins HemF, HemY and HemH as well potential complexes between them within *T. elongatus* cells, immunogold labelled antibodies against these proteins were subjected to cell slices and the results were visualized via electron microscopy. For this purpose, first *T. elongatus* cells were fixed and ultrathin sections of the cells were prepared with a diamond knife and placed on nickel grids. Figure 42 shows longitudinal and cross sections of *T. elongatus* cells.

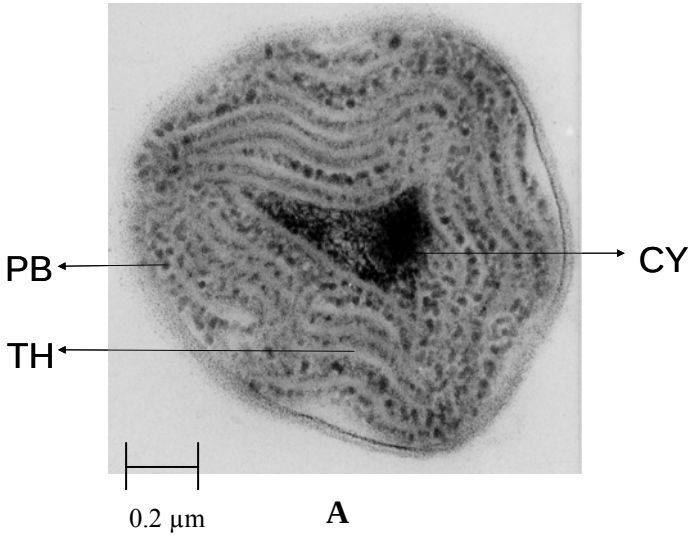

A

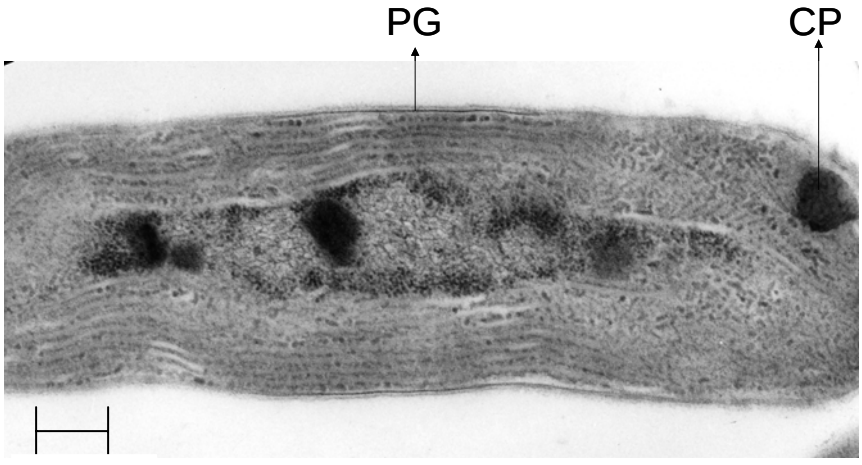

B

Figure 42: Longitudinal (A) and cross (B) thin sections of *T. elongatus* cells. Phycobilisome (PB), thylakoid membrane (TH), cytoplasm (CY), cyanophycin (CP), peptidoglycan (PG) are indicated with the arrows. Magnification of the microscopical views of cells was 3000; size bars are indicated.

Photos were taken at a magnification of 3000 fold with a Zeiss transmission electron microscope EM910. In these sections, different subcellular structures like thylakoid membrane (TH), cytoplasm (CY), cyanophycin (CP), peptidoglycan of *T. elongatus* cell became visible by the electron microscopic approach.

The labelling procedure was started by incubation of the sections with one of purified antibodies (α-HemF, α-HemY or α-HemH). After washing, the sections were incubated in protein A/G gold and washed again. Figure 43 panels A, B and C show the sections of cells after incubation with α-HemF, α-HemY and α-HemH antibodies, respectively. In the case of a specific interaction of a gold labelled antibody with its protein, black dots on an ultrathin section of the *T. elongatus* cell indicate the localization of the protein within the cell.

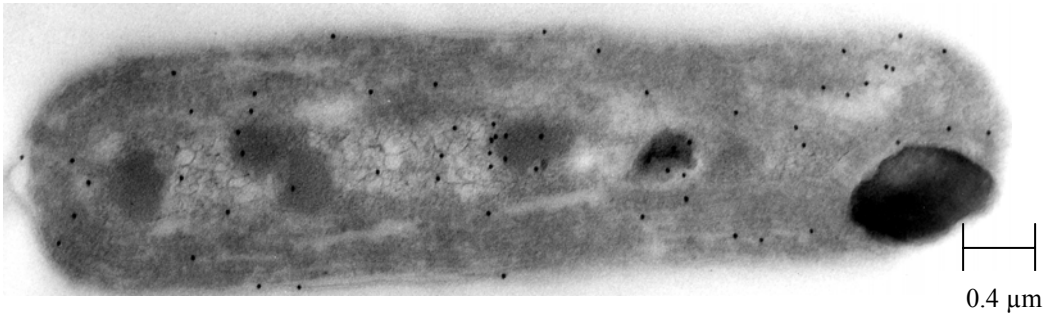

A

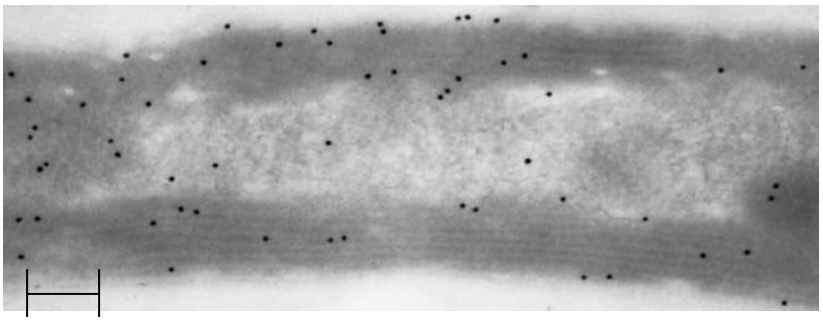

B

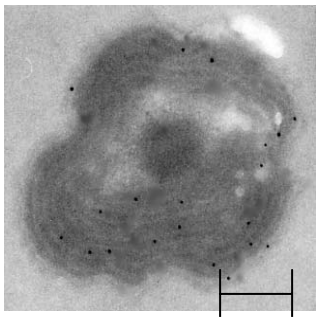

C

Figure 43: Cellular localization of *T. elongatus* HemF, HemY and HemH are shown. Sections of *T. elongatus* cells after immunogold labelling. A: Incubation with gold labelled antibody raised against HemF. B: With gold labelled antibody raised against HemY. C: With gold labelled antibody raised against HemH. Magnification of the microscopical views of cells was 3000; size bars are indicated.

Fig. 43 shows the result of the localization of HemF, HemY and HemH within a *T. elongatus* cell. For detection the sections were examined in a Zeiss transmission electron microscope EM910 with an acceleration voltage of 80 kV. Images were recorded onto negative film (Kodak SO-163). While HemY as well as HemH were found localized mostly in the thylakoid membranes (fig 43, panels B and C), HemF was distributed throughout the whole cell, i.e. also in the cytoplasma (fig 43, panel A).

III.2.9 Detection of HemY – HemH Complexes by Double-Immunogold Labelling and Electron Microscopy

For the determination of a possible complex formation *in vivo* between the terminal enzymes in tetrapyrrole biosynthesis, the localization of HemY and HemH in a *T. elongatus* cell was visualized after performing a double labelling experiment. First, HemH was detected with the α-HemH antibody followed by small protein A/G-gold particles (10 nm in diameter). For blocking bound α-HemH antibodies which might not be decorated by protein A/G gold-particles the FC-parts of these antibodies were blocked with protein A. Subsequently, the α-HemY antibody was applied to the identical side of the ultrathin section, followed by an attachment of large protein A/G gold-particles (15 nm in diameter). Complexes between these two enzymes were indicated by the close distance between the different sized gold-particles (black circles in Fig. 43, panel C and D). The identical experiment was performed with the α –HemF as first applied antibody and either α –HemY or α-HemH as second antibody (fig. 43, panel A and B). For detection the sections were examined in a Zeiss transmission electron microscope EM910 with an acceleration voltage of 80 kV. In the resulting images, dots with different sizes belonging to either 10 nm or 15 nm gold particle were detected. Four electron microscopic images of *T. elongatus* sections after double-immunogold labelling are shown in figure 44.

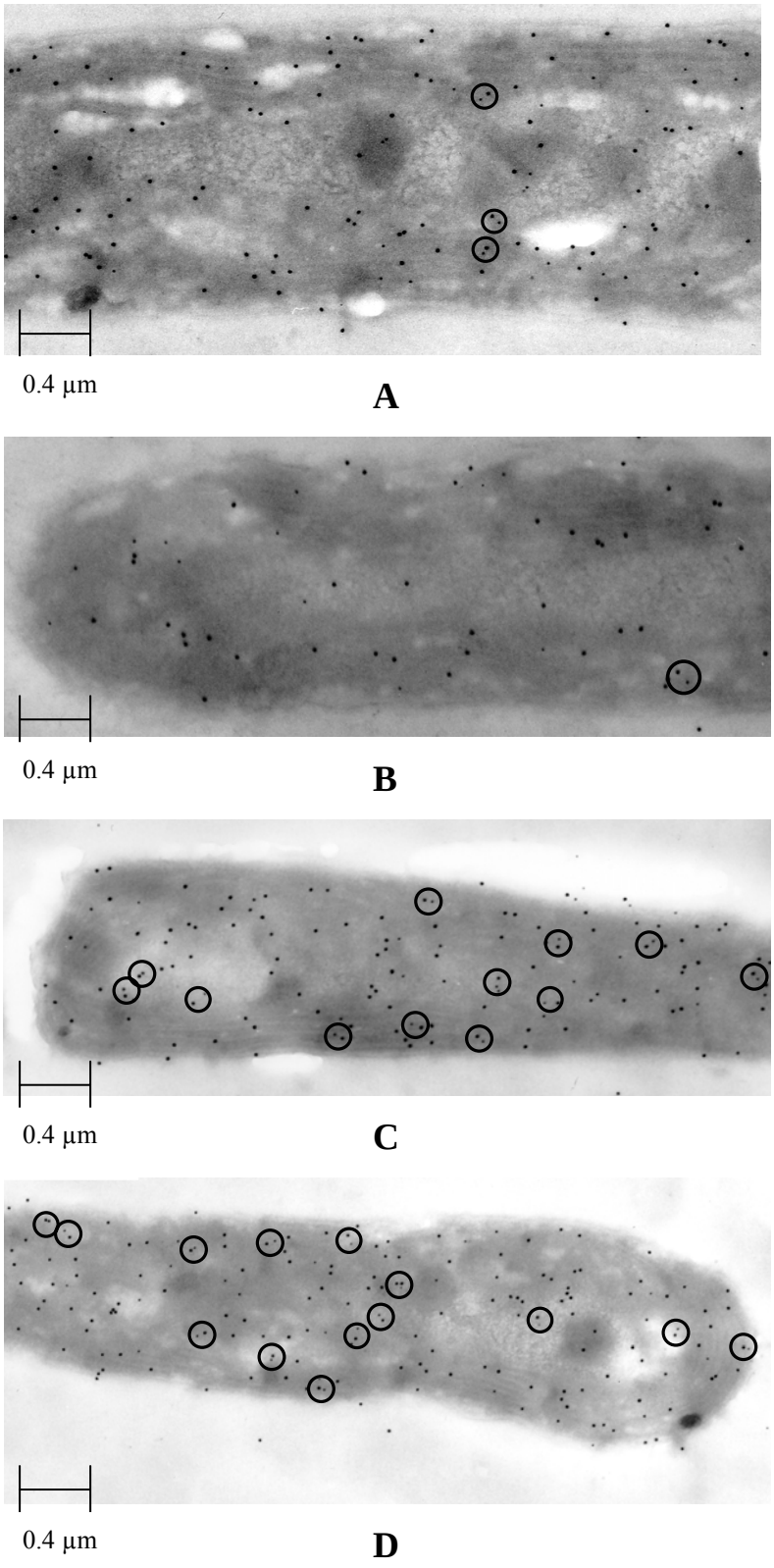

Figure 44: Detection of HemY–HemH complex in *T. elongatus* cells with double-immunogold labelling. Circled areas represent probable complexes of two proteins. The following antibody combinations were applied. A: Gold labelled antibodies raised against HemF (15 nm) and HemH (10 nm), B: Gold labelled antibodies raised against HemF (15 nm) and HemY (10 nm). C and D: Gold labelled antibodies raised against HemY (15 nm) and HemH (10 nm). Magnification of the microscopical views of cells was 3000; size bars are indicated.

By comparing fig. 44, panels A and B with panels C and D, the existance of a complex between HemY and HemH was confirmed. Panel C and D demonstrate that more than 60% of the detected HemH proteins are in close vicinity to HemY in the cells. In contrast to that panel A and B show that only about 10% of HemH and HemY co-localize with HemF making complex formation with HemF very unlikely.

III.2.10 The HemY-HemH Complex in *T. elongatus*

During the last decade, many scientific approaches were performed in order to elucidate a probable protein complex between the terminal enzymes in tetrapyrrole synthesis. For mammalian cells it was demonstrated that PPO and FC are both located in the mitochondria. PPO is associated with the mitochondrial inner membrane, and its active site faces the intermembrane space, whereas FC is present as an integral component of the mitochondrial inner membrane with its active site on the matrix side (Dailey, 2000). The subcellular localizations of PPO and FC in plant and algal cells are less well characterized. Different isoforms of PPO and FC have been reported to be targeted to either chloroplasts or mitochondria after their synthesis in the cytoplasm (Lermontova *et al.*, 1997; Watanabe *et al*., 2001; Suzuki *et al*., 2002). In *Chlamydomonas reinhardtii,* a motile single celled green alga, PPO and and FC are located only associated to the chloroplast membrane (Van Lis *et al*., 2005).

Due to the phototoxic nature of the substrate intermediates of CPO, PPO and FC, substrate channelling was proposed based on crystal structure solved by Koch and coworkers. Earlier data analyzing the kinetic determinants of eukaryotic PPO and FC suggestedd that substrate channelling could occur between these enzymes (Ferreira *et al*., 1988). Moreover it was previously stated by a study of *B. subtilis* ferrochelatase mutants that FC is involved in substrate channelling (Olsson *et al*., 2002).

In this work, localization experiments showed for the first time that in the cyanobacterium *T. elongatus* HemF is distributed throughout the whole *T. elongatus* cell, while HemY as well as HemH could be localized within the thylakoid membranes.

Further *in vitro* co-immunoprecipitation analyses described in this thesis proved the existance of a protein complex between HemY and HemH, but not for HemF with either HemY or HemH. These observations confirmed the existance of this HemY and HemH complex. Thus, these results are in a good agreement with the assumption that it is important for the organism to keep the protoporphyrin intermediate at a low concentration and prevent solvet exposure.

So, with these informations we can propose a model for localization of these three enzymes in the cyanobacterium *T. elongatus*. Here we compare the localization for a eukaryotic and a cyanobacterial cell to our understanding based on the *in vitro* and *in vivo* results (fig. 45 and 46).

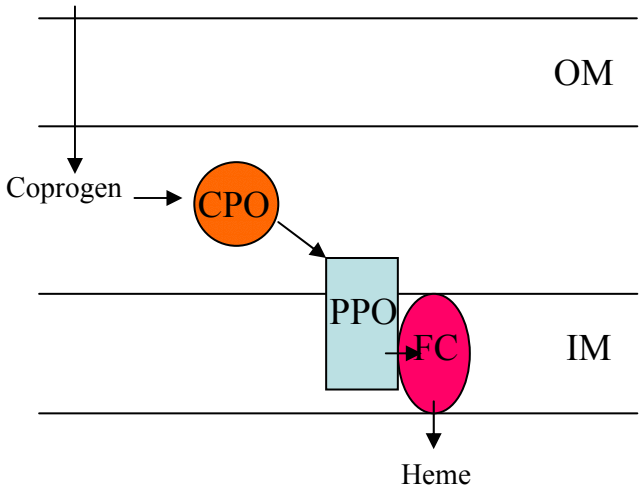

Figure 45: A proposed model for the eukaryotic terminal three enzymes of the heme biosynthetic pathway localized in the mitochondria. CPO: coprotoporphyrinogen oxidase; PPO: protoporphyrinogen oxidase; FC: ferrochelatase; OM: outer mitochondrial membrane; IM: inner mitochondrial membrane.

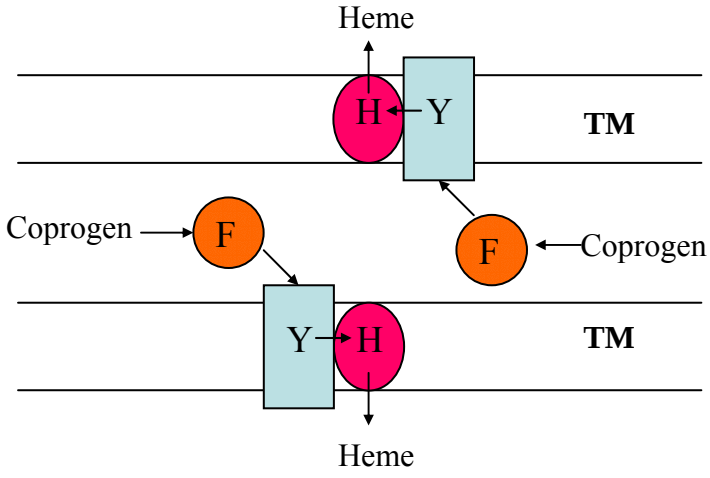

Figure 46: A proposed model for the cyanobacterium terminal three enzymes of the heme biosynthetic pathway. F: coprotoporphyrinogen oxidase; Y: protoporphyrinogen oxidase; H: ferrochelatase; TM: thylakoid membrane.

Thus, the existance of HemY-HemH complex was verified for the first time by two independent biochemical techniques: 1. Co-immunoprecipitation experiments using antibodies directed against recombinantly produced *T. elongatus* HemY and HemH. 2. I*n vivo* immunogold labelling experiments analyzed via electron microscopy using native *T. elongatus* cells.

IV Summary

The fidelity of protein biosynthesis is dependent on the reliable charging of each tRNA with its cognate amino acid. However, many bacteria lack a glutaminyl-tRNA synthetase. In these organisms $tRNA^{Gln}$ is initially mischarged with glutamate by a non-discriminating glutamyl-tRNA synthetase (GluRS). This enzyme thus charges both $tRNA^{Glu}$ and $tRNA^{Gln}$ with glutamate. The resulting misacylated Glu-$tRNA^{Gln}$ is then converted to Gln-$tRNA^{Gln}$ by a tRNA-dependent amidotransferase through the amide addition to the tRNA-bound glutamate. This thesis provided experimental proof that *Thermosynechococcus elongatus* GluRS is indeed a non-discriminating tRNA synthetase. For this purpose the kinetic parameters for the synthesis of Glu-$tRNA^{Glu}$ and Glu-$tRNA^{Gln}$ were determined. Therefore *T. elongatus* $tRNA^{Glu}$ and $tRNA^{Gln}$ were purified. It was shown that *T. elongatus* GluRS accommodates and charges both $tRNA^{Glu}$ as well as $tRNA^{Gln}$. Obtained results were discussed in the light of solved *T. elongatus* GluRS crystal structure.

Coproporphyrinogen oxidase (CPO), protoporphyrinogen oxidase (PPO) and ferrochelatase (FC) catalyze the three terminal steps of the heme biosynthetic pathway to form protoheme IX. For the protection of the highly toxic intermediate protoporphyrin IX, a protein complex between CPO, PPO and FC was proposed based on the solved crystal structure of tobacco PPO (Koch *et al*., 2004).

It was objective in a second part of this thesis to proof the existance and determine the localization of the proposed complex in *T. elongatus* cells. Co-immunoprecipitation experiments and double-immunogold labelling in combination with electron microscopy were employed.

First recombinant *T. elongatus* HemF (CPO), HemY (PPO) and HemH (FC) were produced and chromatographically purified subsequently, polyclonal rabbit antibodies were raised against the three enzymes. Complex formation of PPO with FC was demonstrated for *T. elongatus* cell free extracts via co-immunoprecipitation for the first time. These *in vitro* findings were further confirmed using electron microscopy and double-immunogold labelled PPO and FC. PPO - FC complexes were detected in *T. elongatus* thylakoid membranes while CPO was not involved in complex formation. Obtained data lay the basis for the in-depth analysis of the cellular arrangement of tetrapyrrole biosynthetic enzymes.

V Outlook

Complex formation of Protoporphyrinogen IX Oxidase and Ferrochelatase:

In this study *in vitro* co-immunoprecipitation analyses and *in vivo* localization of PPO/FC in *T. elongatus* cells via electron microscopy proved the existance of the former hypothesized complex between these enzyme. Further studies using molecular analyses could be performed in order to reveal the surface contacts between PPO and FC. Therefore, mutagenesis analyses of the amino acid residues, which are proposed to be involved in complex formation by the structural model (Koch et al., 2004), should contribute to the elucidation of the nature of such a protein/protein formation within the thylakoid-membrane.

Additionally, the co-crystallazation experiments could be continously persued. Since both of the respective enzymes, PPO and FC, are membrane associated proteins, it could be shown that it was difficult, however possible to isolate recombinantly purified proteins at high yields and concentrations for crystallization. More attempts should be made in order to reach this goal.

The complex formation between PPO and FC is currently believed to be required, because the intermediate substrate for the ferrochelatase, i.e. protoporphyrinogen IX, is phototoxic to the cell. Thus, substrate channelling seems to be essential for the protection of the cell. During the entire tetrapyrrole biosynthesis pathway, all intermediates, when accumulated, lead to toxic stress symptoms and are, e.g. for humans, well-known for diseases called porphyrias.

So, here the question arises whether the cells protect themselves similarly to PPO and FC. Future experiments could focus on the potential complex formation between other tetrapyrrol-synthesizing enzymes, such as HemB, HemC and HemD, respectively.

VI References

Akhtar, M. (1991) Mechanism and stereochemistry of the enzymes involved in the conversion of uroporphyrinogen III into haem. In *Biosynthesis of tetrapyrroles*. (Jordan, P. M., ed.) Elsevier Science Ltd., Amsterdam, pp. 67-99.

Al-Karadaghi, S., Hansson, M., Nikonov, S., Jonsson, B. and Hederstedt, L. (1997) Crystal structure of ferrochelatase: the terminal enzyme in heme biosynthesis. *Structure* **5**, 1501-10.

Battersby, A. R. (2000) Tetrypyrroles: the pigments of life. *Nat. Prod. Rep.* **17**, 507-26. Rewiew.

Beale, S. I. and Castelfranco, P. A. (1973) ^{14}C incorporation from exogenous compounds into δ-aminolevulinic acid by greening cucumber cotyledons. *Biochem. Biophys. Res. Commun.* **52**, 143-9.

Beale, S. I. and Weinstein, J. D. (1990) Tetrapyrrole metabolism in photosynthetic organisms. In *Biosynthesis of heme and chlorophylls.* (Dailey, H. A., ed.) McGraw-Hill Publishing, New York, pp. 287-392.

Beale, S. I. and Weinstein, J. D. (1991) Biochemistry and regulation of photosynthetic pigment formation in plants and algae. *In Biosynthesis of tetrapyrroles*. (Jordan, P. M., ed.) Elsevier Science Ltd., Amsterdam, pp. 155-235.

Beale, S. I. (1993) Biosynthesis of phycobilins. *Chem. Rev.* **93**, 785-802.

Beale, S. I. and Yeh, J. I. (1999) Deconstructing heme. *Nature Struct. Biol.* **6**, 903-5.

Breckau, D., Mahlitz, E., Sauerwald, A., Layer, G. and Jahn, D. (2003) Oxygen-dependent coproporphyrinogen III oxidase (HemF) from *Escherichia coli* is stimulated by manganese. *J. Biol. Chem.* **278**, 46625-31.

Brenner, D. A and Bloomer, J. R. (1980) Fluorometric assay for measurement of protoporphyrinogen oxidase activity in mammalian tissue. *Clin. Chim. Acta.* **100**, 259–66.

Brenner, D.A. and Frasier, F. (1991) Cloning of murine ferrochelatase. *Proc. Natl. Acad. Sci. U S A.* **88**, 849-53.

Brenner, D. A., Didier, J. M., Frasier, F., Christensen, S. R., Evans, G. A. and Dailey, H. A. (1992) A molecular defect in human protoporphyria. *Am. J. Hum. Genet.* **50**,1203-10.

Bult, C. J., White, O., Olsen, G. J., Zhou, L., Fleischmann, R. D., Sutton, G. G., Blake, J. A., FitzGerald, L. M., Clayton, R. A., Gocayne, J. D., Kerlavage, A. R., Dougherty, B. A., Tomb, J. F., Adams, M. D., Reich, C. I., Overbeek, R., Kirkness, E. F., Weinstock, K. G., Merrick, J. M., Glodek, A., Scott, J. L., Geoghagen, N. S. and Venter, J. C. (1996) Complete genome sequence of the methanogenic archaeon, *Methanococcus jannaschii*. *Science.* **273**, 1058-73.

Camadro, J. M., Thome, F., Brouillet, N. and Labbe P. (1994) Purification and properties of protoporphyrinogen oxidase from the yeast Saccharomyces cerevisiae. Mitochondrial location and evidence for a precursor form of the protein. *J. Biol. Chem.* **269**, 32085-91.

Carrio, M. M., Villaverde, A. (2001) Protein aggregation as bacterial inclusion bodies is reversible. *FEBS Lett.* **489**, 29-33.

Chadwick, D. J. and Ackrill, K. (eds.). (1994). *The Biosynthesis of Tetrapyrrole Pigments*. Ciba Foundation Symposia, 180, Wiley and Sons, Chichester, UK.

Chang, C. K. (1994) Haem *d*1 and other haem cofactors from bacteria. In *The biosynthesis of tetrapyrrole pigments; Ciba Foundation Symposium 180*. (Chadwick, D. J. and Ackrill, K., eds.) Wiley, Chichester, pp. 228-46.

Corradi, H. R., Corrigall, A. V., Boix, E., Mohan, C. G., Sturrock, E. D., Meissner, P. N. and Acharya, K. R. (2006) Crystal structure of protoporphyrinogen IX oxidase from *Myxococcus xanthus* and its complex with the inhibitor aciflurfen. *J. Bio. Chem.* **281**, 38625-33.

Corrigall, A. V., Siziba, K. B., Maneli, M. H., Shephard, E. G., Ziman, M., Dailey, T. A., Dailey, H. A., Kirsch, R. E. and Meissneer, P. N. (1998) Purification of and kinetic studies on a cloned protoporphyrinogen oxidase from the aerobic bacterium *Bacillus subtilis*. *Arch. Biochem. Biophys.* **358**, 251-6.

Curnow, A. W., Hong, K., Yuan, R., Kim, S., Martins, O., Winkler, W., Henkin, T. M. and Soll, D. (1997) Glu-tRNAGln amidotransferase: a novel heterotrimeric enzyme required for correct decoding of glutamine codons during translation. *Proc. Natl. Acad. Sci. U. S. A.* **94**, 11819-26.

Dailey, H. A. (1987) Metal inhibition of ferrochelatase. *Ann. N. Y. Acad. Sci.* **514**, 81-6.

Dailey, H. A. (ed.) (1990) *Biosynthesis of heme and chlorophylls.* McGraw-Hill Publishing, New York.

Dailey, T. A., Meissner, P. and Dailey, H. A. (1994) Expression of a Cloned protoporphyrinogen oxidase. *J. Biol. Chem.* **269**, 813-5.

Dailey, H. A. and Dailey, T. A. (1996) Protoporphyrinogen oxidase of *Myxococcus xanthus*. Expression, purification, and characterization of the cloned enzyme. *J. Biol. Chem.* **271**, 8714-8.

Dailey, T. A. And Dailey H. A. (1996) Human protoporphyrinogen oxidase: expression, purification, and characterization of the cloned enzyme. *Protein. Sci.* **5**, 98-105.

Dailey, T. A. and Dailey, H. A. (1998) Identification of an FAD superfamily containing protoporphyrinogen oxidases, monoamine oxidases and phytoene desaturase. *J. Biol. Chem.* **273**, 13658-62.

Dailey, H. A. (2002) Terminal steps of haem biosynthesis. *Biochem. Soc. Trans.* **30**, 590-5.

Ferreira, G.C., Andrew, T. L., Karr, S. W. and Dailey, H. A. (1988) Organization of the terminal two enzymes of the heme biosynthetic pathway. Orientation of protoporphyrinogen oxidase and evidence for a membrane complex. *J. Biol. Chem.* **263**, 3835-9.

Francklyn, C.S. (2001) Charging two for the price of one. *Nat. Struct. Biol.* **8**, 189-91.

Frankenberg, N., Erskine, P. T., Cooper, J. B., Shoolingin-Jordan, P. M., Jahn, D. and Heinz, D. W. (1999) High resolution crystal structure of a Mg2+ dependent porphobilinogen synthase. *J. Mol. Biol.* **289**, 591-602.

Frankenberg, N. and Lagarias, J. C. (2003) Phycocyanobilin:ferredoxin oxidoreductase of Anabaena sp. PCC 7120. Biochemical and spectroscopic. *J. Biol. Chem.* **278**, 9219-26.

Frankenberg, N., Moser, J. and Jahn, D. (2003) Bacterial heme biosynthesis and its biotechnological application. *Appl. Microbiol. Biotechnol.* **63**, 115-27.

Friedmann, H. C., Klein, A. and Thauer, R. K. (1991) Biochemistry of coenzyme F430, a nickel porphinoid involved in methanogenesis. *In Biosynthesis of tetrapyrroles*. (Jordan, P. M., ed.) Elsevier Science Ltd., Amsterdam, pp. 139-54.

Hansson, M. and Hederstedt, L. (1992) Cloning and characterization of the *Bacillus subtilis hemEHY* Gene Cluster, which encodes protoheme IX biosynthetic enzymes. *J. Biol. Chem.* **174**, 8081-93.

Hansson, M. and Hederstedt, L. (1994) *Bacillus subtilis* HemY is a periphal membrane protein essential for protoheme IX synthesis which can oxidize coproporphyrinogen III and protoporphyrinogen IX. *J. Biol. Chem.* **176**, 5962-70.

Heinemann, I. U., Diekmann, N., Masoumi, A., Koch, M., Messerschmidt, A., Jahn, M. and Jahn, D. (2007) Functional definition of the tobacco protoporphyrinogen IX oxidase substrate-binding site. *Biochem. J.* **402**, 575-80.

Ibba, M. And Soll, D. (2000) Aminoacyl-tRNA synthesis. *Annual Review of Biochemistry.* 69, 617-50.

Ilag, L. L. and Jahn, D. (1992) Activity and spectroscopic properties of the *Escherichia coli* glutamate 1- semialdehyde aminotransferase and the putative active site mutant K256R. *Biochemistry* **31,** 7143-51.

Jackson, A. H., Jones, D. M., Philip, G., Lash, T. D., del C. Batlle, A. M. and Smith, S. G. (1980) Synthetic and biosynthetic studies of porphyrins, part IV. Further studies of the conversion of coproporphyrinogen-III to protoporphyrinogen-IX: mass spectrometric investigations of the incubation of specifically deuteriated coproporphyrinogen-III with chicken red cell haemolysates. *Int. J. Biochem.* **12**, 681-8.

Jacobs, J. M. and Jacobs, N. J. (1984) Protoporphyrinogen oxidation, an enzymatic step in heme and chlorophyll synthesis: partial characterization of the reaction in plant organelles and comparison with mammalian and bacterial systems. *Arch. Biochem. Biophys.* **229**, 312-9.

Jacobs, J. M. and Jacobs, N. J. (1987) Oxidation of protoporphyrinogen to protoporphyrin, a step in chlorophyll and haem biosynthesis. Purification and partial characterization of the enzyme from barley organelles. *Biochem. J.* **244**, 219-24.

Jahn, D., Verkamp, E. and Söll, D. (1992) Glutamyl-transfer RNA: a precursor of heme and chlorophyll biosynthesis. *Trends Biochem. Sci.* **17**, 215-8.

Jordan, P. M. (ed.) (1991) *Biosynthesis of tetrapyrroles.* Elsevier Science Ltd., Amsterdam.

Kaneko, T., Suzuki, T., Kapushoc, S. T., Rubio, M. A., Ghazvini, J., Watanabe, K., Simpson, L., Suzuki, T. (2003) Wobble modification differences and subcellular localization of tRNAs in Leishmania tarentolae: implication for tRNA sorting mechanism. *EMBO J.* **22**, 657-67.

Kennedy, G. Y., Jackson, A. H., Kenner, G. W. and Suckling, C. J. (1970) Isolation, structure and synthesis of a tricarboxylic porphyrin from the harderian glands of the rat. *FEBS Lett.* **6**, 9-12.

Kikuchi, G., Kumar, A. M., Tamalge, P. and Shemin, D. (1958) The enzymatic synthesis of δ-aminolevulinic acid. *J. Biol. Chem.* **233**, 1214-19.

Koch, M., Breithaupt, C., Kiefersauer, R., Freigang, J., Huber, R. and Messerschmidt, A. (2004) Crystal structure of protoporphyrinogen IX oxidase: a key enzyme in haem and chlorophyll biosynthesis. *EMBO J.* **23**, 1720-28.

Kohno, H., Furukawa, T., Tokunaga, R., Taketani, S. and Yoshinaga, T. (1996) Mouse coproporphyrinogen oxidase is a copper-containing enzyme: expression in *Escherichia coli* and site-directed mutagenesis. *Biochim. Biophys. Acta.* **1292**, 156-62.

Laemmli, U. K. (1970) Cleavage of structural proteins during the assembly of the head of bacteriophage T4. *Nature* **227,** 680-5.

Lascelles, J. (1964) Tetrapyrrole biosynthesis and its regulation. *Microbial and molecular biology series.* (Davis, B. D., ed.) W. A. Benjamin, New York.

Layer, G., Verfurth, K., Mahlitz, E. and Jahn, D. (2002) Oxygen-independent coproporphyrinogen-III oxidase HemN from Escherichia coli. *J. Biol. Chem.* **277**, 34136-42.

Layer, G., Moser, J., Heinz, D. W., Jahn, D. and Schubert, W. D. (2003) Crystal structure of coproporphyrinogen III oxidase reveals cofactor geometry of Radical SAM enzymes. *EMBO J.* **22**, 6214-24.

Lee, D. S., Flachsova, E., Bodnarova, M., Demeler, B., Martasek, P. and Raman, C. S. (2005) Structural basis of hereditary coproporphyria. *Proc Natl Acad Sci U S A.* **102**, 14232-7.

Lermontova, I., Kruse, E., Mock, H. P. and Grimm, B. (1997) Cloning and characterization of a plastidal and a mitochondrial isoform of tobacco protoporphyrinogen IX oxidase. *Proc. Natl. Acad. Sci.* **94**, 8895-900.

Lüer, C., Schauer, S., Möbius, K., Schulze, J., Schubert, W. D., Heinz, D. W., Jahn, D. and Moser, J. (2005) Complex formation between Glutamyl-tRNA reductase and Glutamate-1-semialdehyde-2,1-aminomutase in *Escherichia coli* during the initial reactions of porphyrin biosynthesis. *J. Biol. Chem.* **280**, 18568-72.

Luo, J. (1993) Order of uroporphyrinogen III decarboxylation on incubation of porphobilinogen and uroporphyrinogen III with erythrocyte uroporphyrinogen decarboxylation. *Biochem. J.* **289**, 529-32.

Martens, J. H., Barg, H., Warren, M. J. and Jahn, D. (2002) Microbial production of vitamin B_{12}. *Appl. Microbiol. Biotechnol.* **58**, 275-85.

Medlock, A. E. and Dailey, H. A. (1996) Human coproporphyrinogen oxidase is not a metalloprotein. *J. Biol. Chem.* **271**, 32507-10.

Medlock, A., Swartz, L., Dailey, T. A., Dailey, H. A. and Lanzilotta, W. N. (2007) Substrate interactions with human ferrochelatase. *Proc. Natl. Acad. Sc.i U. S. A.* **104**, 1789-93.

Meissner, P. N., Dailey, T. A., Hift, R. J., Ziman, M., Corrigall, A. V., Roberts, A. G., Meissner, D. M., Kirsch, R. E. and Dailey, H. A. (1996) A R59W mutation in human protoporphyrinogen oxidase results in decreased enzyme activity and is prevalent in South Africans with variegate porphyria. *Nat. Genet.* **13**, 95-7.

Moser, J., Lorenz, S., Hubschwerlen, C., Rompf, A. and Jahn, D. (1999) *Methanopyrus kandleri* glutamyl-tRNA reductase. *J. Biol. Chem.* **274**, 30679-85.

Moser, J., Schubert, W. D., Beier, V., Bringemeier, I., Jahn, D. and Heinz, D. W. (2001) V-shaped structure of glutamyl-tRNA reductase, the first enzyme of tRNAdependent tetrapyrrole biosynthesis. *EMBO J.* **20**, 6583-90.

Murphy, G. M., Hawk, J. L., Magnus, I. A., Barrett, D. F., Elder, G. H. and Smith, S. G. (1986) Homozygous variegate porphyria: two similar cases in unrelated families. *J. R. Soc. Med.* **79**, 361-3.

Nakamura, Y., Kaneko, T., Sato, S., Ikeuchi, M., Katoh, H., Sasamoto, S., Watanabe, A., Iriguchi, M., Kawashima, K., Kimura, T., Kishida, Y., Kiyokawa, C., Kohara, M., Matsumoto, M., Matsuno, A., Nakazaki, N., Shimpo, S., Sugimoto, M., Takeuchi, C., Yamada, M. and Tabata, S. (2002) Complete genome structure of the thermophilic cyanobacterium *Thermosynechococcus elongatus* BP-1. *DNA Res.* **9**, 123-30.

Neuberger, A. (1953) Metabolism of aminolevulinic acid and the biosynthesis of heme. *Expos. Annu. Biochim. Med.* **8**, 31-9.

Nureki, O., Suzuki, K., Hara-Yokoyama, M., Kohno, T., Matsuzawa, H., Ohta, T., Shimizu, T., Morikawa, K., Miyazawa, T. and Yokoyama, S. (1992) Glutamyl-tRNA synthetase from *Thermus thermophilus* HB8. Molecular cloning of the gltX gene and crystallization of the overproduced protein. *Eur. J. Biochem.* **204**, 465-72.

O'Brian, M. R. and Thöny-Meyer, L. (2002) Biochemistry, regulation and genomics of haem biosynthesis in prokaryotes. *Adv. Microb. Physiol.* **46**, 257-318.

Olsson, U., Billberg, A., Sjovall, S., Al-Karadaghi, S. and Hansson, M. (2002) In vivo and in vitro studies of Bacillus subtilis ferrochelatase mutants suggest substrate channeling in the heme biosynthesis pathway. *J. Bacteriol.* **184**, 4018-24.

Panek, H. and O'Brian, M. R. (2002) A whole genome view of prokaryotic haem biosynthesis. *Microbiology.* **148**, 2273-82.

Phillips, J. D., Whitby, F. G., Warby, C. A., Labbe, P., Yang, C., Pflugrath, J. W., Ferrera, J. D., Robinson, H., Kushner, J. P. and Hill, C. P. (2004) Crystal structure of the oxygen dependant coproporphyrinogen oxidase (Hem13p) of *Saccharomyces cerevisiae*. *J. Biol. Chem.* **279**, 38960-68.

Raczniak, G., Becker, H. D., Min, B. and Soll, D. (2001) A single amidotransferase forms asparaginyl-tRNA and glutaminyl-tRNA in Chlamydia trachomatis. *J. Biol. Chem.* **276**, 45862-7.

Rao, S. and Rossmann, M. (1973) Comparison of super-secondary structures in proteins. *J. Mol. Biol.* **76**, 241-56.

Righetti, P. G., Gianazza, E., Gelfi, C. and Chairi, M. (1990) In *Gel electrophoresis of proteins: a practical approach.* (Hames, B. D. and Rickwood, D., eds.) 2nd ed., Oxford University Press, Oxford, pp. 149-214.

Sambrook, J., Fritsch, E. F. and Maniatis, T. (1989) Liquid media for *E. coli*. In *Molecular cloning: a laboratory manual.* 2nd ed., vol. **3**, Cold Spring Harbor Laboratory Press, New York.

Sano, S. and Granick, S. (1961) Mitochondrial coproporphyrinogen oxidase and protoporphyrin formation. *J. Biol. Chem.* **236**, 1173-80.

Sarkani, R. P. (1999) Porphyria from Sir Walter Raleight to molecular biology. *Adv. Exp. Med. Biol.* **455**, 235-41.

Schulze, J. O., Masoumi, A., Nickel, D., Jahn, M., Jahn, D., Schubert, W. D. and Heinz, D. W. (2006) Crystal structure of a non-discriminating glutamyl-tRNA synthetase. *J. Mol. Biol.* **361**, 888-97.

Scott, A. I. and Santander, P. J. (1991) The biosynthesis of vitamin B12. In *Biosynthesis of tetrapyrroles*. (Jordan, P. M., ed.) Elsevier Science Ltd., Amsterdam, pp. 101-138.

Sekine, S., Nureki, O., Shimada, A., Vassylyev, D. G. and Yokoyama, S. (2001) Structural basis for anticodon recognition by discriminating glutamyl-tRNA synthetase. *Nat. Struct. Biol.* **8**, 203-6.

Sekine, S., Nureki, O., Dubois, D. Y., Bernier, S., Chenevert, R., Lapointe, J., Vassylyev, D. G. and Yokoyama, S. (2003) ATP binding by glutamyl-tRNA synthetase is switched to the productive mode by tRNA binding. *EMBO J.* **22**, 676-88.

Shemin, D. and Russell, C. S. (1953) δ-aminolevulinic acid, its role in the biosynthesis of porphyrins and purines. *J. Am. Chem. Soc.* **75**, 4873-4.

Shoolingin-Jordan, P. M., Spencer, P., Sarwar, M., Erskine, P. E., Cheung, K. M., Cooper, J. B. and Norton, E. B. (2002) 5-Aminolaevulinic acid dehydratase: metals, mutants and mechanism. *Biochem. Soc. Trans.* **30**, 584-90.

Siepker, L. J., Ford, M., deKock, R. and Kramer, S. (1987) Purification of bovine protoporphyrinogen oxidase: immunological cross-reactivity and structural relationship to ferrochelatase. *Biochem. Biophys. Acta.* **913**, 349-58.

Smith, D. R., Doucette-Stamm, L. A., Deloughery, C., Lee, H., Dubois, J., Aldredge, T., Bashirzadeh, R., Blakely, D., Cook, R., Gilbert, K., Harrison, D., Hoang, L., Keagle, P.,

Lumm, W., Pothier, B., Qiu, D., Spadafora, R., Vicaire, R., Wang, Y., Wierzbowski, J., Gibson, R., Jiwani, N., Caruso, A., Bush, D. and Reeve, J. N. (1997) Complete genome sequence of *Methanobacterium thermoautotrophicum* deltaH: functional analysis and comparative genomics. *J. Bacteriol.* **179**, 7135-55.

Suzuki, T., Masuda, T., Singh, D. P., Tan, F. C., Tsuchiya, T., Shimada, H., Ohta, H., Smith, A. G. and Takamiya, K. (2002) Two types of ferrochelatase in photosynthetic and nonphotosynthetic tissues of cucumber: their difference in phylogeny, gene expression, and localization. *J Biol Chem.* **277**, 4731-7.

Thauer, R. K. and Bonacker, L. G. (1994) Biosynthesis of coenzyme F430, a nickel porphinoid involved in methanogenesis. In *The biosynthesis of tetrapyrrole pigments; Ciba Foundation Symposium 180*. (Chadwick, D. J. and Ackrill, K., eds.) Wiley, Chichester, pp. 210-27.

van Lis, R., Atteia, A., Nogaj, L. A. and Beale, S. I. (2005) Subcellular localization and light-regulated expression of protoporphyrinogen IX oxidase and ferrochelatase in Chlamydomonas reinhardtii. *Plant. Physiol.* **139**,1946-58.

Wang, K.F., Dailey, T.A. and Dailey, H.A. (2001) Expression and characterization of the terminal heme synthetic enzymes from the hyperthermophile Aquifex aeolicus. *FEMS Microbiol. Lett.* **202**, 115-9.

Warren, M. J. and Jordan, P. M. (1987) Investigation into the nature of substrate binding to the dipyrromethane cofactor of *Escherichia coli* porphobilinogen deaminase. *Biochemistry* **27**, 9020-30.

Warren, M. J., Bolt, E. and Woodcock, S. C. (1994) 5-Aminolaevulinic acid synthase and uroporphyrinogen methylase: two key control enzymes of tetrapyrrole biosynthesis and modification. In *The biosynthesis of tetrapyrrole pigments; Ciba Foundation Symposium 180*. (Chadwick, D. J. and Ackrill, K., eds.) Wiley, Chichester, pp. 26-49.

Warren, M. J. and Phelan, V. (2005) UV/Visible spectroscopic investigations of the 'pigments of life'. *Lab. Asia* **27**, 7-8.

Watanabe, N., Che, F. S., Iwano, M., Takayama, S., Yoshida, S. and Isogai, A. (2001) Dual targeting of spinach protoporphyrinogen oxidase II to mitochondria and chloroplasts by alternative use of two in-frame initiation codons. *J. Biol. Chem.* **276,** 20474-81.

Wilcox, M. and Nirenberg, M. (1968) Transfer RNA as a cofactor coupling amino acid synthesis with that of protein. *Proc. Natl. Acad. Sci. U. S. A.* **61**, 229-36.

Wu, C. K., Dailey, H. A., Rose, J. P., Burden, A., Sellers, V. M. and Wang, B. C. (2001) The 2.0 A structure of human ferrochelatase, the terminal enzyme of heme biosynthesis. *Nat. Struct. Biol.* **8**, 156-60.

Danksagung

Bei meinem Doktorvater Prof. Dr. Dieter Jahn möchte ich mich für die Vergabe des Themas, seine stets motivierende Art sowie die Unterstützung und Diskussionsbereitschaft während der vergangenen drei Jahre sehr herzlich bedanken.

Prof. Dr. Ralf Mendel danke ich für die Übernahme des Zweitgutachtens für diese Arbeit.

Prof. Dr. Petra Dersch sei gedankt für die Übernahme des Vorsitzes der Promotionskommission.

Besonders bedanken möchte ich mich bei Dr. Martina Jahn. Sie war für mich in den vier Jahren nicht nur meine Ansprechpartnerin bei fachlichen Problemen und Fragen, sondern half mir auch bei sprachlichen Hindernissen sowie wie eine Freundin bei der Eingewöhnung in Deutschland und anderen Schwierigkeiten. Sie war meine beste Chance in Deutschland.

Außerdem danke ich auch Ilka Heinemann, Nina Diekmann, Claudia Schulz und Simone Virus für die nette Aufnahme in Labor 253/212, die stete Hilfe sowie die wirklich freundschaftliche Atmosphäre.

Natürlich geht auch ganz herzlicher Dank an die gesamte AG Jahn für das entspannte Arbeitsklima. Es hat Spaß gemacht, hier zu arbeiten - und auch die vielen „sonstigen Aktivitäten“ sollen nicht unerwähnt bleiben.

Außerdem möchte ich mich an dieser Stelle noch einmal bei meinen Eltern dafür bedanken, dass sie mir das Studium ermöglicht haben.

Herzlicher Dank natürlich auch an alle, die mir im Laufe der drei Jahre immer wieder Mut gemacht haben.